Report No. GDL/GMF-99-02

BUOYANT TURBULENT JETS AND FLAMES: II. REFRACTIVE INDEX, EXTINCTION AND SCATTERING PROPERTIES OF SOOT

S. S. Krishnan and G. M. Faeth
Department of Aerospace Engineering
The University of Michigan
Ann Arbor, Michigan 48109-2140

Prepared for:

U.S. Department of Commerce
National Institute of Standards and Technology
Laboratory for Building and Fire Research
Washington, D.C. 20234

Annual Report
Grant No. 60NANB8D0081
H. R. Baum, NIST Scientific Officer

October 1999

Notice

This report was prepared for the Laboratory for Building and Fire Research of the National Engineering Laboratory, National Institute of Standards and Technology, under Grant Number 60NANB80081. The statements and conclusions contained in this report are those of the authors and do not necessarily reflect the views of the National Institute of Standards and Technology, or the Laboratory for Building and Fire Research.

BUOYANT TURBULENT JETS AND FLAMES: II. REFRACTIVE INDEX, EXTINCTION AND SCATTERING PROPERTIES OF SOOT

October 1999

Sponsored by:

U.S. Department of Commerce
National Institute of Standards and Technology
Laboratory for Building and Fire Research
Washington, D.C. 20234

BUOYANT TURBULENT JETS AND FLAMES: II. REFRACTIVE INDEX, EXTINCTION AND SCATTERING PROPERTIES OF SOOT

Abstract

Extinction and scattering properties at wavelengths of 250-5200 nm were studied for soot emitted from large buoyant turbulent diffusion flames where soot properties are independent of position in the overfire region and characteristic flame residence time. Flames burning in still air and fueled with both gas (acetylene, ethylene, propane and propylene) and liquid (benzene, toluene, cyclohexane and n-heptane) hydrocarbon fuels were considered. Extinction and scattering measurements were interpreted to find soot optical properties using Rayleigh-Debye-Gans/polydisperse-fractal aggregate (RDG/PFA) theory after establishing that this theory provided good predictions of scattering patterns and ratios of total scattering/absorption cross sections. Effects of fuel type on soot optical properties were comparable to experimental uncertainties. Measured depolarization ratios were correlated with the primary particle size parameter, completing RDG/PFA methodology needed to make soot extinction and scattering predictions. Measurements of dimensionless extinction coefficients were in good agreement with earlier measurements for similar soot populations and were relatively independent of wavelength for wavelengths of 400-800 nm where a mean value of 8.4, averaged over fuel type and wavelength, was observed. The refractive index function for absorption was in good agreement with earlier reflectometry measurements in the visible but was larger than these measurements in the infrared. Similarly, present measurements of the refractive index function for scattering agreed with earlier reflectometry measurements for wavelengths of 400-550 nm but otherwise increased with increasing wavelength more rapidly than the rest. Finally, ratios of total scattering/absorption cross sections were relatively large in the visible and near-infrared, with maximum values as large as 0.9, suggesting greater potential for scattering from soot particles to affect flame radiation properties than previously thought.

Acknowledgments

This research was supported by the U.S. Department of Commerce, National Institute of Standards and Technology, Grant Number 60NANB80081, with H. R. Baum of the Laboratory for Building and Fire Research serving as Scientific Officer. The assistance of K.-C. Lin and J.-S. Wu is also gratefully acknowledged.

Table of Contents

	Page
Abstract	iv
Acknowledgments	v
List of Tables	vii
List of Figures	viii
Nomenclature	ix
1. Introduction	1
2. Experimental Methods	3
3. Theoretical Methods	5
4. Results and Discussion	7
5. Conclusions	20
References	21
Appendix A: Krishnan et al. (1999a)	25
Appendix B: Krishnan et al. (1999b)	66

List of Tables

Table		Page
1	Summary of publications	2
2	Summary of the dimensionless extinction coefficients and refractive index properties of overfire soot in the visible.	9

List of Figures

Figure	Caption	Page
1.	Measured dimensionless extinction coefficients of soot for various fuels at wavelengths of 250-5200 nm. Measurements of Dobbins et al. (1994), Choi et al. (1995), Mulholland and Choi (1998), Zhou et al. (1998) and the present investigation.	8
2.	Measured and predicted scattering patterns for soot in the overfire region of ethylene/air flames in the visible (351.2-632.8 nm).	12
3.	Measurements of depolarization ratios for various fuels as a function of primary particle size parameter in the visible (351.2-632.8 nm). Measurements of Köylü and Faeth (1994a,b), Wu et al. (1997) and the present investigation.	13
4.	Measured mean values of the refractive index functions E(m) and F(m) of soot in the visible as a function of wavelength.	15
5.	Measured mean real and imaginary parts of the complex refractive indices of soot in the visible as a function of wavelength.	16
6.	Measured and predicted total scattering/absorption cross section ratios for various fuels as a function of wavelength in the visible (351.2-632.8 nm).	18
7.	Estimates of total scattering/absorption cross section ratios for various fuels as a function of wavelength for wavelengths of 300-5200 nm.	19

Nomenclature

C	=	optical cross section
d_p	=	primary particle diameter
D_f	=	mass fractal dimension
$E(m)$	=	refractive index function for absorption = $\mathrm{Im}((m^2-1)/(m^2+2))$
f_v	=	soot volume fraction
$F(m)$	=	refractive index function for scattering = $\lvert(m^2-1)/(m^2+2)\rvert^2$
i	=	$(-1)^{1/2}$
I	=	light intensity
k	=	wave number = $2\pi/\lambda$
k_f	=	fractal prefactor
K_e	=	dimensionless extinction coefficient
L	=	light path length
m	=	soot refractive index = $n + i\kappa$
n	=	real part of soot refractive index
N	=	number of primary particles per aggregate
N_g	=	geometric mean of the number of particles per aggregate
q	=	modulus of scattering vector = $2k \sin(\theta/2)$
Q	=	volumetric optical cross section

R_g	=	radius of gyration of an aggregate
x_p	=	primary particle size parameter $= \pi d_p/\lambda$
θ	=	angle of scattering from forward direction
κ	=	imaginary part of refraction of soot
λ	=	wavelength of radiation
ρ_{sa}	=	ratio of total scattering to absorption
ρ_v	=	depolarization ratio

Subscripts

a	=	absorption
av	=	average value
e	=	extinction
h	=	horizontal polarization
ij	=	incident (i) and scattered (j) polarization directions
s	=	total scattering
v	=	vertical polarization
o	=	initial value

Subscripts

a	=	aggregate properties
p	=	primary particle property

$(\bar{\ })$ = mean value over a polydisperse aggregate population

1. Introduction

An investigation of the structure and optical properties of soot is described. The findings of this research have applications to the development of nonintrusive methods for measuring soot properties and to estimating the continuum radiation properties of soot in flame environments. The main emphasis of the investigation was on the refractive index, extinction and scattering properties (the optical properties) of soot emitted from large buoyant turbulent flames fueled with hydrocarbons and burning in still air.

Information about the optical properties of soot is needed to develop reliable nonintrusive (optical) measurements of soot properties and estimates of continuum radiation due to soot in flame environments. Substantial information about the optical properties of soot is already known, as follows: soot consists of nearly monodisperse spherical primary particles that collect into mass fractal aggregates having broad size distributions, soot primary particle diameters and aggregate sizes vary widely but soot fractal properties appear to be relatively universal, soot optical properties in the visible can be approximated reasonably well by Rayleigh-Debye-Gans scattering from polydisperse mass fractal aggregates (called RDG-PFA theory), and current estimates of soot optical properties in flame environments are mainly limited by excessive uncertainties about soot refractive index properties, see Faeth and Köylü (1995) and references cited therein. Motivated by these observations, the objective of the present investigation was to measure soot optical properties at visible and near-infrared wavelengths, emphasizing the properties of dimensionless extinction coefficients and refractive index indices.

Earlier studies of soot dimensionless extinction coefficient and refractive index properties in the present wavelength range are briefly reviewed in the following, more details can be found in Charalampopoulos (1992), Faeth and Köylü (1995), Jullien and Botet (1987), Köylü and Faeth (1993), Tien and Lee (1982), Viskanta and Mengüc (1987) and references cited therein. Some past determinations of soot refractive indices involve *ex situ* reflectivity measurements of compressed soot samples (Batten, 1985; Dalzell and Sarofim, 1969; Felske et al., 1984; Stagg and Charalampopoulos, 1993); these results have been questioned, however, due to potential changes of soot properties caused by sample collection and compression as well as potential effects of surface irregularities on measured reflectance properties (Charalampopoulos, 1992; Felske et al., 1984; Tien and Lee, 1982). In order to avoid these error sources, other studies involved *in situ* measurements of extinction and scattering (Chang and Charalampopoulos, 1990; Charalampopoulos, 1992; Lee and Tien, 1980; Vaglieco et al., 1990); unfortunately, these studies have a number of deficiencies as well: soot structure generally was not

Table 1. Summary of Publications

This is a summary of publications, reports and theses under the present grant concerning soot optical properties that were in print, in press, submitted, presented or in preparation during the report period.

Archival Publications (articles and book chapters):

Krishnan, S.S., Lin, K.-C., and Faeth, G.M. (1999) "Optical Properties in the Visible of Overfire Soot in Large Buoyant Turbulent Diffusion Flame," *J. Heat Trans.*, in press.

Krishnan, S.S., Lin, K.-C., and Faeth, G.M. (1999) "Extinction and Scattering Properties of Soot Emitted from Large Buoyant Turbulent Diffusion Flames," *J. Heat Trans.*, submitted.

Faeth, G.M., Krishnan, S.S., and Xu, F. (1999) "Physical and Optical Properties of Soot," *Prog. Energy Combust. Sci.*, in preparation.

Papers:

Krishnan, S.S., Lin, K.-C., and Faeth, G.M. (1999) "Extinction and Scattering of Soot Emitted From Turbulent Diffusion Flames for Wavelengths of 250-5200 nm," *34th National Heat Transfer Conference*, Pittsburgh, PA, submitted.

Krishnan, S.S., Lin, K.-C., and Faeth, G.M., (1999) "Refractive Index Properties of Soot Emitted from Buoyant Turbulent Diffusion Flames," *Proceedings of the Joint Meeting of the United States Sections*, The Combustion Institute, Pittsburgh, pp. 560-563.

Krishnan, S.S., Lin, K.-C., and Faeth, G.M. (1999) "Scattering and Extinction Properties of Overfire Soot in Large Buoyant Turbulent Diffusion Flames," *Proc. ASME National Heat Transfer Conference*, Albuquerque, NM.

Krishnan, S.S., Lin, K.-C., Wu, J.-S., and Faeth, G.M. (1999) "Optical Properties of Soot in the Overfire Region of Large Buoyant Diffusion Flames," *Annual Conference on Fire Research*, National Institute of Standards and Technology, Gaithersburg, MD, NISTIR 6242, pp. 29-30.

Reports and Theses:

Krishnan, S.S., Farias, T.L., Wu, J.-S., Köylü, Ü.Ö., and Faeth, G.M. (1998) "Mixing and Radiation Properties of Buoyant Luminous Flame Environments: II. Structure and Optical Properties of Soot," Report No. GDL/GMF-98-03, The University of Michigan, Ann Arbor.

Krishnan, S.S. (2000) "Optical Properties of Soot Emitted from Buoyant Turbulent Diffusion Flames," Ph.D. Thesis, The University of Michigan, Ann Arbor, in preparation.

---

2. Experimental Methods

Apparatus. The following discussion of experimental methods is brief, see Köylü and Faeth (1994), Wu et al. (1997) and Krishnan et al.(1999a,b) for more details.

Present test flames were large buoyant turbulent diffusion flames burning in still air within the long residence time regime. The test flames were provided by gas and liquid-fueled burners injecting fuel gases vertically upward. Soot properties were measured by collecting the combustion products in a hood having a 152 mm diameter vertical exhaust duct. Measurements were made at the exit of the exhaust duct where properties across the flow were nearly uniform; nevertheless, soot concentrations were measured along the optical path so that extinction measurements could be referenced to conditions at the duct axis where all other optical measurements were made. Note that using a collection system in this way does not affect soot structure and optical properties because they are universal in the overfire region for present test conditions (Köylü and Faeth, 1994a). A water-cooled burner having a diameter of 50 mm described by Sivathanu and Faeth (1990) was used for the gas-fueled flames. Uncooled burners having diameters of 51 and 102 mm were used for the liquid-fueled flames, adjusting the fuel flow rate to attain steady pool fires with the liquid surface roughly 10-20 mm below the burner exit.

Sampling Measurements. Aside from routine sampling measurements of gas temperatures and compositions at the measuring location, sampling measurements included soot structure and gravimetric volume fractions. Other soot properties of interest during the present study, e.g., soot density and composition, were drawn from Köylü and Faeth (1992, 1994a) and Wu et al. (1997) for similar soot populations.

The first step of the present calculations involved the determination of the mean number of primary particles per unit volume at the measurement location from the gravimetric measurements of soot volume fraction and the TEM measurement of primary particle diameter, as follows:

$$n_p = 6f_v/(\pi d_p^3) \tag{1}$$

Then, noting that $\overline{Q}_a^a = \overline{Q}_e^a - \overline{Q}_s^a$ so that $\overline{Q}_a^a$ can be found from present measurements of $\overline{Q}_e^a$ and $\overline{Q}_s^a$, the refractive index functions, E(m) and F(m) can be computed as follows:

$$E(m) = k^2 \overline{Q}_a^a/(4\pi x_p^3 n_p) \tag{2}$$

$$F(m) = k^2(qd_p)^{D_f}\, \overline{Q}_{vv}^a(qd_p)/(k_f x_p^6 n_p) \tag{3}$$

where qd_p must be large enough so that scattering is in the large-angle (power-law) regime where Eq. (3) is appropriate. This requirement was established by noting the behavior of scattering at the limiting conditions of small-angle (Guinier) and large-angle (power-law) scattering, as follows:

$$\overline{Q}_{vv}^a(qd_p)/\ Q_{vv}^p = (\overline{N}^2/\overline{N})\exp(q^2\overline{R}_g^2/3), \quad \text{Guinier regime} \tag{4}$$

$$\overline{Q}_{vv}^a(qd_p)/\ Q_{vv}^p = k_f(qd_p)^{-D_f}, \quad \text{power-law regime} \tag{5}$$

where the expression for $\overline{R}_g^2$ in the Guinier regime can be found in Köylü and Faeth (1994a) while the value of $k_f = 8.5$ was adopted from the determination of Köylü et al. (1995). The volumetric primary particle Rayleigh scattering cross section used to normalize Eqs. (4) and (5) is given by:

$$Q_{vv}^p = n_p x_p^6\, F(m)/k^2 \tag{6}$$

It is evident that $\overline{Q}_{vv}^a(qd_p)/\ Q_{vv}^p$ provides a simple determination of soot fractal dimensions because D_f is the slope of this function in the power-law regime. Finally, E(m) and F(m) provide two nonlinear algebraic equations that can be solved to find the real and imaginary parts of the soot refractive indices.

The dimensionless extinction coefficient is a useful optical property that provides a simple relationship between extinction and soot volume fractions (Dobbins et al., 1994;

neutral density filters and a photodetector. The extinction measurements employed similar but rigidly-mounted collection optics, designed following Manickavasagam and Mengüc (1993) to reduce contributions of forward scattering to less than 1%. An optical system housing and darkroom conditions in the laboratory minimized optical noise due to ambient lighting.

Rayleigh scattering from propane gas was used to provide an absolute calibration of the scattering measurements. Absolute differential scattering cross sections of soot were found from ratios of the detector signal for soot and propane, based on the Rayleigh scattering properties of propane from Rudder and Bach (1968) and Dyer (1979). Total volumetric scattering cross sections were found by integrating volumetric differential scattering cross sections over the spherical surface while extrapolating to find contributions in the near forward and backward scattering directions as discussed by Wu et al. (1997).

In addition to full extinction and scattering measurements in the visible, extinction measurements were extended to the wavelength range of 250-5200 nm. This involved a Quartz-Tungsten Halogen (QTH) lamp (100W, Oriel 6333) at 600.0, 800.0, 1100.0, 1550.0 and 2017.0 nm and an IR emitter source (Oriel 6363) at 3980.0 and 5205.0 nm. Two detectors were used: 351.2-800.0 nm using a silicon detector (Newport 818-UV), and 248.0-303.0 nm and 1100.0-5205.0 nm using a pyrodetector (Oriel 70128). Interference filters having 10 nm bandwidths were used for wavelengths up to 1550.0 nm and bandwidths of 90-160 nm for wavelengths larger than 1500.0 nm. Calcium fluoride lenses were used for spatial filtering and collimating the incident light due to the large range of wavelengths considered.

3. Theoretical Methods

Analysis of the scattering measurements to find soot optical properties was based on RDG-PFA theory. The main assumptions of RDG-PFA theory are as follows: individual primary particles satisfy the Rayleigh scattering approximation, soot aggregates satisfy the Rayleigh-Debye-Gans (RDG) scattering approximation, primary particles are spherical and monodisperse, primary particles just touch one another, the number of primary particles per aggregate satisfies a log-normal probability distribution function and the aggregates are mass fractal-like objects. These approximations have proven to be satisfactory during past evaluations for a variety of conditions (Köylü and Faeth, 1992, 1994a,b); nevertheless, they still were evaluated using present measurements before the theory was used to find soot optical properties.

Soot structure was found by thermophoretic sampling and analysis using transmission electron microscopy (TEM), following Köylü and Faeth (1992). Sampling was carried by inserting TEM grids into the flow at the exhaust duct axis. Sampling times were selected to achieve less than 10% coverage of the grid surface with soot in order to avoid overlapping aggregates on the grid. Effects of aggregate size on sampling bias were less than 20% from estimates based on Rosner et al. (1991). Samples of 400 primary particles selected from more than 50 aggregates were used to find the mean value of d_p with an experimental uncertainty less than 2% (95% confidence).

Gravimetric volume fractions were measured following Wu et al. (1997). This involved sampling the flow and measuring the volumes of soot and gas collected. The sampling probe was aligned with the exhaust duct axis and had a 13 mm diameter inlet connected to a 47 mm diameter Gelman filter. The filter was connected to a vacuum pump through a flowmeter and valve. The flowmeter was fitted with a manometer and calibrated over the required range of inlet pressures and flow rates using a wet test meter. Soot samples were collected for a timed period using two filters, one in the filter holder and the second to mechanically collect soot from the sample line and filter holder. The mass of soot was found by weighing the filters before and after sampling using an electronic balance. Given these measurements, the soot volume fraction could be computed from the known soot density. Sample times were lengthy and several samples along the optical path and repeat samples were required; therefore, a laser extinction system was used across the sampling duct exit to insure that flame conditions were accurately repeated. In addition, gravimetric soot volume fractions were measured at more locations along the optical path than before. These two changes from the approach used by Wu et al. (1997) are felt to be mainly responsible for better agreement between present and past measurements of the dimensionless extinction coefficients of soot than before.

Optical Measurements. Soot scattering and extinction properties were measured following Köylü and Faeth (1994a,b). Light sources used for measurements at various wavelengths were as follows: 351.2, 457.9, 488.0 and 514.5 nm using an argon-ion laser (4W, Coherent Innova 90-4); 632.8 nm using a He-Ne laser (28 mW, Melles Griot MG53036); 240.0, 303.0 and 405.0 nm using a mercury lamp (100W, Oriel 6333); and 800.0 nm (for extinction measurements only) using a laser diode (700 mW, SDL-2360-P3). The incident beams were passed through a polarization rotator and mechanical chopper and then focused at the axis of the exhaust duct. The collecting optics for scattering measurements were mounted on a turntable so that scattering angles of 5-160 deg could be considered. The collecting optics had a collection angle of 0.7 msr, dichroic sheet polarizer filters (1 and 10 nm bandwidths for laser and lamp sources, respectively),

Choi et al., 1995). This parameter was found for present test conditions by noting that properties were constant along the optical path used for extinction measurements, which implies (Choi et al., 1995):

$$K_e = -\lambda \ln(I/I_o)/(Lf_v) \tag{7}$$

Large soot aggregates exhibit effects of depolarization which influence $\overline{Q}^a_{hh}$ and thus estimates of $\overline{Q}^a_s$ and ρ_{sa}. Unfortunately, effects of depolarization cannot be predicted using RDG-PFA theory and must be handled empirically instead. This was done as suggested by Köylü and Faeth (1994a) by defining a depolarization ratio, ρ_v, and using it analogous to Rayleigh scattering theory, see Rudder and Bach (1968). Thus, values of $\overline{Q}^a_{hh}(\theta)$ were found, as follows:

$$\overline{Q}^a_{hh}(\theta) = [(1-\rho_v)\cos^2\theta + \rho_v]\,\overline{Q}^a_{vv}(\theta) \tag{8}$$

It follows immediately from Eq. (8) that

$$\rho_v = \overline{Q}^a_{hh}(90°)/\overline{Q}^a_{vv}(90°) \tag{9}$$

So that ρ_v could be obtained directly from present measurements in the visible. The general formulation of Eqs. (1)-(9) was used in a variety of ways to analyze and interpret the present measurements, Krishnan et al. (1999a,b) should be consulted for the details.

4. Results and Discussion

Dimensionless Extinction Coefficients. Effects of fuel type on dimensionless extinction coefficients were comparable to experimental uncertainties and the following results will involve values of K_e averaged over all fuels at each wavelength. The resulting values of K_e are plotted as a function of wavelength in Fig. 1, with values of K_e in the visible also summarized in Table 2. Other measurements for overfire soot in the long residence time regime for various fuels due to Dobbins et al. (1994), Choi et al. (1995), Mulholland and Chen (1998) and Zhou et al. (1998) are plotted on the figure for comparison with the present measurements.

The values of K_e from the studies illustrated in Fig. 1 all involve soot emitted from large buoyant turbulent diffusion flames burning a variety of fuels and are in excellent agreement. This supports the idea that effects of fuel type on K_e are small for these conditions, however, this behavior should not be assumed for all flame conditions.

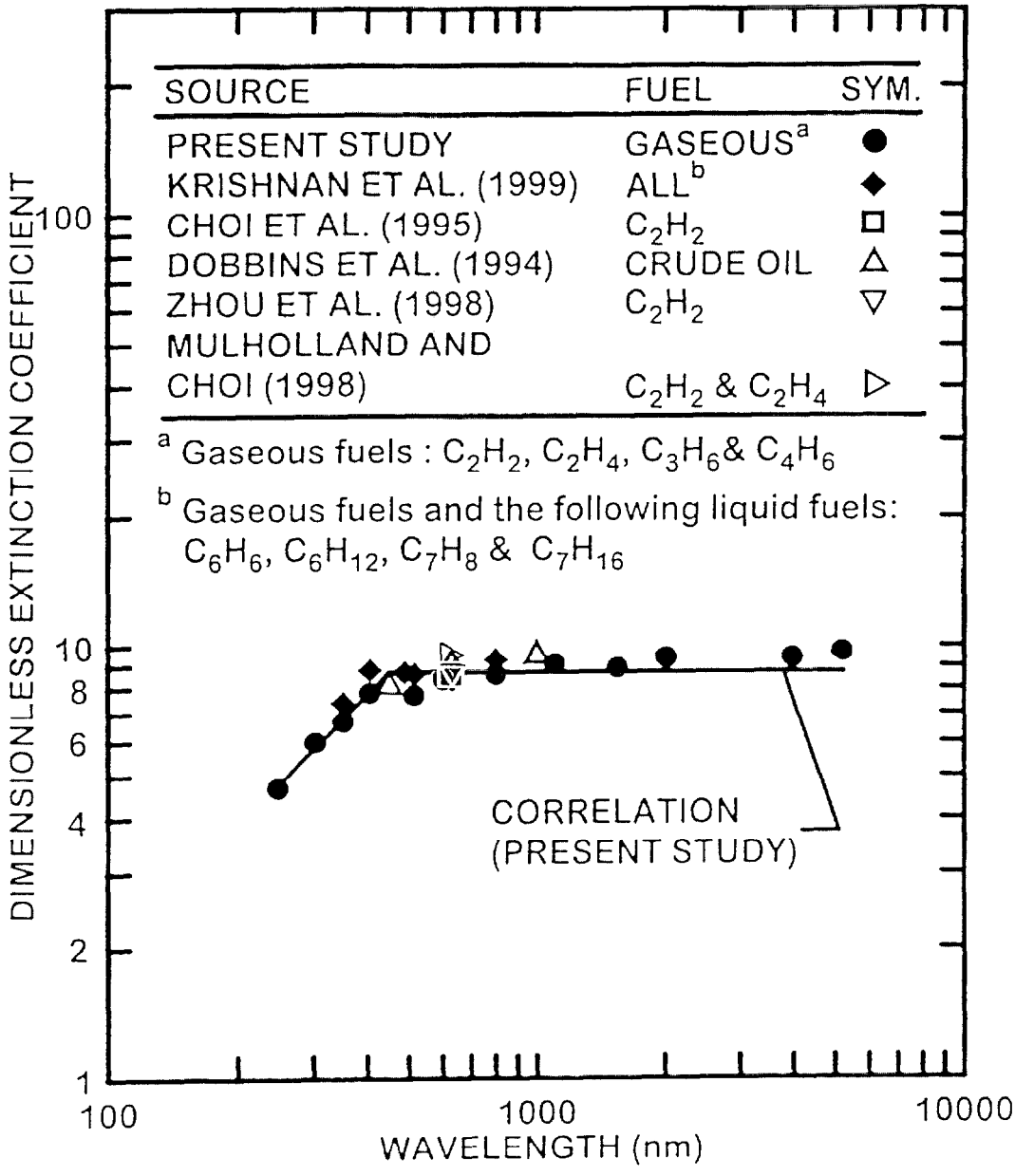

Figure 1 Measured dimensionless extinction coefficients of soot for various fuels at wavelengths of 250-5200 nm. Measurements of Dobbins et al. (1994), Choi et al. (1995), Mulholland and Choi (1998), Zhou et al. (1998) and the present investigation.

For example, Dobbins et al. (1994) and Colbeck et al. (1997) review measurements of K_e that exhibit significant differences among large diffusion flames, premixed flames and smoldering flames. Effects of primary particle size and aggregate size on the extinction properties of soot from RDG-PFA theory also support such behavior.

Values of K_e in Fig. 1 increase rapidly with increasing wavelength at wavelengths smaller than 400 nm which agrees with Vaglieco et al. (1990) for amorphous carbon and soot in the near ultraviolet. For wavelengths of 400-5200 nm, however, values of K_e are relatively constant, yielding an average of 8.7 with a standard deviation of 1.5 which is plotted on the figure.

Table 2 Summary of the dimensionless extinction coefficient and refractive index properties of overfire soot in the visible[a]

λ (nm)	E(m)	F(m)	F(m)/E(m)[b]	n	κ	K_e
351.2	0.24(0.06)	0.13(0.03)	0.63	1.38	0.44	7.4(1.3)
405.0[c]	---	---	0.76	---	---	8.8(1/0)[c]
457.9[d]	0.27(0.06)	0.26(0.07)	0.87	1.64	0.62	8.7(1.5)
488.0	0.28(0.04)	0.25(0.07)	0.93	1.60	0.62	8.7(1.9)
514.5	0.29(0.04)	0.27(0.06)	0.98	1.62	0.66	8.6(1.5)
632.8	0.27(0.04)	0.44(0.15)	1.17	1.99	0.89	8.4(1.0)
800.0[c]	---	---	---	---	---	9.3(1.5)[f]

[a]Standard deviations based on measurements for soot emitted from flames for eight fuels are shown in parenthesis, except as noted.
[b]Values of F(m)/E(m) from the correlation for all fuels in visible.
[c]Only extinction measurements were made at 405.0 and 800.0 nm.
[d]Benzene and toluene were excluded at 457.9 nm.
[e]Measurements were not made for the gaseous fuels and n-heptane at 405.0 nm.
[f]Measurements were not made for the gaseous fuels at 800.0 nm.

Scattering Patterns. Scattering problems were used to evaluate RDG-PFA theory for the present overfire soot before applying this theory to find soot optical properties. This approach is justified because scattering patterns are affected by the optical theory used but are relatively independent of soot refractive index properties.

characterized, Rayleigh and Mie scattering approximations were used to analyze the measurements that have not proven to be very effective for soot aggregates, questionable approximations involving either graphitic-based dispersion models or Kramers-Kronig causality relationships were adopted in some cases, and there has only been limited consideration of effects of fuel type on soot refractive index properties (Dobbins and Megaridis, 1991; Faeth and Köylü 1995; Köylü and Faeth, 1994a,b,1996).

A recent study of the refractive index properties of soot due to Wu et al. (1997) sought to resolve concerns about earlier work. These experiments considered soot emitted from buoyant turbulent diffusion flames in the long residence time regime where soot properties are relatively independent of position in the fuel-lean (overfire) region and residence time (Sivathanu and Faeth, 1990; Köylü and Faeth, 1992). Measurements included soot density, structure, gravimetric volume fraction and scattering and absorption properties in the visible wavelength range. These data were analyzed to find soot dimensionless extinction coefficients, fractal dimensions and refractive index properties based on RDG-PFA scattering theory. RDG-PFA theory was successfully evaluated and soot fractal indices were independent of fuel type and in good agreement with earlier work. On the other hand, dimensionless extinction coefficients were significantly smaller (by 40%) than earlier measurements reported by Dobbins et al. (1993) and Choi et al. (1995). This last difficulty clearly raises concerns about the associated measurements of refractive index properties reported by Wu et al. (1997).

In view of these observations, the present study of soot optical properties in the visible was undertaken, considering soot emitted from buoyant turbulent diffusion flames in the long residence time regime. The approach was similar to Wu et al. (1997) where measurements of gravimetric soot volume fractions and soot extinction and scattering properties were analyzed using RDG-PFA theory to find dimensionless extinction coefficients, fractal dimensions and refractive index properties. Flame conditions included a variety of gaseous and liquid hydrocarbon fuels burning in still air. Complete measurements of extinction and scattering properties were undertaken in the visible (351.2-800.0 nm); in addition, new extinction measurements and analysis were undertaken to extend these results toward both the ultraviolet and infrared (250-5200 nm).

The present discussion of the research is brief, more details about the investigation can be found on the articles, papers, reports and theses describing aspects of the investigation that are summarized in Table 1 and are cited in the list of references. Finally, key references summarizing the present work are included in the appendices of this report, e.g., Krishnan et al. (1999a,b) in Appendices A and B, respectively.

Typical examples of these evaluations are illustrated by the measured and predicted scattering patterns of ethylene soot at wavelength of 352.2-632.8 nm appearing in Fig. 2, see Köylü and Faeth (1994a), Wu et al. (1997) and Krishnan et al. (1999a) for other examples. The agreement between measurements and predictions is seen to be excellent. There is no deterioration of performance at small wavelengths where large x_p create concerns about the validity of RDG-PFA theory. Similarly, there is no deterioration of performance at large wavelengths where large values of the refractive indices also cause concerns about the validity of RDG-PFA theory. Similar performance was achieved at other conditions, implying acceptable use of RDG/PFA theory for soot at values of x_p as large as 0.46 for the rather large soot aggregates emitted from the large buoyant turbulent flames.

Depolarization Ratios. A limitation of RDG-PFA theory, noted earlier, is that it provides no estimates of depolarization ratios that are needed to accurately compute differential scattering cross sections from Eq. (8). Thus, values of ρ_v were studied by exploiting the available data in the literature from Köylü and Faeth (1994a,b), Wu et al. (1997) and Krishnan et al. (1999a,b) using Eq. (9) to find ρ_v. Available measurements of ρ_v are plotted as a function of x_p in Fig. 3. Measurements illustrated in the plot include results from Köylü and Faeth (1994a,b), Wu et al. (1997) and Krishnan et al. (1999b). Results for soot in the overfire region of buoyant turbulent diffusion flames in the long residence time regime, due to Köylü and Faeth (1994a), Wu et al. (1997), Krishnan et al. (1999b) and the present investigation, are relatively independent of fuel type and are in reasonable agreement with each other, yielding the following correlation for ρ_v:

$$\rho_v = 0.14x_p \tag{10}$$

which also is shown on the plot. The standard error of the power of x_p in Eq. (10) is 0.1, the standard error of the coefficient is 0.03, and the correlation coefficient of the fit is 0.83, which is reasonably good. In contrast, the measurements for underfire soot in laminar diffusion flames due to Köylü and Faeth (1994a) are consistently smaller (by roughly 35%) than results for the overfire soot, although the variation of ρ_v with x_p is similar. This behavior suggests that the coefficient of Eq. (10) may be a function of aggregate size because the underfire soot involved $\overline{N}$ in the range 30-80 whereas the overfire soot involved $\overline{N}$ in the range 260-552 (Krishnan et al. 1999a,b).

Refractive Index Properties. The refractive index function E(m) was found from Eqs. (1) and (2) based on present measurements of volumetric extinction and total scattering cross sections, the gravimetric measurements of soot volume fraction and the

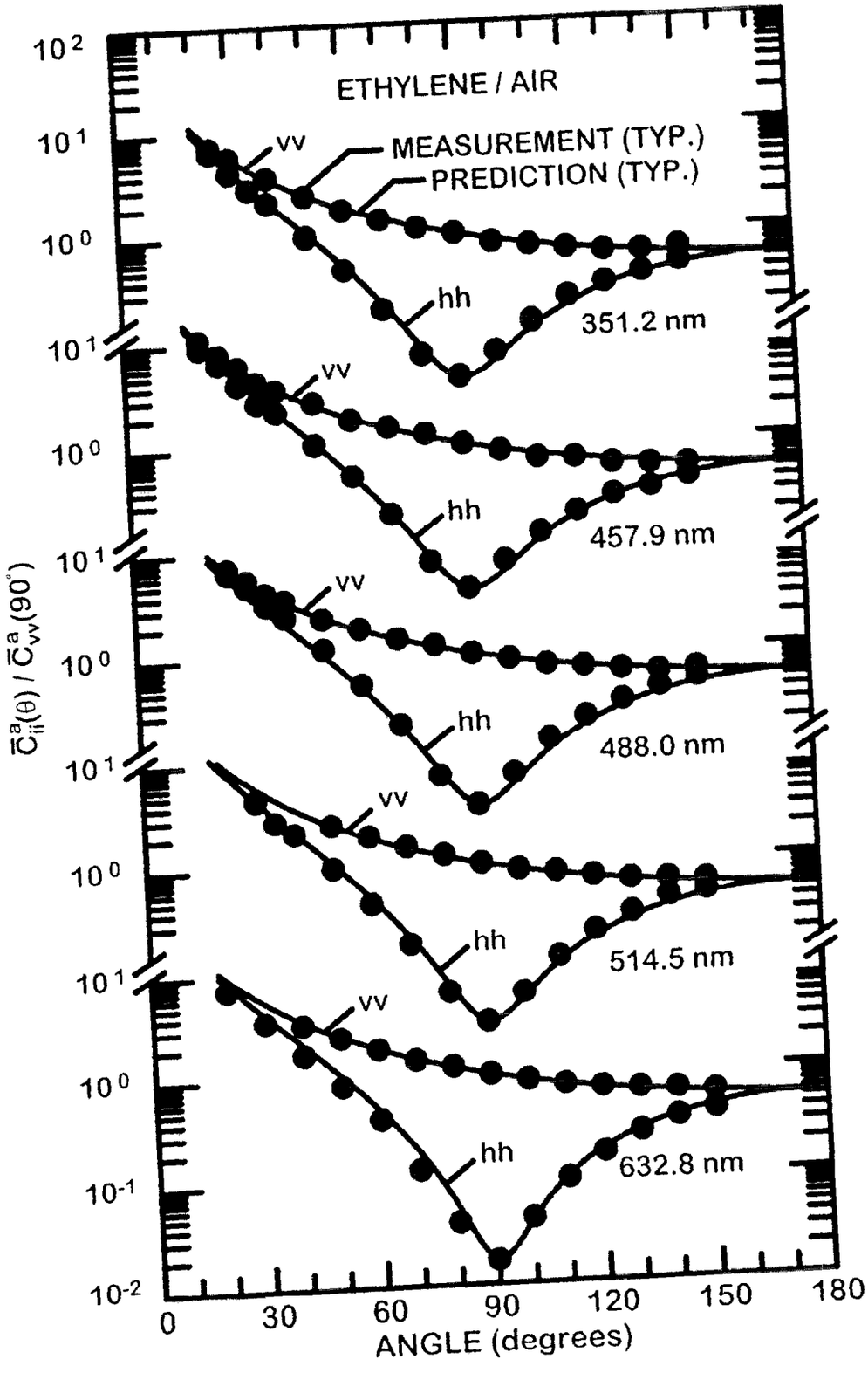

Figure 2 Measured and predicted scattering patterns for soot in the overfire region of ethylene/air flames in the visible (351.2-632.8 nm).

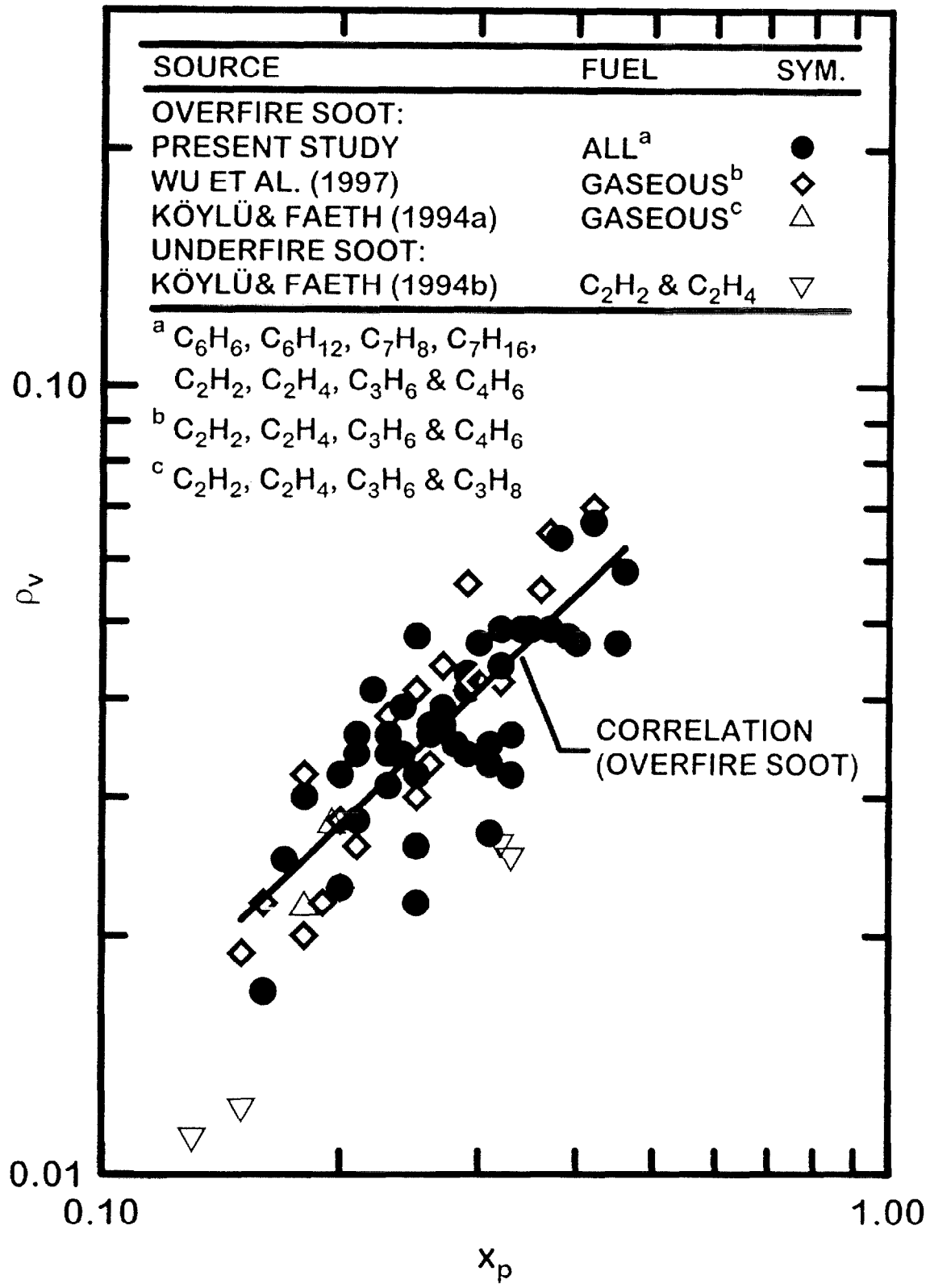

Figure 3 Measurements of depolarization ratios for various fuels as a function of primary particle size parameter in the visible (351.2-632.8 nm). Measurements of Köylü and Faeth (1994a,b), Wu et al. (1997) and the present investigation.

TEM measurements of primary particle diameters. The refractive index function F(m) was found from Eq. (3) based on present measurements of absolute vv cross sections in the large angle regime, the present gravimetric measurements of soot volume fractions, TEM measurements of primary particle diameter, present measurements of fractal dimensions, and the value of the fractal prefactor from Köylü et al. (1995) for similar soot populations. It was found that differences among E(m) and F(m) for various fuel types were comparable to experimental uncertainties; therefore, results for various fuels are averaged at each wavelength. These results are plotted in Fig. 4 and are summarized in Table 2 for the visible spectral range. Other measurements illustrated in Fig. 4 include the *ex situ* reflectometry results of Dalzell and Sarofim (1969) and Stagg and Charalampopoulos (1993) and the *in situ* measurements of Köylü and Faeth (1996) and the present study.

The present measurements of E(m) in Fig. 4 generally fall within the span of the other measurements for wavelengths greater than 400 nm. The only measurements of E(m) at shorter wavelengths are the extended results of Köylü and Faeth (1996), however, present results are thought to be more reliable because they do not involve the approximations used to extend the results of Köylü and Faeth (1996), they consider many more fuels, and they provide a reasonable explanation of the behavior of K_e at small wavelengths.

Present measurements of F(m) in Fig. 4 agree with Köylü and Faeth (1996) for wavelengths greater than 400 nm but only agree with the *ex situ* studies for the wavelength range 500-550 nm. Present results are consistent with the qualitative trends of F(m) observed by Wu et al. (1999), not plotted in Fig. 4, although the magnitudes of F(m) differ from the present results due to the problems discussed in connection with the measurements of K_e. Finally, somewhat reduced values of E(m) and F(m) for the *ex situ* measurements compared to the present *in situ* measurements, as seen in Fig. 4, are consistent with problems of correcting *ex situ* measurements for effects of surface voidage as discussed by Felski et al. (1984).

Given E(m) and F(m), the real and imaginary parts of the refractive indices of soot can be found as a function of wavelength. Similar to the other refractive index properties of soot, effects of fuel type on n and κ were comparable to experimental uncertainties. Thus, values of n and κ averaged over the present results for soot from all the fuels are plotted as a function of wavelength in Fig. 5 and are tabulated as a function of wavelength in Table 2. Several earlier measurements are also shown on the plots as discussed in connection with E(m) and F(m), e.g., the *in situ* results extended from Köylü and Faeth (1996) and the *ex situ* results from the reflectometry measurements of Dalzell

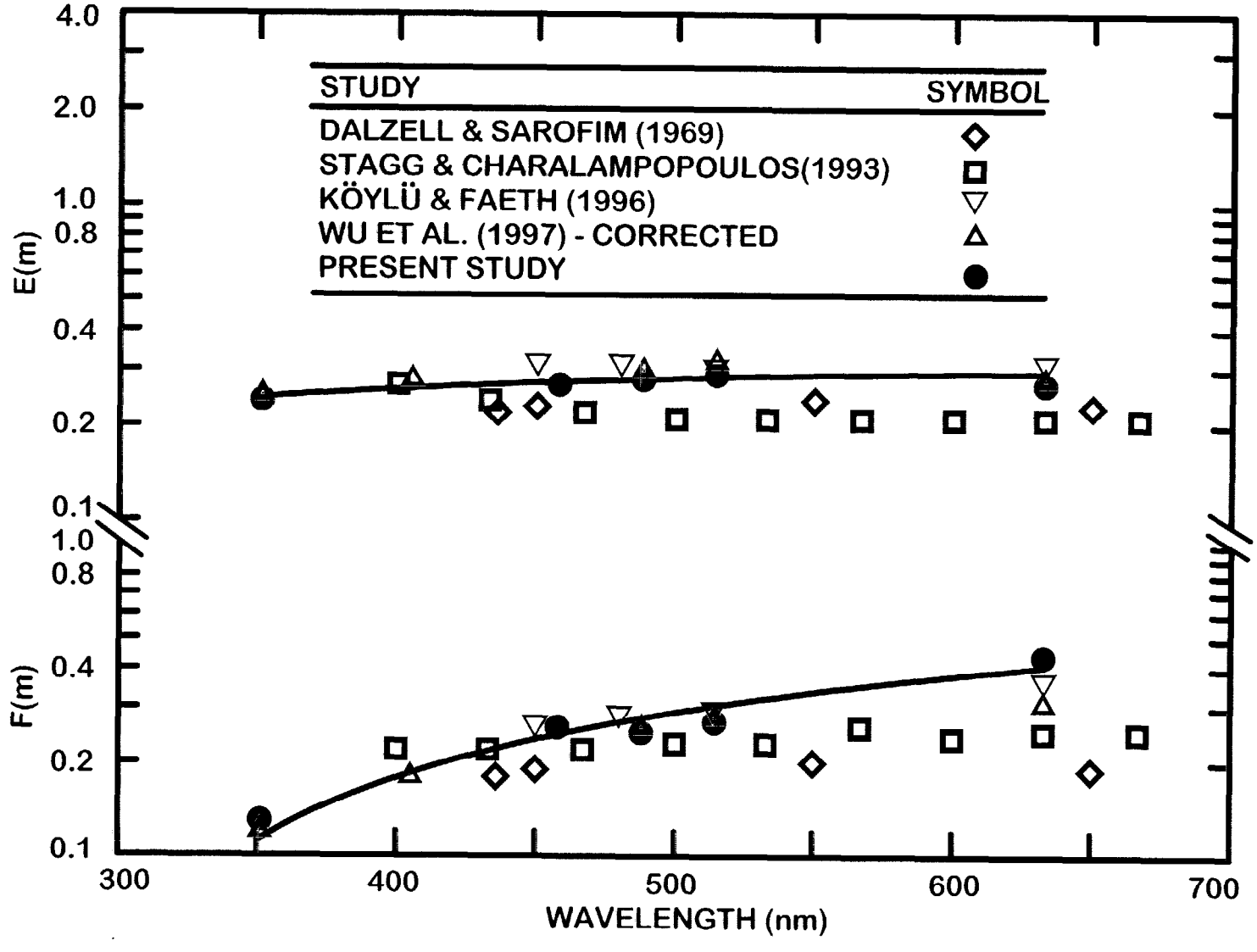

Figure 4 Measured mean values of the refractive index functions E(m) and F(m) of soot in the visible as a function of wavelength.

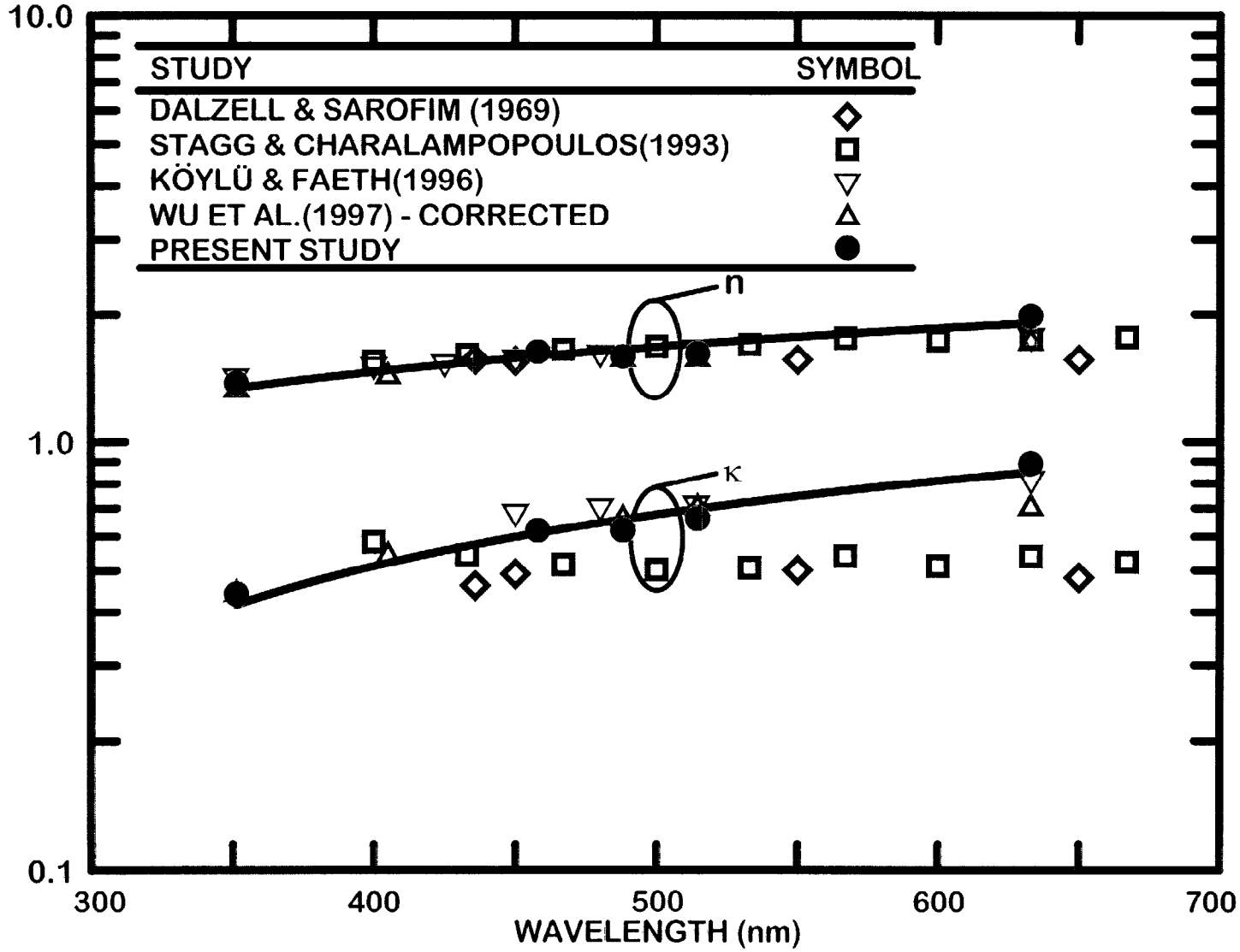

Figure 5 Measured mean real and imaginary parts of the complex refractive indices of soot in the visible as a function of wavelength.

and Sarofim (1969) and Stagg and Charalampopoulos (1993). Present values of n agree with the other measurements well within experimental uncertainties. On the other hand, present values of κ only agree with the other measurements within experimental uncertainties for wavelengths of 400-550 nm and generally increase with increasing wavelength more rapidly than the rest. This behavior follows because F(m) and κ have similar trends, as discussed earlier in connection with the results for F(m) in Fig. 4. An exception not shown on the plot, however, is a recent theoretical estimate of $\kappa = 0.8$ at 632.8 nm due to Mulholland and Mountain (1999) that is in excellent agreement with present measurements at this wavelength.

Total Scattering/Absorption Ratios. Measurements and predictions of ρ_{sa} were obtained as described by Krishnan et al. (1999b). Unfortunately all the soot structure properties needed to complete RDG-PFA predictions of ρ_{sa} were not available for butadiene and cyclohexane; therefore, results for these two fuels will not be considered in the following.

Measured and predicted values of ρ_{sa} are illustrated for wavelengths of 351.1-632.8 nm in Fig. 6. These results are for overfire soot in large buoyant turbulent diffusion flames burning n-heptane, benzene, toluene, ethylene, propylene and acetylene in still air. Measured values of ρ_{sa} are relatively large, in the range 0.1-0.9, tending to increase with increasing propensity to soot as indicated by increasing primary particle diameters. These results suggest significant effects of scattering for the conditions of the present measurements, which is expected in view of the relatively large aggregates found in the overfire region of large buoyant diffusion flames. Finally, RDG-PFA theory is in reasonably good agreement with the measurements. The various trends of ρ_{sa} seen in Fig. 6 with respect to fuel type and wavelength are consistent with RDG-PFA theory and the structure properties of the various soot types considered in the figure as discussed by Krishnan et al. (1990b).

Soot Scattering Predictions. Given the RDG-PFA scattering and refractive index properties of the present overfire soot aggregates, it is of interest to estimate the potential importance of scattering from such soot in flame environments. This was done by finding ρ_{sa} for the six fuels where required structure properties were known as discussed by Krishnan et al. (1999b). The results of these computations are illustrated in Fig. 7.

The results shown in Fig. 7 indicate maximum values of ρ_{sa} for wavelengths of 450-600 nm, with n-heptane soot reaching a maximum before the rest because these soot

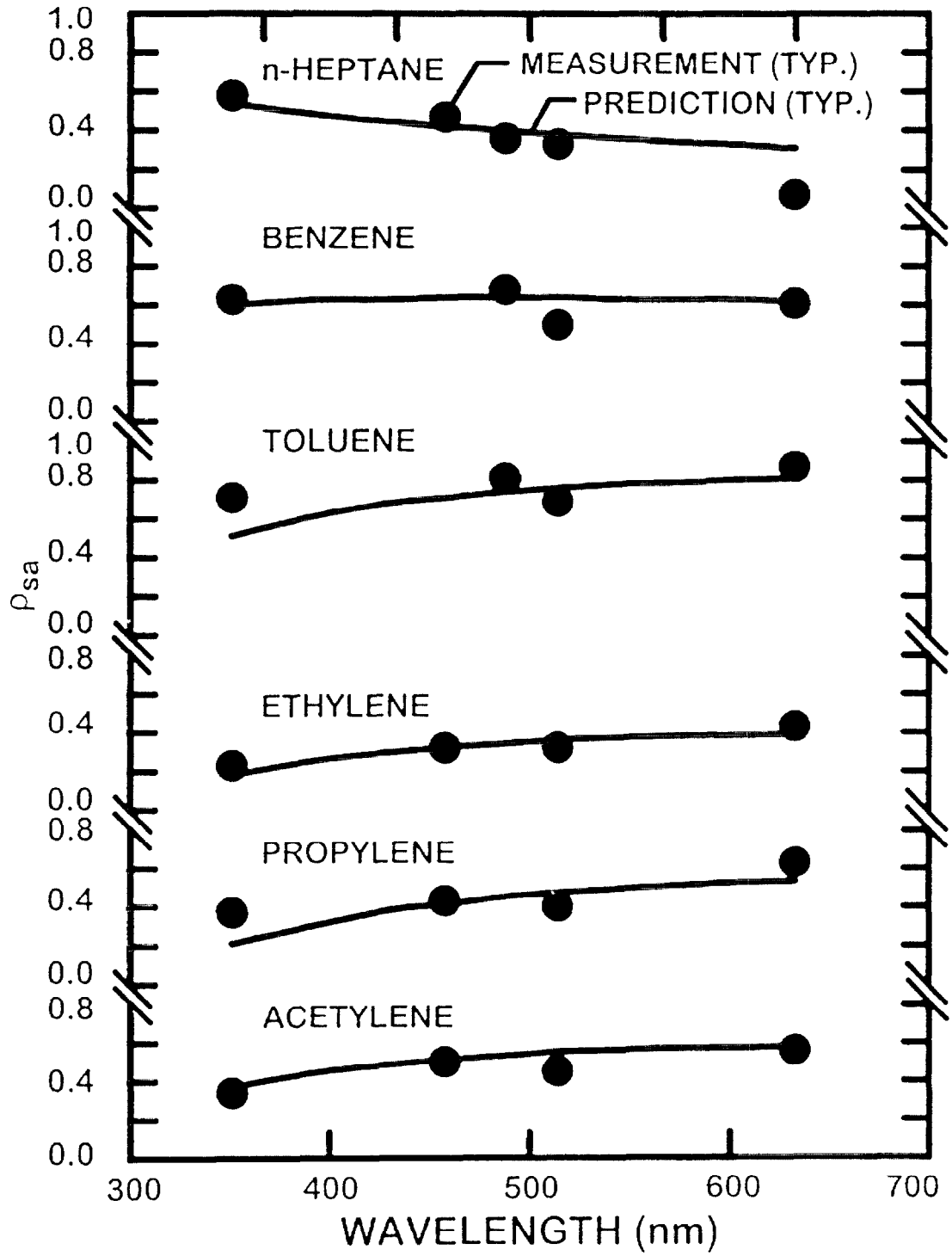

Figure 6 Measured and predicted total scattering/absorption cross section ratios for various fuels as a function of wavelength in the visible (351.2-632.8 nm).

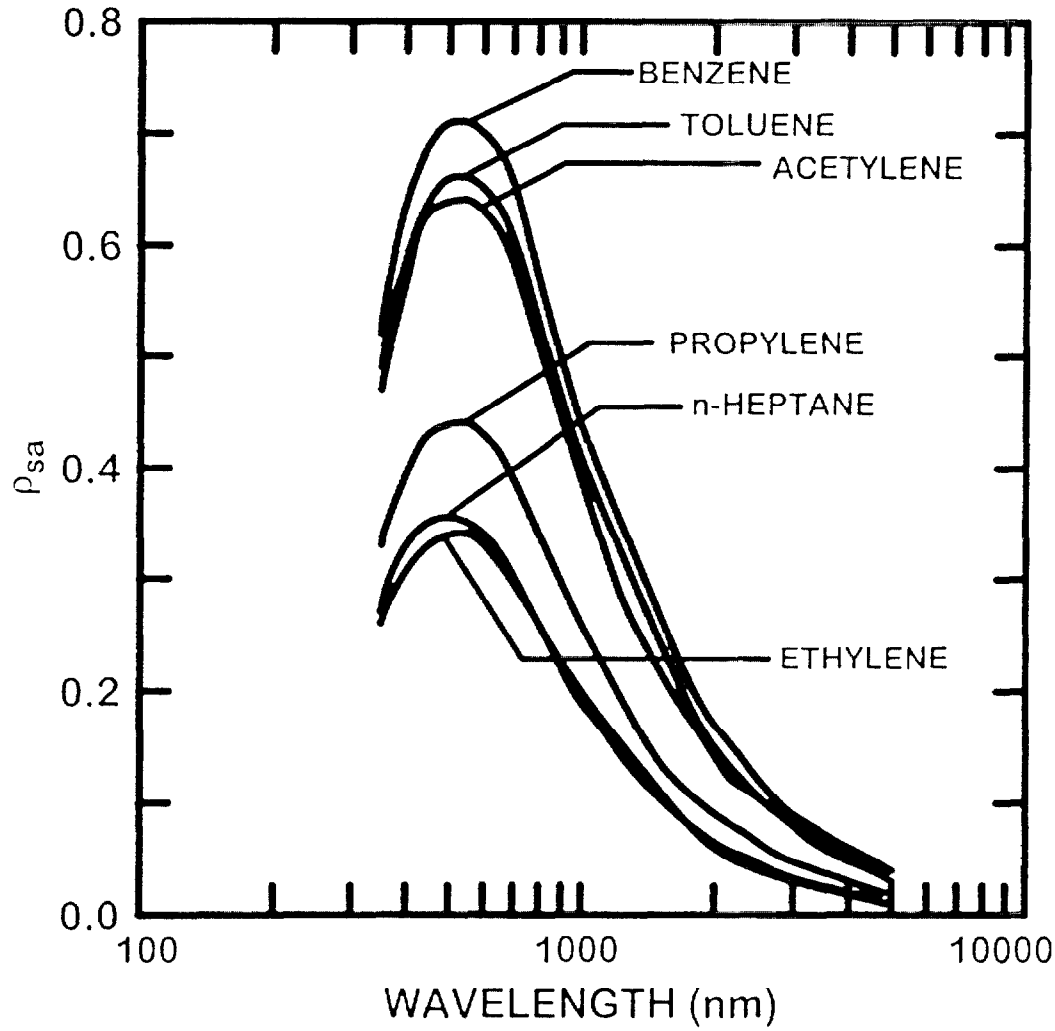

Figure 7 Estimates of total scattering/absorption cross section ratios for various fuels as a function of wavelength for wavelengths of 300-5200 nm.

aggregates have small primary particle diameters. Nevertheless, relatively large values of ρ_{sa} are maintained well into the infrared, particularly for the very large soot aggregates resulting from the combustion of benzene, toluene and acetylene, where scattering is still roughly 20% of absorption at wavelengths approaching 2000 nm. This behavior suggests that scattering should be considered for accurate estimates of continuum radiation from soot in flame environments, at least for large soot aggregates similar to those considered during the present investigation and representative of natural fires.

5. Conclusions

In situ observations of soot optical properties were undertaken for wavelengths of 250-2500 nm considering soot emitted from buoyant turbulent diffusion flames in the long residence time regime where the properties of soot in the overfire region are independent of position and characteristic flame residence time. Soot was observed for a variety of gas and liquid hydrocarbon fuels (acetylene, ethylene, propylene, butadiene, benzene, cyclohexane, toluene and n-heptane) burning in still air. Data analysis was based on RDG-PFA scattering theory for soot, which was evaluated successfully for primary particle size parameters as large as 0.46 at a wavelength of 351.2 nm and real and imaginary parts of the complex refractive index of soot that reached values of 1.99 and 0.89 at a wavelength of 632.8 nm. Major conclusions of the study are as follows:

1. Measured scattering patterns and ratios of total scattering/absorption cross sections in the visible were in good agreement with the predictions of RDG-PFA theory.

2. Measured depolarization ratios yielded a simple correlation in terms of the primary particle size parameter alone which completes the methodology needed to estimate soot scattering properties using RDG-PFA theory. Effects of aggregate size on this correlation were observed, however, and merit further study in the future.

3. Present dimensionless extinction coefficients were relatively independent of fuel type, increasing rapidly with increasing wavelength in the near ultraviolet but becoming relatively independent of wavelength over the range 400-5200 nm. Present measurements were in good agreement with earlier measurements for similar soot populations due to Dobbins et al. (1994), Choi et al. (1995), Mulholland and Choi (1998) and Zhou et al. (1998).

4. Present *in situ* measurements of the ratios of the scattering/absorption refractive index function, F(m)/E(m), were independent of fuel type and were in good agreement with earlier *ex situ* measurements in the literature. Present *in situ* measurements of the refractive index function for absorption, E(m), were also independent of fuel type and were in good agreement with earlier *in situ* measurements but were somewhat larger than earlier *ex situ* reflectometry measurements in the infrared.

5. Present soot refractive indices did not exhibit an approach to a resonance condition in the near uv that is observed for graphite; instead, present refractive indices declined continuously with decreasing wavelength as the near uv was approached, similar to the findings of Vaglieco et al. (1990) for amorphous carbon and soot.

6. Ratios of total scattering/absorption cross sections, ρ_{sa} were relatively large in the visible and near infrared (reaching maximum values as large as 0.9) suggesting potential for greater effects of scattering from soot particles on the properties of flame radiation than previously thought.

Extending these conditions to other types of soot should be approached with caution. In particular, the present soot has been exposed to oxidation in flame environments and involves relatively large soot aggregates due to large characteristic flame residence times; thus, such soot may not be representative of unoxidized and weakly aggregated soot typical of fuel-rich soot growth regions.

References

Batten, C.E., 1985, "Spectral Optical Constants of Soots from Polarized Angular Reflectance Measurements," *Appl. Optics* , Vol. 24, pp. 1193-1199.

Chang, H.Y., and Charalampopoulos, T. T., 1990, "Determination of the Wavelength Dependence of Refractive Indices of Flame Soot," *Proc. R. Soc. London A*, Vol. 430, pp. 577-591.

Charalampopoulis, T.T., 1992, "Morphology and Dynamics of Agglomerated Particulates in Combustion Systems Using Light Scattering Techniques," *Prog. Energy Combust. Sci.*, Vol. 18, pp. 13-45.

Choi, M.Y., Mulholland, G.W., Hamins, A., and Kashiwagi, T., 1995, "Comparisons of the Soot Volume Fraction Using Gravimetric and Light Extinction Techniques," *Combust. Flame*, Vol. 102, pp. 161-169.

Colbeck, I., Adkinson, B., and Johar, Y., 1997, "The Morphology and Optical Properties of Soot Produced by Diferent Fuels," *J. Aerosol Sci.*, Vol. 28, pp. 715-723.

Dalzell, W.H., and Sarofim, A.F., 1969, "Optical Constants of Soot and Their Application to Heat Flux Calculations," *J. Heat Trans.*, Vol. 91, pp. 100-104.

Dobbins, R.A., and Megaridis, C.M., 1991, "Absorption and Scattering of Light by Polydisperse Aggregates," *Appl. Optics*, Vol. 30, pp. 4747-4754.

Dobbins, R.A., Mulholland, G.W., and Bryner, N.P., 1994. "Comparison of a Fractal Smoke Optics Model with Light Extinction Measurements," *Atmospheric Environment*, Vol. 28, pp. 889-897.

Dyer, T.M., 1979, "Rayleigh Scattering Measurements of Time-Resolved Concentration in a Turbulent Propane Jet," *AIAA J.*, Vol. 17, pp. 912-914.

Faeth, G. M., and Köylü, Ü.Ö., 1995, "Soot Morphology and Optical Properties in Nonpremixed Turbulent Flame Environments," *Combust. Sci. Tech.*, Vol. 108, pp. 207-229.

Felske, J.D., Charalampopoulos, T.T., and Hura, H., 1984, "Determination of the Refractive Indices of Soot Particles from the Reflectivities of Compressed Soot Pellets," *Combust. Sci. Tech.*, Vol. 37, pp. 263-284.

Jullien, R., and Botet, R., 1987, *Aggregation and Fractal Aggregates*, World Scientific Publishing Co., Singapore, pp. 45-60.

Köylü, Ü.Ö., 1992, "Emission, Structure and Optical Properties of Overfire Soot in Buoyant Turbulent Diffusion Flames," Ph.D. Thesis, The University of Michigan, Ann Arbor, Michigan.

Köylü, Ü.Ö., and Faeth, G.M., 1992, "Structure of Overfire Soot in Buoyant Turbulent Diffusion Flames at Long Residence Times," *Combust. Flame*, Vol.89, pp. 140-156.

Köylü, Ü.Ö., and Faeth, G.M., 1993, "Radiative Properties of Flame-Generated Soot," *J. Heat Trans.*, Vol. 111, pp. 409-417.

Köylü, Ü.Ö., and Faeth, G.M., 1994a, "Optical Properties of Overfire Soot in Buoyant Turbulent Diffusion Flames at Long Residence Times," *J. Heat Trans.*, Vol. 116, pp. 152-159.

Köylü, Ü.Ö., and Faeth, G.M., 1994b, "Optical Properties of Soot in Buoyant Laminar Diffusion Flames," *J. Heat Trans.*, Vol. 116, pp. 971-979.

Köylü, Ü.Ö., and Faeth, G.M., 1996, "Spectral Extinction Coefficients of Soot Aggregates from Turbulent Diffusion Flames," *J. Heat Trans.*, Vol. 118, pp. 415-421.

Köylü, Ü.Ö., Faeth, G.M., Farias, T.L., and Carvalho, M.G., 1995, "Fractal and Projected Structure Properties of Soot Aggregates," *Combust. Flame*, Vol. 100, pp. 621-633.

Krishnan, S.S., Lin, K.-C., and Faeth, G.M., 1999a, "Optical Properties in the Visible of Overfire Soot in Large Buoyant Turbulent Diffusion Flames," *J. Heat Trans.*, in press.

Krishnan, S.S., Lin, K.-C., and Faeth, G.M., 1999b, "Extinction and Scattering Properties of Soot Emitted from Large Buoyant Turbulent Diffusion Flames," *J. Heat Trans.*, in preparation.

Lee, S.C., and Tien, C.L., 1980, "Optical Constants of Soot in Hydrocarbon Flames," *Eighteenth Symposium (International) on Combustion,* The Combustion Institute, Pittsburgh, pp. 1159-1166.

Manickavasagam, S., and Mengüc, M.P., 1993, "Effective Optical Properties of Coal/Char Particles Determined from FT-IR Spectroscopy Experiments," *Energy and Fuel*, Vol.7, pp.860-869.

Mulholland, G. W., and Choi, M. Y., 1998, "Measurement of the Mass Specific Extinction Coefficient for Acetylene and Ethane Using the Large Agglomerate Optics Facility," *Twenty-Seventh Symposium (International) on Combustion*, The Combustion Insitute, Pittsburgh, PA, pp. 1515-1522.

Mulholland, G. W., and Mountain, R.D., 1999, "Coupled Dipole Calculations of Extinction Coefficient and Polarization Ratio for Smoke Agglomerates," *Combust. Flame*, Vol. 119, pp. 56-68.

Rosner, D.E., Mackowski, D.W., and Garcia-Ybarra, P., 1991, "Size- and Structure-Insensitivity of the Thermophoretic Transport of Aggregated 'Soot' Particles in Gases," *Combust. Sci. Tech.*, Vol. 80, pp. 87-101.

Rudder, R.R., and Bach, D. R., 1968, "Rayleigh Scattering of Ruby-Laser Light by Neutral Gases," *J. Opt. Soc. Amer.*, Vol. 58, pp. 1260-1266.

Sivathanu, Y.R., and Faeth, G.M., 1990, "Soot Volume Fractions in the Overfire Region of Turbulent Diffusion Flames," *Combust. Flame*, Vol. 81, pp. 133-149.

Stagg, B.J., and Charalampopoulos, T.T., 1993, "Refractive Indices of Pyrolytic Graphite, Amorphous Carbon, and Flame Soot in the Temperature Range 25 to 600°C.," *Combust. Flame*, Vol. 94, pp. 381-396.

Tien, C. L., and Lee, S. C., 1982, "Flame Radiation," *Prog. Energy Combust. Sci.*, Vol. 8, pp. 41-59.

Vaglieco, B.M., Beretta, F., and D'Alessio, A., 1990, "In Situ Evaluation of the Soot Refractive Index in the UV-Visible from the Measurements of Scattering and Extinction Coefficients in Rich Flames," *Combust. Flame,* Vol. 79, pp. 259-271.

Viskanta, R., and Mengüc, M.P., 1987, "Radiation Heat Transfer in Combustion Systems," *Prog. Energy Combust. Sci.*, Vol. 13, pp. 511-524.

Wu, J.-S., Krishnan, S.S., and Faeth, G.M., 1997, "Refractive Indices at Visible Wavelengths of Soot Emitted from Buoyant Turbulent Diffusion Flames," *J. Heat Trans.*, Vol. 119, pp. 230-237.

Zhou, Z.-O., Ahmed, T.U. and Choi, M.Y., 1998, "Measrements of Dimensionless Soot Extinction Constant Using a Gravimetric Sampling Technique," *Experimental Thermal and Fluid Science*, Vol. 18, pp. 27-32.

Appendix A: Krishnan et al. (1999a)

OPTICAL PROPERTIES IN THE VISIBLE OF OVERFIRE SOOT IN LARGE BUOYANT TURBULENT DIFFUSION FLAMES

S. S. Krishnan,[1] K.-C. Lin[2] and G. M. Faeth[3]

Department of Aerospace Engineering

The University of Michigan

Ann Arbor, Michigan 48109-2140

Abstract

Nonintrusive measurements of the optical properties of soot at visible wavelengths (351.2 - 800.0 nm) were completed for soot in the overfire region of large (2-7 kW) buoyant turbulent diffusion flames burning in still air at standard temperature and pressure, where soot properties are independent of position and characteristic flame residence time for a particular fuel. Soot from flames fueled with gaseous (acetylene, ethylene, propylene and butadiene) and liquid (benzene, cyclohexane, toluene and n-heptane) hydrocarbon fuels were studied. Scattering and extinction measurements were interpreted to find soot optical properties using Rayleigh-Debye-Gans/polydisperse-fractal-aggregate theory after establishing that this theory provided good predictions of scattering patterns over the present test range. Effects of fuel type on soot optical

[1] Graduate Student Research Assistant

[2] Research Fellow. Now with Taitec, Inc., Wright-Patterson AFB, Ohio

[3] Professor, Fellow ASME, gmfaeth@umich.edu

properties were comparable to experimental uncertainties. Dimensionless extinction coefficients were relatively independent of wavelength for wavelengths of 400-800 nm and yielded a mean value of 8.4 in good agreement with earlier measurements. Present measurements of the refractive index function for absorption, E(m), were in good agreement with earlier independent measurements of Dalzell and Sarofim (1968) and Stagg and Charalampopoulos (1993). Present values of the refractive index function for scattering, F(m), however, only agreed with these earlier measurements for wavelengths of 400-550 nm but otherwise increased with increasing wavelength more rapidly than the rest. The comparison between present and earlier measurements of the real and imaginary parts of the complex refractive index was similar to E(m) and F(m).

Nomenclature

C	=	optical cross section
d	=	burner diameter
d_p	=	primary particle diameter
D_f	=	mass fractal dimension
$E(m)$	=	refractive index function for absorption = $\mathrm{Im}((m^2-1)/(m^2+2))$
f_v	=	soot volume fraction
$F(m)$	=	refractive index function for scattering = $\lvert(m^2-1)/(m^2+2)\rvert^2$
i	=	$(-1)^{1/2}$
I	=	light intensity

k	=	wave number = $2\pi/\lambda$
k_f	=	fractal prefactor
K_e	=	dimensionless extinction coefficient
L	=	light path length
m	=	soot refractive index = $n+i\kappa$
M	=	molecular weight
n	=	real part of soot refractive index
N	=	number of primary particles per aggregate
N_g	=	geometric mean of the number of particles per aggregate
q	=	modulus of scattering vector = $2k \sin(\theta/2)$
Q	=	volumetric optical cross section
$\dot{Q}$	=	burner heat release rate
R_g	=	radius of gyration of an aggregate
t_r	=	characteristic flame residence time
x_p	=	primary particle size parameter = $\pi d_p/\lambda$
θ	=	angle of scattering from forward direction
κ	=	imaginary part of refractive index of soot
λ	=	wavelength of radiation
ρ_{sa}	=	ratio of total scattering to absorption cross sections
σ_D	=	standard deviation of D_f

σ_g = standard deviation of number of particles per aggregate from geometric mean

Subscripts

a = absorption

av = average value

e = extinction

h = horizontal polarization

ij = incident (i) and scattered (j) polarization directions

s = total scattering

v = vertical polarization

o = initial value

Superscripts

a = aggregate property

p = primary particle property

$(\bar{\ })$ = mean value over a polydisperse aggregate population

Introduction

Information about the optical properties of soot is needed to develop reliable nonintrusive (optical) measurements of soot properties and estimates of continuum radiation due to soot in flame environments. Substantial information about the optical

properties of soot is already known, as follows: soot consists of nearly monodisperse spherical primary particles that collect into mass fractal aggregates having broad size distributions, soot primary particle diameters and aggregate sizes vary widely but soot fractal properties appear to be relatively universal, soot optical properties in the visible can be approximated reasonably well by Rayleigh-Debye-Gans scattering from polydisperse mass fractal aggregates (called RDG-PFA theory), and current estimates of soot optical properties in flame environments are mainly limited by excessive uncertainties about soot refractive index properties, see Faeth and Köylü (1995) and references cited therein. Motivated by these observations, the objective of the present investigation was to measure soot optical properties at visible wavelengths, emphasizing dimensionless extinction coefficients and refractive indices.

Earlier studies of soot dimensionless extinction coefficient and refractive index properties in the visible are briefly reviewed in the following, more details can be found in Charalampopoulos (1992), Faeth and Köylü (1995), Jullien and Botet (1987), Köylü and Faeth (1993), Tien and Lee (1982), Viskanta and Mengüc (1987) and references cited therein. Some past determinations of soot refractive indices involve *ex situ* reflectivity measurements of compressed soot samples (Batten, 1985; Dalzell and Sarofim, 1969; Felske et al., 1984); these results have been questioned, however, due to potential changes of soot properties caused by sample collection and compression as well as

potential effects of surface irregularities on measured reflectance properties (Charalampopoulos, 1992; Felske et al., 1984; Tien and Lee, 1982). In order to avoid these error sources, other studies involved *in situ* measurements of extinction and scattering (Chang and Charalampopoulos, 1990; Charalampopoulos, 1992; Lee and Tien, 1980; Vaglieco et al., 1990); unfortunately, these studies have a number of deficiencies as well: soot structure generally was not characterized, Rayleigh and Mie scattering approximations were used to analyze the measurements that have not proven to be very effective for soot aggregates, questionable approximations involving either graphitic-based dispersion models or Kramers-Krönig causality relationships were adopted in some cases, and there has only been limited consideration of effects of fuel type on soot refractive index properties (Dobbins and Megaridis, 1991; Faeth and Köylü, 1995; Köylü and Faeth, 1994a, b, 1996).

A recent study of the refractive index properties of soot due to Wu et al. (1997) sought to resolve concerns about earlier work. These experiments considered soot emitted from buoyant turbulent diffusion flames in the long residence time regime where soot properties are relatively independent of position in the fuel-lean (overfire) region and residence time (Sivathanu and Faeth, 1990; Köylü and Faeth, 1992). Measurements included soot density, structure, gravimetric volume fraction and scattering and absorption properties. These data were analyzed to find soot dimensionless extinction coefficients, fractal dimensions and refractive index properties based on RDG-PFA

scattering theory. RDG-PFA theory was successfully evaluated and soot refractive indices were independent of fuel type and in good agreement with earlier work. On the other hand, dimensionless extinction coefficients were significantly smaller (by 40%) than earlier measurements reported by Dobbins et al. (1993) and Choi et al. (1995). This last difficulty clearly raises concerns about the associated measurements of refractive index properties reported by Wu et al. (1997).

In view of these observations, the present study of soot optical properties in the visible was undertaken, considering soot emitted from buoyant turbulent diffusion flames in the long residence time regime. The approach was similar to Wu et al. (1997) where measurements of gravimetric soot volume fractions and soot extinction and scattering properties were analyzed using RDG-PFA theory to find dimensionless extinction coefficients, fractal dimensions and refractive index properties. Flame conditions included a variety of gaseous and liquid hydrocarbon fuels burning in still air.

Experimental Methods

Apparatus. Present test flames were large buoyant turbulent diffusion flames burning in still air within the long residence time regime. The test flames were provided by gas and liquid-fueled burners injecting fuel gases vertically upward. Soot properties were measured by collecting the combustion products in a hood having a 152 mm diameter vertical exhaust duct. Measurements were made at the exit of the exhaust duct where properties across the flow were nearly uniform; nevertheless, soot concentrations

were measured along the optical path so that extinction measurements could be referenced to conditions at the duct axis where all other optical measurements were made. Note that using a collection system in this way does not affect soot structure and optical properties because they are universal in the overfire region for present test conditions (Köylü and Faeth, 1994a). A water-cooled burner having a diameter of 50 mm described by Sivathanu and Faeth (1990) was used for the gas-fueled flames. Uncooled burners having diameters of 51 and 102 mm were used for the liquid-fueled flames, adjusting the fuel flow rate to attain steady pool fires with the liquid surface roughly 10-20 mm below the burner exit.

Sampling Measurements. Aside from routine sampling measurements of gas temperatures and compositions at the measuring location, sampling measurements included soot structure and gravimetric volume fractions. Other soot properties of interest during the present study, e.g., soot density and composition, were drawn from Köylü and Faeth (1992, 1994a) and Wu et al. (1997) for similar soot populations.

Soot structure was found by thermophoretic sampling and analysis using transmission electron microscopy (TEM), following Köylü and Faeth (1992). Sampling was carried by inserting TEM grids into the flow at the exhaust duct axis. Sampling times were selected to achieve less than 10% coverage of the grid surface with soot in order to avoid overlapping aggregates on the grid. Effects of aggregate size on sampling bias were less than 20% from estimates based on Rosner et al. (1991). Samples of 400

primary particles selected from more than 50 aggregates were used to find the mean value of d_p with an experimental uncertainty less than 2% (95 % confidence).

Gravimetric volume fractions were measured following Wu et al. (1997). This involved sampling the flow and measuring the volumes of soot and gas collected. The sampling probe was aligned with the exhaust duct axis and had a 13 mm diameter inlet connected to a 47 mm diameter Gelman filter. The filter was connected to a vacuum pump through a flowmeter and valve. The flowmeter was fitted with a manometer and calibrated over the required range of inlet pressures and flow rates using a wet test meter. Soot samples were collected for a timed period using two filters, one in the filter holder and the second to mechanically collect soot from the sample line and filter holder. The mass of soot was found by weighing the filters before and after sampling using an electronic balance. Given these measurements, the soot volume fraction could be computed from the known soot density. Sample times were lengthy and several samples along the optical path and repeat samples were required; therefore, a laser extinction system was used across the sampling duct exit to insure that flame conditions were accurately repeated. In addition, gravimetric soot volume fractions were measured at more locations along the optical path than before. These two changes from the approach used by Wu et al. (1997) are felt to be mainly responsible for better agreement between present and past measurements of the dimensionless extinction coefficients of soot than before.

Optical Measurements. Soot scattering and extinction properties were measured following Köylü and Faeth (1994a,b). Light sources used for measurements at various wavelengths were as follows: 351.2, 457.9, 488.0 and 514.5 nm using an argon-ion laser (4W, Coherent Innova 90-4); 632.8 nm using a He-Ne laser (28 mW, Melles Griot MG53036); 405.0 nm using a mercury lamp (100W, Oriel 6333); and 800.0 nm (for extinction measurements only) using a laser diode (700 mW, SDL-2360-P3). The incident beams were passed through a polarization rotator and mechanical chopper and then focused at the axis of the exhaust duct. The collecting optics for scattering measurements were mounted on a turntable so that scattering angles of 5-160 deg could be considered. The collecting optics had a collection angle of 0.7 msr, dichroic sheet polarizer filters (1 and 10 nm bandwidths for laser and lamp sources, respectively), neutral density filters and a photodetector. The extinction measurements employed similar but rigidly-mounted collection optics, designed following Manickavasagam and Mengüc (1993) to reduce contributions of forward scattering to less than 1 %. An optical system housing and darkroom conditions in the laboratory minimized optical noise due to ambient lighting.

Rayleigh scattering from propane gas was used to provide an absolute calibration of the scattering measurements. Absolute differential scattering cross sections of soot were found from ratios of the detector signal for soot and propane, based on the Rayleigh scattering properties of propane from Rudder and Bach (1968) and Dyer (1979). Total

volumetric scattering cross sections were found by integrating volumetric differential scattering cross sections over the spherical surface while extrapolating to find contributions in the near forward and backward scattering directions as discussed by Wu et al. (1997); the corrections of the total volumetric scattering cross sections due to these extrapolations did not exceed 25%.

Theoretical Methods

Dimensionless extinction coefficients. The dimensionless extinction coefficient is a useful optical property that provides a simple relationship between extinction and soot volume fractions (Dobbins et al., 1993; Choi et al., 1995). This parameter was found for present test conditions based on Dobbins et al. (1993), as follows:

$$K_e = -\lambda \ln (I/I_o)/(Lf_v) \qquad (1)$$

Values of f_v were nearly constant (varying 14 to 20%) over the present optical path; nevertheless, an appropriate average value was used in Eq. (1) based on several gravimetric measurements of f_v along the path. Experimental uncertainties of K_e (95% confidence) varied between 14% (acetylene at 351.2 nm) and 24% (n-heptane at 800 nm), dominated by uncertainties in the soot volume fraction determinations along the optical path.

Refractive Index Properties. Measurements of refractive index properties were based on RDG-PFA theory, adopting the approach of Wu et al. (1997); therefore, only

results from RDG-PFA theory specifically used during the present study are discussed in the following. The main assumptions of RDG-PFA theory are as follows: individual primary particles satisfy the Rayleigh scattering approximation, soot aggregates satisfy the Rayleigh-Debye-Gans (RDG) scattering approximation, primary particles are spherical and monodisperse, primary particles just touch one another, the number of primary particles per aggregate satisfies a log-normal probability distribution function, and the aggregates are mass fractal-like objects that satisfy the following relationship (Jullien and Botet, 1987):

$$N = k_f (R_g/d_p)^{D_f}. \tag{2}$$

These approximations have proven to be satisfactory during past evaluations for soot at a variety of conditions (Köylü and Faeth, 1992, 1994a, b, 1996); they were also evaluated by comparing predicted and measured scattering patterns during the present investigation, as discussed later.

Values of the measured volumetric vv scattering cross section, $\overline{Q}_{vv}^{a}(qd_p)$, satisfied power-law behavior at large angles, similar to results illustrated for soot emitted from gas fueled flames by Wu et al. (1997). Thus, values of the fractal dimension, D_f, needed to find the refractive index function for scattering, F(m), were found based on the results of RDG-PFA theory in the large-angle regime, as follows:

$$D_f = -d\ln(\overline{Q}_{vv}^{a}(qd_p))/d\ln(qd_p) \tag{3}$$

where all parameters on the right-hand-side (RHS) of Eq. (3) are known from the measurements. Experimental uncertainties (95% confidence) of the D_f measurements are less than 5%.

Values of the refractive index function for absorption, E(m), were found from RDG-PFA theory, as follows:

$$E(m) = \lambda(\overline{Q}_e^a - \overline{Q}_s^a)/(6\pi f_v) \tag{4}$$

where $\overline{Q}_e^a$ and $\overline{Q}_s^a$ are the measured volumetric extinction and total scattering cross sections while f_v is the gravimetrically measured soot volume fraction. Experimental uncertainties (95% confidence) of E(m) varied between 14% (acetylene at 351.2 nm) and 24% (n-heptane at 632.8 nm). Corresponding values of the refractive index function for scattering, F(m), were found from RDG-PFA theory in the large-angle regime, as follows:

$$F(m) = 2\lambda^4 (qd_p)^{D_f} \overline{Q}_{vv}^a (qd_p)/(3\pi^3 d_p^3 k_f f_v) \tag{5}$$

where all parameters on the RHS of this equation are either known or measured after adopting $k_f = 8.5$ based on the measurements of Köylü et al. (1995) for soot similar to the present measurements, e.g., soot emitted from large buoyant turbulent-diffusion flames in the long residence time regime and fueled with acetylene, propylene, ethylene and propane. The experimental uncertainties (95 percent confidence) of F(m) varied between 19% (acetylene at 351.2 nm) and 26% (n-heptane at 632.8 nm). Finally, given values of E(m) and F(m), their definitions provide two equations to solve for the real and

imaginary parts of the soot refractive index, $m = n+i\kappa$; the experimental uncertainties of n and κ are comparable to $E(m)$ and $F(m)$, respectively.

Results and Discussion

Test Conditions. Present test conditions are summarized in Table 1. The flames involved both gaseous (acetylene, ethylene, propylene, butadiene) and liquid (benzene, cyclohexane, toluene, n-heptane) hydrocarbon fuels burning in still air from burners having diameters of 50-102 mm with heat release rates of 2-7 kW. Characteristic residence times were computed using the correlation of Sivathanu and Faeth (1990) finding values of 254-333 ms which places present flames in the long residence time regime (Köylü and Faeth, 1992). Present measurements were confined to the fuel-lean overfire region of the flames.

Soot structure properties for present test conditions are summarized in Table 2. Primary particle diameters are in the range 32-51 nm, with standard deviations of 17-21 percent of mean values and were reasonably monodisperse as concluded by Köylü and Faeth (1992) for similar conditions. For the present ranges of primary particle diameters and wavelengths, values of the primary particle size parameters, $x_p = 2\pi d_p/\lambda$, were in the range 0.16-0.46, with the maximum value being the largest yet considered for evaluating RDG-PFA predictions of soot optical properties. The mean numbers of primary particles per aggregate were known for soot from a number of the fuels from Köylü (1992) and Köylü and Faeth (1994a) and these values are summarized in the table. The values of d_p

and $\overline{N}$ yield typical aggregate dimensions of 1000-10,000 nm which is larger than the visible wavelength range and provides significant potential for scattering (Faeth and Köylü, 1995). Values of the fractal dimensions were measured as described in connection with Eq. (3) and were found to be properly independent of wavelength for a given fuel within experimental uncertainties; therefore, mean values of D_f for each fuel are summarized in the table. It is evident that effects of fuel type are also small, yielding a mean value of $D_f = 1.79$ with a standard deviation of 0.05 when averaged over all wavelengths and fuels.

Dimensionless Extinction Coefficients. Present measurements of dimensionless extinction coefficients are plotted as a function of fuel type (fuel molecular weight) and wavelength in Fig. 1. The mean value of present measurements averaged over all fuels and wavelengths is 8.4 with a standard deviation of 1.5. In addition, the mean value averaged over all fuels at each wavelength is shown as a dashed line on the plots for reference purposes. These average values of K_e at each wavelength considered during the present measurements are summarized in Table 3. There is a tendency for overfire soot from acetylene and n-heptane to yield dimensionless extinction coefficients near uncertainty limits that are smaller and larger than the rest, respectively. It is felt, however, that these differences may be due to experimental difficulties. In particular, acetylene soot involved the presence of a tarry residue not seen for soot from the other fuels which could cause overestimation of the soot volume fraction while n-heptane

measurements involved small soot concentrations and signal-to-noise ratios of extinction measurements. Thus, in view of the rather similar values of dimensionless extinction coefficients of the other six fuels, it is concluded that effects of soot type on this parameter are small. Similar small effects of fuel type were also observed by the soot refractive inex properties considered during the present investigation as will be discussed subsequently. Notably, Sivathanu et al. (1993) find similar relatively small effects of fuel type on the specific absorption coefficients of soot in premixed flames fueled with methane, propane and ethylene.

Values of the dimensionless extinction coefficient, averaged over all the fuels at each wavelength, are plotted as a function of wavelength in Fig. 2. Other measurements of K_e for soot formed from the combustion of crude oil from Dobbins et al. (1993) and from the combustion of acetylene from Choi et al. (1995) are also shown on the plot for comparison with the present measurements. Clearly, the results of all three studies are in excellent agreement. In addition, the results of Choi et al. (1995) tend to support the idea that present results for acetylene were affected by the tarry residue. Taken together, these results suggest remarkably little variation of K_e for wavelengths of 400-800 nm. In contrast, the earlier measurements of Wu et al. (1997) for soot emitted from acetylene-, propylene-, ethylene- and propane-fueled flames in the long residence time regime yielded a smaller value of K_e = 5.1 with a standard deviation of 0.5, although their observations of small effects of fuel type and wavelength were similar to the present

study. Repeated testing could not confirm the findings of Wu et al. (1997) during the present study, however, and their observations will not be considered any further in the following.

It is interesting that K_e is relatively independent of wavelength in the visible in spite of the strong variation of absorption and scattering cross sections for the RDG scattering approximation. For example, $Q_a^p \sim 1/\lambda$ and $Q_s^p \sim Q_{vv}^p \sim 1/\lambda^4$ for primary particles under the RDG scattering approximation. Scattering from aggregates of primary particles under RDG-PFA theory exhibits a reduced sensitivity to changes of wavelength; nevertheless, the general trend toward decreasing optical cross sections with increasing wavelength when refractive indices remain constant is similar. Thus, the relatively small variation of K_e with wavelength for the present test range requires compensating variations of the refractive index functions, E(m) and F(m). Results to be considered subsequently will show that this is the case.

Scattering Patterns. The RDG-PFA scattering theory was evaluated for soot resulting from combustion of each fuel at each wavelength in order to justify the present approach to find soot refractive index properties nonintrusively. Typical examples of this evaluation can be seen from the scattering patterns illustrated in Fig. 3. The results shown in this illustration represent the limiting scattering conditions for the present experiments: toluene at a wavelength of 351.2 nm which represents the largest value of x_p and thus potentially most questionable condition for the use of the evaluation; and ethylene at a

wavelength of 632.8 nm which represents the smallest value of x_p and thus potentially the least questionable conditions for the use of the RDG scattering approximation but still a concern because soot refractive indices tend to increase with increasing wavelength which could lead to failure of the RDG scattering approximation (Wu et al., 1997). The agreement between measurements and predictions is seen to be excellent at both limits, justifying the use of RDG scattering theory to find refractive index properties for present conditions. Furthermore, plots of vv cross sections as functions of the modulus of the scattering vector (see Wu et al. (1997) for typical examples) and the invariance of fractal dimensions with wavelength discussed earlier, all show that present scattering measurements properly reached the large-angle (power-law) regime required to use Eqs. (3) and (5) in order to find refractive index properties.

The refractive index function E(m) was found from Eq. (4) based on present measurements of volumetric extinction and total scattering cross sections, and the gravimetric measurements of soot volume fraction. The resulting values of E(m) are plotted as a function of fuel type (fuel molecular weight) and wavelength in Fig. 4. Mean values of E(m), averaged over all the fuels, are shown on the plots for each wavelength; these average values of E(m) are also summarized in Table 3. Effects of fuel type for E(m) are qualitatively similar to those for the related property K_e with values for acetylene and n-heptane departing from the mean values to a somewhat larger degree than the rest (joined by ethylene for E(m) to a greater degree than for K_e). Nevertheless,

effects of fuel type on these plots are within experimental uncertainties and it is concluded that E(m) is independent of fuel type over the present test range.

The refractive index function, F(m), was found from Eq. (5), based on present measurements of absolute vv cross sections in the large angle regime, present gravimetric measurements of soot volume fraction, TEM measurements of primary particle diameter, present measurements of the fractal dimensions, and values of the fractal prefactor from Köylü et al. (1995). The resulting values of F(m) are plotted as a function of fuel type (fuel molecular weight) and wavelength in Fig. 5. Mean values, averaged over all the fuels, are also shown on the plots for each wavelength; these average values of F(m) are also summarized in Table 3. In this case, values for acetylene continued to be smaller than the rest which may be attributable to the tarry residue observed for this soot, discussed in connection with the dimensionless extinction coefficient measurements. Scatter of the measurements of F(m) also progressively increase with increasing wavelength due to progressively increasing difficulties in maintaining adequate signal-to-noise ratios for the Rayleigh scattering measurements from propane gas used to provide an absolute calibration of the soot scattering measurements. Thus, effects of fuel type on these plots do not exhibit any consistent trends and are comparable to experimental uncertainties and it is concluded that F(m) is independent of fuel type over the test range, similar to E(m).

Present mean values of E(m) and F(m), averaged over all fuels types, are plotted as a function of wavelength in the visible in Fig. 6. Present results were used in conjunction with the earlier laser extinction measurements of Köylü and Faeth (1996) in order to obtain another nonintrusive estimate of E(m) and F(m). This was done by matching the values of E(m) for the two data sets of 514.5 nm and then using present measurements of ρ_{sa} to compute values of E(m) from the extinction measurements of Köylü and Faeth (1996) in the visible. Then values of F(m) were obtained from these estimates of E(m) using a general correlation for the ratio F(m)/E(m) developed from present measurements which is summarized in Table 4. These calculations were completed for acetylene, propylene and ethylene soot which were the only fuels considered during both studies; notably, Köylü and Faeth (1996) did not observe significant effects of fuel type during their investigation. The agreement between values of E(m) and F(m) from the present investigation and those extended from Köylü and Faeth (1996) is excellent for wavelengths greater than 400 nm but present results are somewhat smaller than the extended results as the near uv is approached. The present values of E(m) and F(m) progressively increase with increasing wavelength in the near uv similar to the observations of Vaglieco et al. (1990), and do not suggest an approach to a resonance condition for soot which would cause E(m) and F(m) to peak in this region, similar to the behavior of graphite, see Chang and Charalampopoulos (1990) and Lee and Tien (1980). Increasing E(m) and F(m) with increasing wavelength over the present test

range is not unexpected, however, because this behavior is needed to explain why K_e is relatively independent of wavelength in the visible for soot aggregates that satisfy RDG-PFA scattering behavior.

Several earlier measurements of E(m) and F(m) are illustrated in Fig. 6. These measurements include the classical *ex situ* reflectometry measurements for soot in the fuel-lean region of acetylene and propane/air diffusion flames (taken as the average for the two fuels) due to Dalzell and Sarofim (1969) and the more recent *ex situ* reflectometry measurements for soot in premixed propane/air flames due to Stagg and Charalampopoulos (1993). Other *ex situ* reflectometry measurements for soot in the fuel-lean regions of acetylene and propane/air diffusion flames due to Batten (1985) have been omitted from the plot because they yield values of E(m) and F(m) roughly half the values of the rest and these results have not been subsequently duplicated. Finally, earlier well known *in situ* measurements of soot refractive index properties in the visible due to Lee and Tien (1980), Chang and Charalampopoulos (1990) and Vaglieco et al. (1990) have not been included on the plots due to the difficulties with these measurements mentioned earlier, e.g., they all involve questionable models for the optical properties of soot, some involve questionable soot transport properties in cases where dynamic scattering measurements were used to estimate soot aggregate properties, and some involve questionable approximations associated with either graphitic-based dispersion

models or Kramers-Kronig causality relationships used to close the procedure to find soot refractive indices.

Present measurements of E(m) illustrated in Fig. 6 generally fall within the span of the other measurements, agreeing within experimental uncertainties with the other measurements for wavelengths greater than 400 nm. The only measurements of E(m) at shorter wavelengths are the extended results of Köylü and Faeth (1996) that are significantly larger than the present results at 351.2 nm, as discussed earlier. In this region, however, present results are thought to be more reliable because they do not involve the approximations used to extend the results of Köylü and Faeth (1996), they consider many more fuels, and given the behavior of the results of Köylü and Faeth (1996) at this wavelength, it would be very difficult to rationalize the behavior of K_e observed in Fig. 2 near this wavelength.

Present measurements of F(m) in Fig. 6 agree with the results extended from Köylü and Faeth (1996) for wavelengths greater than 400 nm but only agree with the *ex situ* studies for the wavelength range 400-550 nm. Overall, present measurements increase more rapidly with increasing wavelengths than the *ex situ* measurements illustrated in Fig. 6. Present results are consistent with the qualitative trends of F(m) observed by Wu et al. (1997), not plotted in Fig. 6, although the magnitudes of F(m) differ from present results due to the problems discussed in connection with the measurements of K_e. In addition, the rapid increase of F(m) with wavelength in the

visible is also consistent with values of K_e relatively independent of wavelength in the visible as discussed earlier. Finally, somewhat reduced values of E(m) and F(m) for the *ex situ* measurements compared to the present *in situ* measurements, as seen in Fig. 6, is consistent with problems of correcting the *ex situ* measurements for effects of surface voidage of the compressed soot samples used for reflectometry measurements in the visible -- a criticism of the *ex situ* measurements of soot refractive index properties that has been raised by Felske et al. (1984).

Refractive Indices. Given E(m) and F(m), the real and imaginary parts of the refractive indices of soot can be found as a function of wavelength. Similar to the other refractive index properties of soot, effects of fuel type on n and κ were comparable to experimental uncertainties. Thus, values of n and κ averaged over the present results for soot from all the fuels, are plotted as a function of wavelength in Fig. 7; these average values of n and κ are also summarized in Table 3. Several earlier measurements are also shown on the plots as discussed in connection with E(m) and F(m), e.g., the *in situ* results extended from Köylü and Faeth (1996) and the *ex situ* results from the reflectometry measurements of Dalzell and Sarofim (1969) and Stagg and Charalampopoulos (1993). Present values of n agree with the other measurements well within experimental uncertainties. On the other hand, present values of κ only agree with the other measurements within experimental uncertainties for wavelengths of 400-550 nm and generally increase with increasing wavelength more rapidly than the rest. An exception

not shown on the plot, however, is a recent theoretical estimate of $\kappa = 0.8$ at 632.8 nm made by Mulholland and Mountain (1999) based on the measurements of the specific extinction coefficients of acetylene and ethylene soot due to Mulholland and Choi (1998), combined with a coupled dipole calculation, which is in excellent agreement with present measurements at this wavelength.

Conclusions

In situ observations of soot optical properties were undertaken for wavelengths of 351.2 - 800.0 nm considering soot emitted from buoyant turbulent diffusion flames in the long residence time regime where the properties of soot in the overfire region are independent of position and characteristic flame residence time. Soot was observed for a variety of gas and liquid hydrocarbon fuels (acetylene, ethylene, propylene, butadiene, benzene, cyclohexane, toluene and n-heptane) burning in still air. Data analysis was based on RDG-PFA scattering theory for soot, which was evaluated successfully for primary particle size parameters as large as 0.46 at a wavelength of 351.2 nm and real and imaginary parts of the complex refractive index of soot that reached values of 1.99 and 0.89 at a wavelength of 632.8 nm. Major conclusions of the study are as follows:

1. Present dimensionless extinction coefficients were relatively independent of fuel type and wavelength (for wavelengths of 400-800 nm) yielding an average value of 8.4 and a standard deviation of 1.5. These results are in excellent agreement

with earlier measurements of Dobbins et al. (1993) and Choi et al. (1995) for similar overfire soot populations, resolving discrepancies between these and earlier studies and the findings of Wu et al. (1997).

2. Present values of the refractive index function for absorption, E(m), were relatively independent of fuel type and agreed within experimental uncertainties with earlier *ex situ* reflectometry measurements of Dalzell and Sarofim (1969) and Stagg and Charalampopoulos (1993) for the wavelength range where they could be compared (400-630 nm).

3. Present values of the refractive index function for scattering, F(m), were relatively independent of fuel type and agreed with the earlier *ex situ* reflectometry measurements of Dalzell and Sarofim (1969) and Stagg and Charalampopoulos (1993) for wavelengths of 400-550 nm; otherwise, present values of F(m) increased more rapidly with increasing wavelength than observed before, although such behavior is consistent with dimensionless extinction coefficients being relatively independent of wavelength over the present test range.

4. Present values of the real and imaginary parts of the refractive indices of soot were relatively independent of fuel type. Present values of real part of the refractive index of soot agreed with the *ex situ* measurements of Dalzell and Sarofim (1969) and Stagg and Charalampopoulos (1993) within experimental uncertainties; on the other hand, similar agreement for the imaginary part of the refractive index of soot

was only observed for wavelengths of 400-550 nm while otherwise increasing with increasing wavelength more rapidly than the rest. One exception to this was a recent theoretical estimate of κ at 632.8 nm due to Mulholland and Mountain (1999) which agrees with present results within experimental uncertainties.

5. Present soot refractive indices did not exhibit an approach to a resonance condition in the near uv that is observed for graphite; instead, present refractive indices declined continuously with decreasing wavelength as the near uv was approached, similar to the findings of Vaglieco et al. (1990) for amorphous carbon and soot.

Extending present observations of dimensionless extinction coefficients to other soot populations should be approached with caution; in particular, the present overfire soot involved large aggregates with significant effects of scattering and behavior might be very different for the small soot aggregates found in soot growth regions. On the other hand, relatively weak effects of fuel type on soot refractive index properties in the visible offer substantial reductions of effort for estimating soot optical and radiative properties that definitely merits further study.

Acknowledgments

This research was supported by the Building and Fire Research laboratory of the Institute of Standards and Technology, Grant Nos. 60NANB4D1696 and 60NANB8D0084, with H. R. Baum serving as Scientific Officer.

References

Batten, C.E., 1985, "Spectral Optical Constants of Soots from Polarized Angular Reflectance Measurements," *Appl. Optics* , Vol. 24, pp. 1193-1199.

Chang, H.Y., and Charalampopoulos, T. T., 1990, "Determination of the Wavelength Dependence of Refractive Indices of Flame Soot," *Proc. R. Soc. London A*, Vol. 430, pp. 577-591.

Charalampopoulis, T.T., 1992, "Morphology and Dynamics of Agglomerated Particulates in Combustion Systems Using Light Scattering Techniques," *Prog. Energy Combust. Sci.*, Vol. 18, pp. 13-45.

Choi, M.Y., Mulholland, G.W., Hamins, A., and Kashiwagi, T., 1995, "Comparisons of the Soot Volume Fraction Using Gravimetric and Light Extinction Techniques," *Combust. Flame*, Vol. 102, pp. 161-169.

Dalzell, W.H., and Sarofim, A.F., 1969, "Optical Constants of Soot and Their Application to Heat Flux Calculations," *J. Heat Trans.*, Vol. 91, pp. 100-104.

Dobbins, R.A., and Megaridis, C.M., 1991, "Absorption and Scattering of Light by Polydisperse Aggregates," *Appl. Optics*, Vol. 30, pp. 4747-4754.

Dobbins, R.A., Mulholland, G.W., and Bryner, N.P., 1993. "Comparison of a Fractal Smoke Optics Model with Light Extinction Measurements," *Atmospheric Environment*, Vol. 28, pp. 889-897.

Dyer, T.M., 1979, "Rayleigh Scattering Measurements of Time-Resolved Concentration in a Turbulent Propane Jet," *AIAA J.*, Vol. 17, pp. 912-914.

Faeth, G. M., and Köylü, Ü.Ö., 1995, "Soot Morphology and Optical Properties in Nonpremixed Turbulent Flame Environments," *Combust. Sci. Tech.*, Vol. 108, pp. 207-229.

Felske, J.D., Charalampopoulos, T.T., and Hura, H., 1984, "Determination of the Refractive Indices of Soot Particles from the Reflectivities of Compressed Soot Pellets," *Combust. Sci. Tech.*, Vol. 37, pp. 263-284.

Jullien, R., and Botet, R., 1987, *Aggregation and Fractal Aggregates*, World Scientific Publishing Co., Singapore, pp. 45-60.

Köylü, Ü.Ö., 1992, "Structure of Overfire Soot in Buoyant Turbulent Diffusion Flames," Ph.D. Thesis, The University of Michigan, Ann Arbor, Michigan.

Köylü, Ü.Ö., and Faeth, G.M., 1992, "Structure of Overfire Soot in Buoyant Turbulent Diffusion Flames at Long Residence Times," *Combust. Flame*, Vol.89, pp. 140-156.

Köylü, Ü.Ö., and Faeth, G.M., 1993, "Radiative Properties of Flame-Generated Soot," *J. Heat Trans.*, Vol. 111, pp. 409-417.

Köylü, Ü.Ö., and Faeth, G.M., 1994a, "Optical Properties of Overfire Soot in Buoyant Turbulent Diffusion Flames at Long Residence Times," *J. Heat Trans.*, Vol. 116, pp. 152-159.

Köylü, Ü.Ö., and Faeth, G.M., 1994b, "Optical Properties of Soot in Buoyant Laminar Diffusion Flames," *J. Heat Trans.*, Vol. 116, pp. 971-979.

Köylü, Ü.Ö., and Faeth, G.M., 1996, "Spectral Extinction Coefficients of Soot Aggregates from Turbulent Diffusion Flames," *J. Heat Trans.*, Vol. 118, pp. 415-421.

Köylü, Ü.Ö., Faeth, G.M., Farias, T.L., and Carvalho, M.G., 1995, "Fractal and Projected Structure Properties of Soot Aggregates," *Combust. Flame*, Vol. 100, pp. 621-633.

Lee, S.C., and Tien, C.L., 1980, "Optical Constants of Soot in Hydrocarbon Flames," *Eighteenth Symposium (International) on Combustion*, The Combustion Institute, Pittsburgh, pp. 1159-1166.

Manickavasagam, S., and Mengüc, M.P., 1993, "Effective Optical Properties of Coal/Char Particles Determined from FT-IR Spectroscopy Experiments," *Energy and Fuel*, Vol.7, pp.860-869.

Mulholland, G. W., and Choi, M. Y., 1998, "Measurement of the Mass Specific Extinction Coefficient for Acetylene and Ethane Using the Large Agglomerate Optics Facility," *Twenty-Seventh Symposium (International) on Combustion*, The Combustion Insitute, Pittsburgh, PA, pp. 1515-1522.

Mulholland, G. W., and Mountain, R.D., 1999, "Coupled Dipole Calculations of Extinction Coefficient and Polarization Ratio for Smoke Agglomerates," *Combust. Flame*, Vol. 119, pp. 56-68.

Rosner, D.E., Mackowski, D.W., and Garcia-Ybarra, P., 1991, "Size- and Structure-Insensitivity of the Thermophoretic Transport of Aggregated 'Soot' Particles in Gases," *Combust. Sci. Tech.*, Vol. 80, pp. 87-101.

Rudder, R.R., and Bach, D. R., 1968, "Rayleigh Scattering of Ruby-Laser Light by Neutral Gases," *J. Opt. Soc. Amer.*, Vol. 58, pp. 1260-1266.

Sivathanu, Y.R., and Faeth, G.M., 1990, "Soot Volume Fractions in the Overfire Region of Turbulent Diffusion Flames," *Combust. Flame*, Vol. 81, pp. 133-149.

Sivathanu, Y.R., Gore, J.P., Janssen, J.M., and Senser, D.W., 1993, "A Study of *In Situ* Specific Absorption Coefficients of Soot Paricles in Laminar Flat Flames," *J. Heat Trans.*, Vol. 115, pp. 653-658.

Stagg, B.J., and Charalampopoulos, T.T., 1993, "Refractive Indices of Pyrolytic Graphite, Amorphous Carbon, and Flame Soot in the Temperature Range 25 to 600°C.," *Combust. Flame*, Vol. 94, pp. 381-396.

Tien, C. L., and Lee, S. C., 1982, "Flame Radiation," *Prog. Energy Combust. Sci.*, Vol. 8, pp. 41-59.

Vaglieco, B.M., Beretta, F., and D'Alessio, A., 1990, "In Situ Evaluation of the Soot Refractive Index in the UV-Visible from the Measurements of Scattering and Extinction Coefficients in Rich Flames," *Combust. Flame,* Vol. 79, pp. 259-271.

Viskanta, R., and Mengüc, M.P., 1987, "Radiation Heat Transfer in Combustion Systems," *Prog. Energy Combust. Sci.*, Vol. 13, pp. 97-160.

Wu, J.-S., Krishnan, S.S., and Faeth, G.M., 1997, "Refractive Indices at Visible Wavelengths of Soot Emitted from Buoyant Turbulent Diffusion Flames," *J. Heat Trans.*, Vol. 119, pp. 230-237.

Table 1. Summary of test conditions[a]

Fuel	Formula (-)	M (kg/kgmol)	d (mm)	$\dot{Q}$ (kW)	t_r[b] (ms)
Gas-fueled flames:					
Acetylene	C_2H_2	26.04	50	6.16	329
Ethylene	C_2H_4	28.05	50	5.14	317
Propylene	C_3H_6	42.08	50	6.58	333
Butadiene	C_4H_6	54.09	50	1.70	254
Liquid-fueled flames:					
Benzene	C_6H_6	78.11	51	3.40	292
Cyclohexane	C_6H_{12}	84.16	102	5.00	315
Toluene	C_7H_8	92.13	51	2.50	274
n-Heptane	C_7H_{16}	100.20	102	4.10	303

[a]Soot properties measured in the overfire region of buoyant turbulent diffusion flames burning in still air in the long residence time regime with ambient pressures and temperature of 99 ± 0.5 kPa and 298 ± 3 K, respectively. Listed in the order of increasing molecular weight for gas and liquid fuels, respectively.
[b]Computed from correlation of Sivathanu and Faeth (1990).

Table 2. Summary of soot structure properties[a]

Fuel	d_p (nm)	$\overline{N}$	N_g	σ_g	$D_f(\sigma_D)$[b]
Gas-fueled flames:					
Acetylene	47	417	214	3.3	1.79(0.01)
Ethylene	32	467	290	2.7	1.80(0.01)
Propylene	41	460	227	3.0	1.79(0.02)
Butadiene	42[c]	---	---	---	1.79(0.03)
Liquid-fueled flames:					
Benzene	50	552	261	3.5	1.77(0.05)
Cyclohexane	37[c]	---	---	--	1.80(0.06)
Toluene	51	526	252	3.2	1.79(0.07)
n-Heptane	35	260	173	2.4	1.79(0.06)

[a]Soot in the overfire region of buoyant turbulent diffusion flames burning in still air in the long residence time regime with ambient pressures and temperatures of 99 ± 0.5 kPa and 298 ± 3 K, respectively. Soot density of 1880 kg/m^3 from Wu et al. (1997); $k_f = 8.5$ with a standard deviation of 0.5 from Köylü et al. (1995). Values of d_p, $\overline{N}$, N_g and σ_g from Köylü et al. (1992) and Köylü and Faeth (1994a) except when noted otherwise. Listed in order of increasing molecular weight for gas and liquid fuels, respectively.

[b]From present scattering measurements in the wide-angle regime averaged over wavelengths of 351.2-632.8 nm with standard deviations for each fuel in parenthesis.

[c]From present TEM measurements.

Table 3. Refractive index properties and dimensionless extinction coefficients in the visible[a]

λ (nm)	E(m)	F(m)	F(m)/E(m)[d]	n	κ	K_e
351.2	0.24(0.06)	0.13(0.03)	0.63	1.38	0.44	7.4(1.3)
405.0[b]	---	---	0.76	---	---	8.8(1.0)[e]
457.9	0.27(0.06)[c]	0.26(0.07)[c]	0.87	1.64	0.62	8.7(1.5)
488.0	0.28(0.04)	0.25(0.07)	0.93	1.60	0.62	8.7(1.9)
514.5	0.29(0.04)	0.27(0.06)	0.98	1.62	0.66	8.6(1.5)
632.8	0.27(0.04)	0.44(0.15)	1.17	1.99	0.89	8.4(1.0)
800.0[b]	---	---	---	---	---	9.3(1.5)[f]

[a]Standard deviations are shown in brackets.

[b]Only extinction measurements were made at 405.0 and 800.0 nm.

[c]Benzene and toluene were excluded at 457.9 nm.

[d]Values of F(m)/E(m) were obtained from the correlation for all fuels in studies made in the visible thus far.

[e]Measurements were not made for the gaseous fuels and n-heptane at 405.0 nm.

[f]Measurements were not made for the gaseous fuels at 800 nm.

Table 4. Correlation of F(m)/E(m)[a]

Wavelength (nm)	351	400	425	450	480	514	633
F(m)/E(m)	0.63	0.75	0.80	0.85	0.91	0.98	1.17

[a]Correlation developed using present measurements for all fuels.

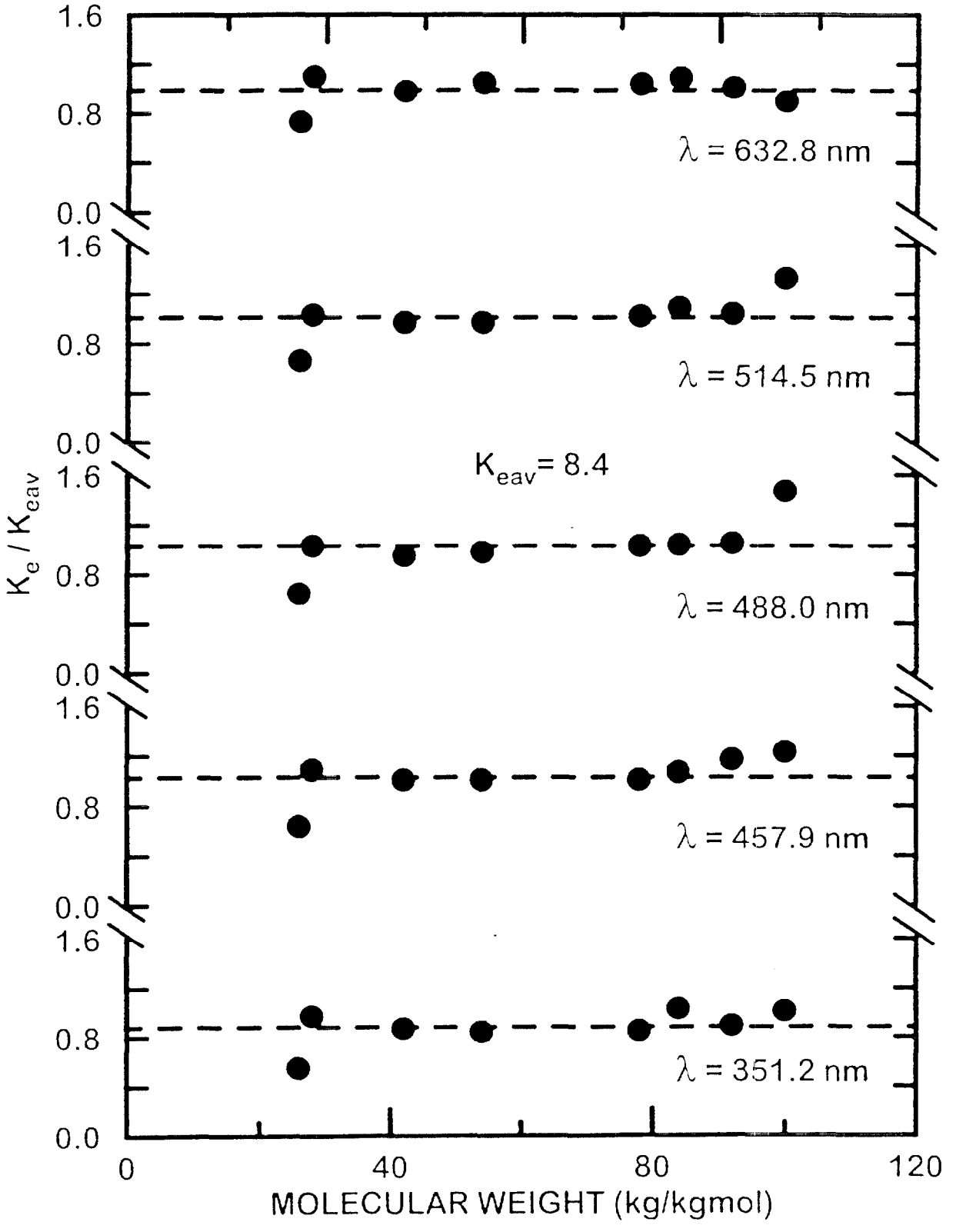

Fig. 1 Measured dimensionless extinction coefficients of soot in the visible as a function of fuel molecular weight and wavelength.

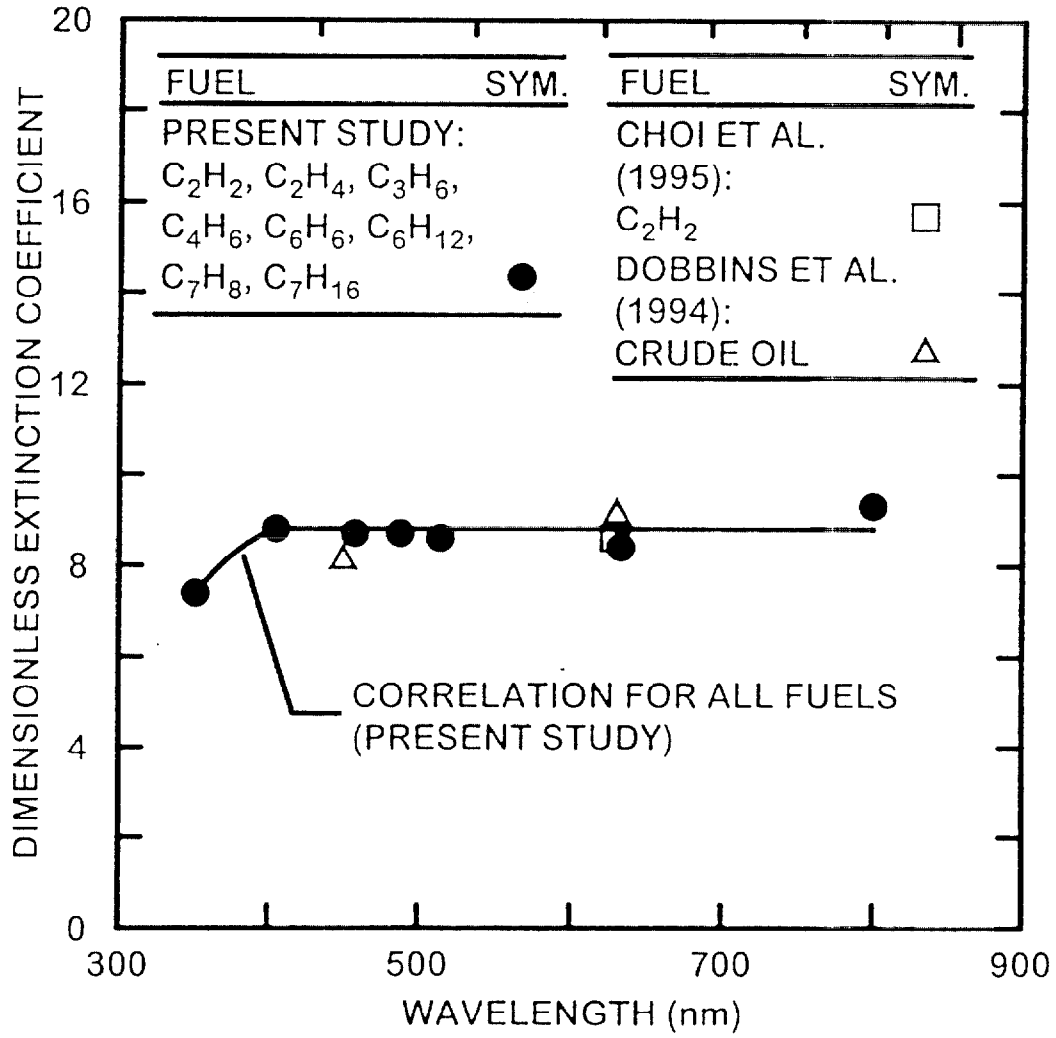

Fig. 2 Measured dimensionless extinction coefficients of soot in the visible as a function of wavelength.

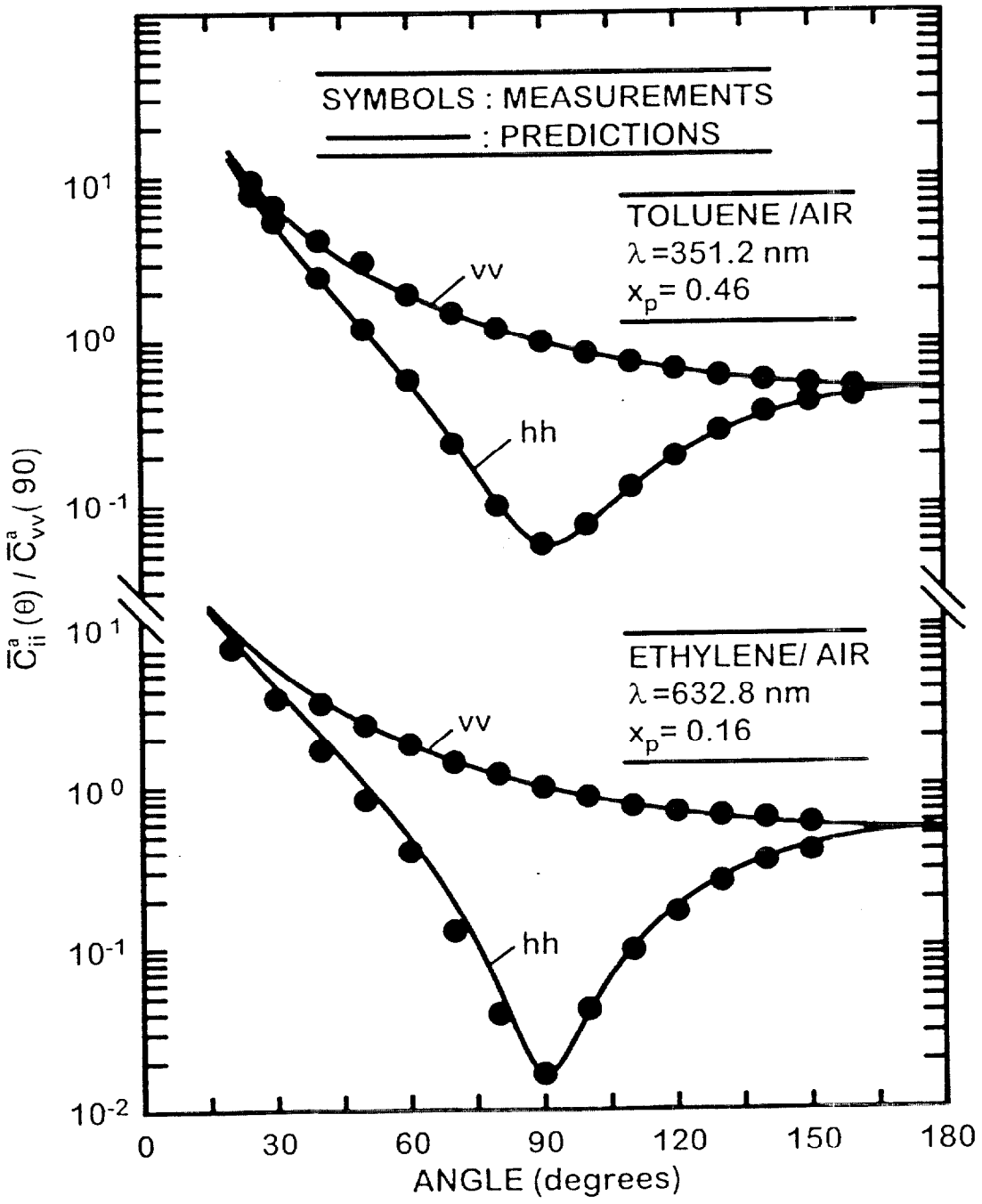

Fig. 3 Typical measured and predicted scattering patterns of soot in the visible.

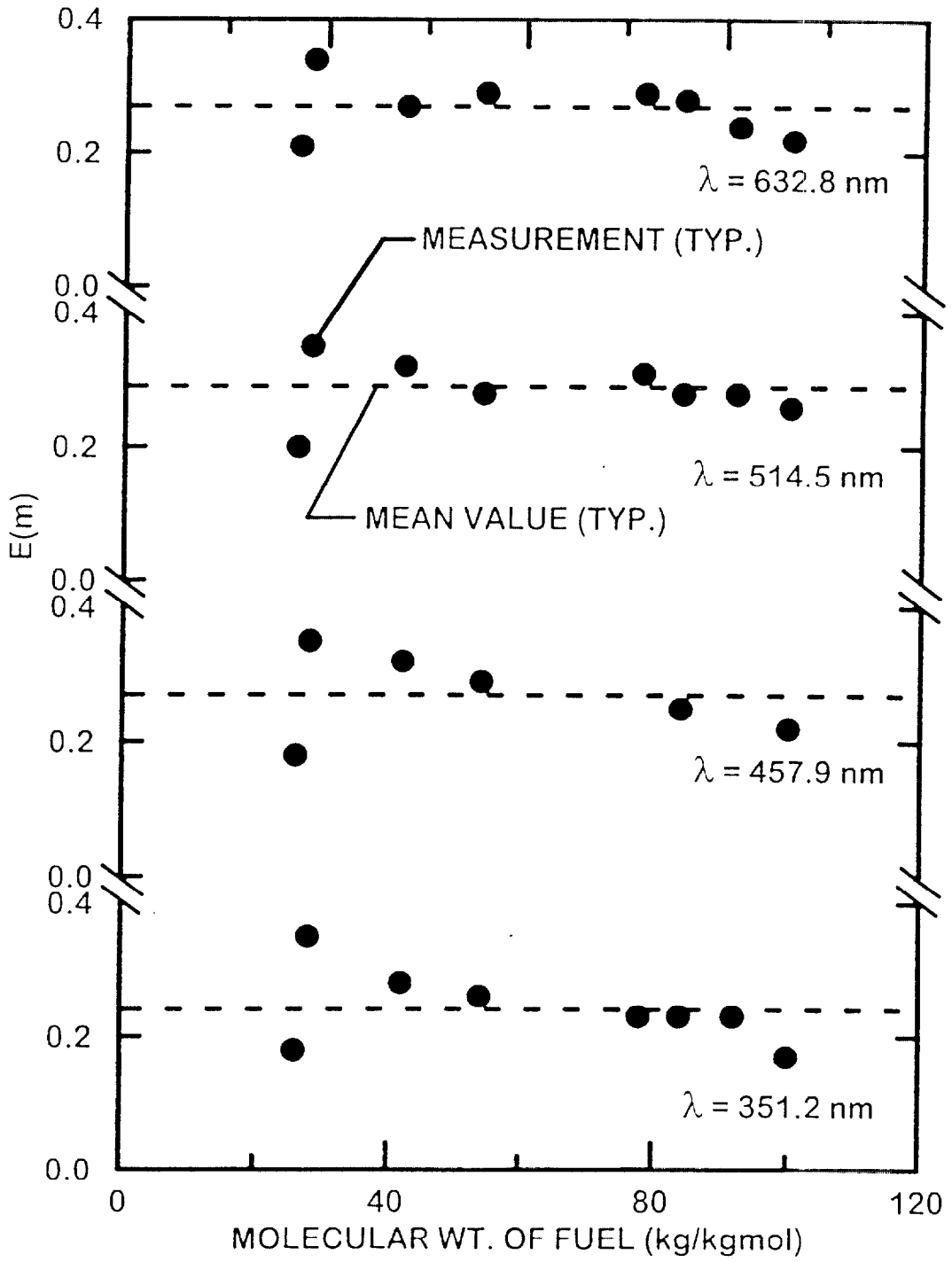

Fig. 4 Measured values of the refractive index function, E(m), of soot in the visible as a function of fuel molecular weight and wavelength.

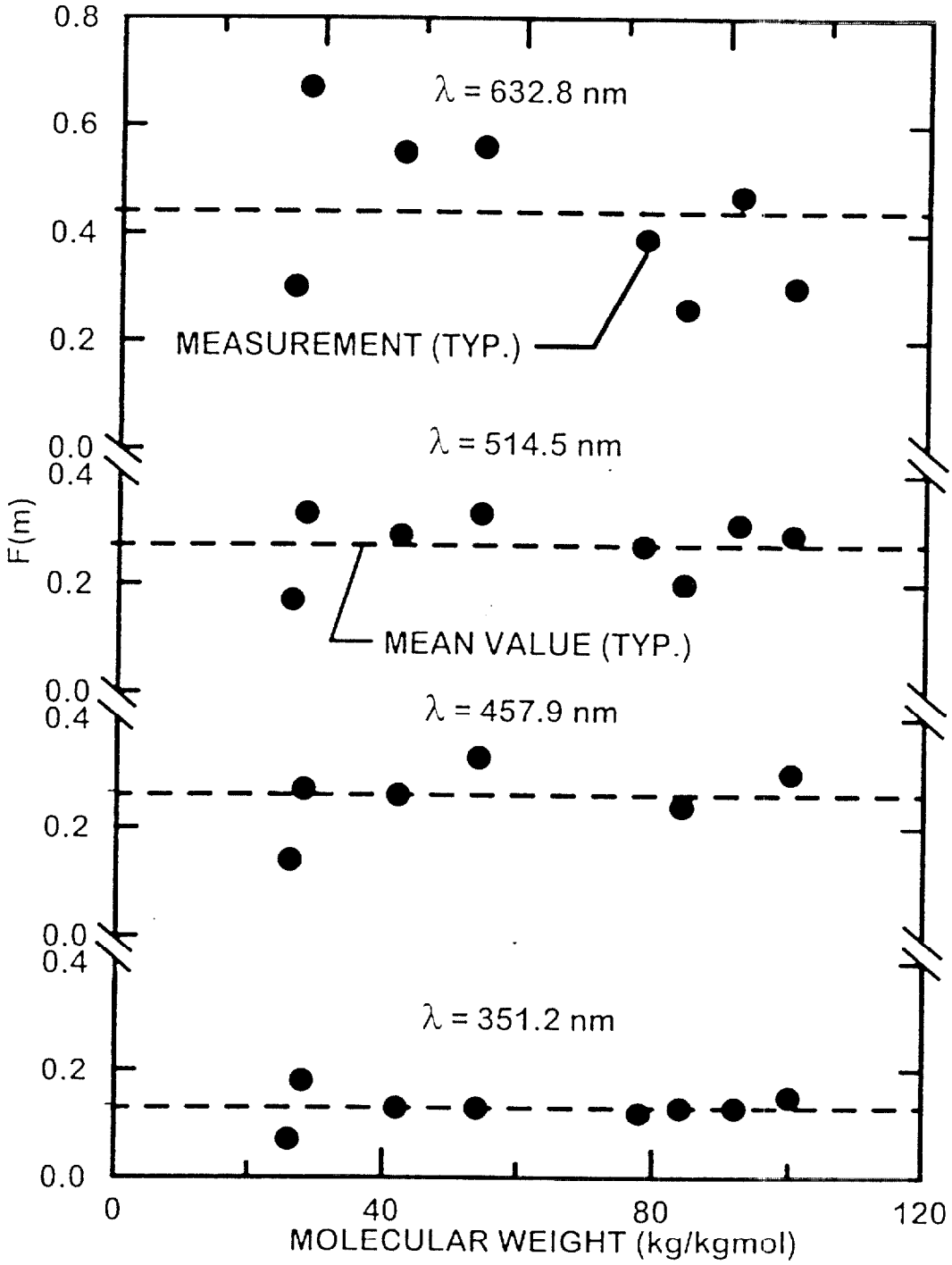

Fig. 5 Measured values of the refractive index function, F(m) of soot in the visible as a function of fuel molecular weight and wavelength

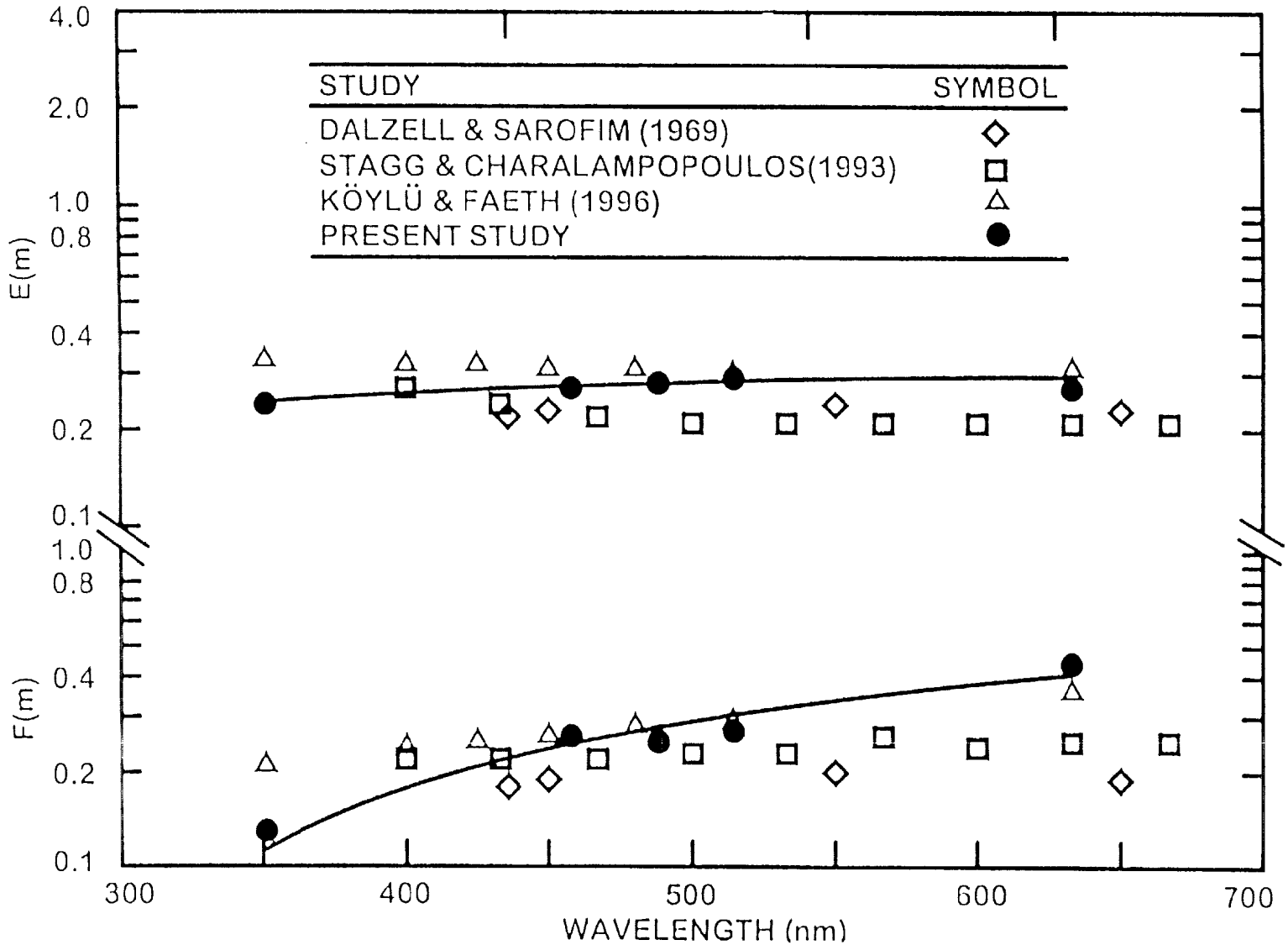

Fig. 6 Measured mean values of the refractive index functions, E(m) and F(m), of soot in the visible as a function of wavelength.

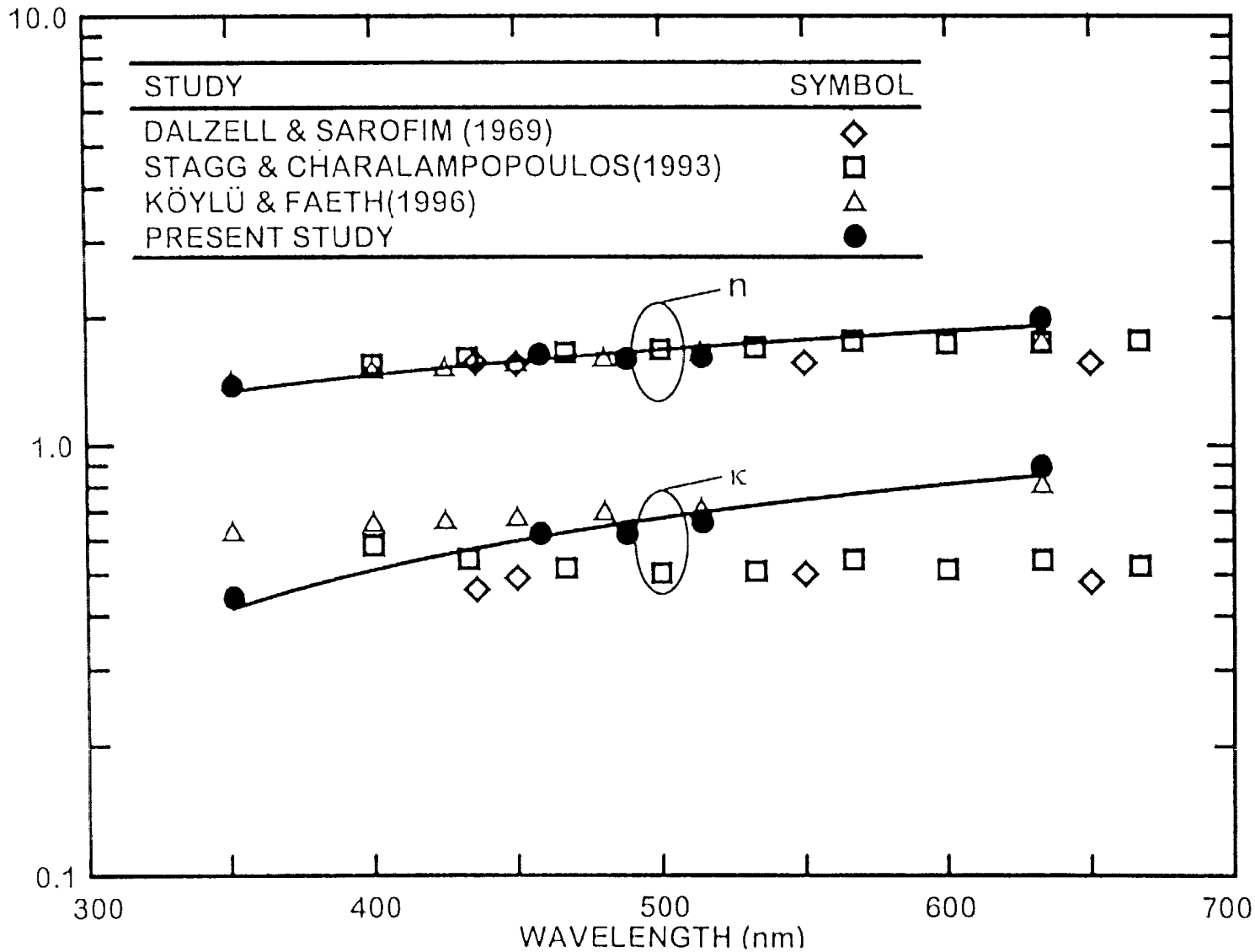

Fig. 7 Measured mean, real and imaginary parts of the complex refractive index of soot in the visible as a function of wavelength.

Appendix B: Krishnan et al. (1999b)

Extinction and Scattering Properties of Soot Emitted from Large Buoyant Turbulent Diffusion Flames

S. S. Krishnan[1], K.-C. Lin[2] and G. M. Faeth[3]
Department of Aerospace Engineering
The University of Michigan
Ann Arbor, Michigan 48109-2140, U.S.A.

Abstract

Extinction and scattering properties at wavelengths of 250-5200 nm were studied for soot emitted from large buoyant turbulent diffusion flames where soot properties are independent of position in the overfire region and characteristic flame residence time. Flames burning in still air and fueled with both gas (acetylene, ethylene, propane and propylene) and liquid (benzene, toluene, cyclohexane and n-heptane) hydrocarbon fuels were considered. Measuring scattering patterns and ratios of total scattering/absorption cross sections were in good agreement with predictions based on the Rayleigh-Debye-Gans (RDG) scattering approximations in the visible. Measured depolarization ratios were correlated by primary particle size parameter, completing RDG methodology needed to make soot scattering predictions. Measurements of dimensionless extinction coefficients were in good agreement with earlier measurements for similar soot populations and were independent of fuel type and wavelength except for reduced values as the near ultraviolet was approached. The ratios of the scattering/absorption refractive index functions were independent of fuel type and were in good agreement with earlier measurements. The refractive index function for absorption was similarly independent of fuel type but was larger than earlier reflectrometry measurements in the infrared. Ratios of total scattering/absorption

---

[1]Graduate Student Research Assistant.
[2]Research Fellow, Now with Taitec, Inc., Wright-Patterson AFB, Ohio.
[3]Professor, Fellow ASME, gmfaeth@umich.edu.

cross sections were relatively large in the visible and near infrared, with maximum values as large as 0.9, suggesting greater potential for scattering from soot particles to affect flame radiation properties than previously thought.

Keywords: Combustion, Radiation, Thermophysical Properties

Nomenclature

C	=	optical cross section
d_p	=	primary particle diameter
D	=	fractal factor, Eq. (19)
D_f	=	mass fractal dimension
$E(m)$	=	refractive index function for absorption = $\mathrm{Im}((m^2-1)/(m^2+2))$
f_v	=	soot volume fraction
$F(m)$	=	refractive index function for scattering = $\lvert(m^2-1)/(m^2+2)\rvert^2$
$g(kP_g,D_f)$	=	aggregate total scattering factor
i	=	$(-1)^{1/2}$
I	=	light intensity
k	=	wave number = $2\pi/\lambda$
k_f	=	fractal prefactor
K_e	=	dimensionless extinction coefficient
L	=	light path length

m	=	soot refractive index = $n+i\kappa$
n	=	real part of soot refractive index
n_p	=	mean number of primary particles per unit volume
N	=	number of primary particles per aggregate
N_g	=	geometric mean of the number of particles per aggregate
q	=	modulus of scattering vector = $2k \sin(\theta/2)$
Q	=	volumetric optical cross section
R_g	=	radius of gyration of an aggregate
x_p	=	primary particle size parameter = $\pi d_p/\lambda$
θ	=	angle of scattering from forward direction
κ	=	imaginary part of refractive index of soot
λ	=	wavelength of radiation
ρ_{sa}	=	ratio of total scattering to absorption cross sections
ρ_v	=	depolarization ratio
σ_D	=	standard deviation of D_f
σ_g	=	standard deviation of number of particles per aggregate from geometric mean

Subscripts

a	=	absorption

av = average value

e = extinction

h = horizontal polarization

ij = incident (i) and scattered (j) polarization directions

s = total scattering

v = vertical polarization

o = initial value

Superscripts

a = aggregate property

p = primary particle property

$(\bar{\ })$ = mean value over a polydisperse aggregate population

Introduction

The extinction and scattering properties of soot at visible and infrared wavelengths must be known in order to develop *in situ* optical techniques for measuring soot structure and concentration properties and reliable estimates of the continuum radiation properties of soot in flame environments. Motivated by these observations, past studies have made significant progress toward resolving the extinction and scattering properties of soot, see reviews by

Charalampopoulos (1992), Faeth and Köylü (1995), Julien and Botet (1987), Tien and Lee (1982), Mengüc (1987), Viskanta and Mengüc (1987) and references cited therein. This work has shown that soot consists of nearly monodisperse spherical primary particles collected into mass fractal aggregates, that primary soot particle diameters and the number of primary particles per aggregate vary widely whereas soot fractal properties are relatively universal, that soot optical properties can be approximated by Rayleigh-Debye-Gans (RDG) scattering from polydisperse mass fractal aggregates (called RDG-PFA theory) at visible wavelengths and that accurate estimates of soot optical properties in the visible and infrared are mainly limited by uncertainties about soot refractive index properties. Earlier work in this laboratory due to Krishnan et al. (1999) sought to improve understanding of soot refractive index properties in the visible by completing *in situ* measurements of soot coefficients and interpreting these results using RDG-PFA theory. The objective of the present investigation was to extend this research, concentrating on additional measurements and analysis of soot extinction and scattering properties in the near ultraviolet, visible and infrared wavelength ranges (wavelengths of 250-5200 nm).

Earlier studies of soot extinction and scattering properties are reviewed by Wu et al. (1997) and references cited therein; therefore, the following discussion will be limited to the findings of the companion study of Krishnan et al. (1999) . Krishnan et al. (1999) carried out *in situ* measurements of the optical properties of soot at wavelengths of 351.2-800.0 nm,

considering soot in the overfire region of large buoyant turbulent diffusion flames burning in still air at standard temperature and pressure and at long characteristic flame residence times where soot properties are independent of position and characteristic flame residence time for a particular fuel (Köylü and Faeth, 1992). Effects of soot type on soot optical properties were considered by studying soot in flames fueled with a variety of gaseous and liquid hydrocarbon fueled (acetylene, ethylene, propylene, butadiene, benzene, cyclohexane, toluene and n-heptane). As noted earlier, extinction and scattering were interpreted to find soot optical properties using RDG-PFA theory after establishing that this theory was effective over the test range by comparing measured and predicted scattering patterns. Effects of fuel type on soot optical properties were comparable to experimental uncertainties. Dimensionless extinction coefficients were relatively independent of wavelength for wavelengths of 400-800 nm and yielded a mean value of 8.4 in good agreement with earlier measurements of Dobbins et al. (1994), Choi et al. (1995), Mulholland and Choi (1998) and Zhou et al. (1998) who considered similar overfire soot populations. Measurements of the refractive index function for absorption, E(m), were in good agreement with earlier *ex situ* reflectrometry measurements of Dalzell and Sarofim (1968) and Stagg and Charalampopoulos (1993). On the other hand, measured values of the refractive index function for scattering, F(m), only agreed with these earlier measurements for wavelengths of 400-550 nm but otherwise increased with increasing wavelength more rapidly

than the rest. These measurements also showed that refractive index function increased rapidly with increasing wavelength in the visible, yielding large levels of scattering as the infrared wavelength range was approached. This behavior raises concerns about approximation of modest refractive index values in the infrared that are required by RDG-PFA theory (Dobbins and Megaridis, 1991; Köylü and Faeth, 1993; Dobbins et al., 1994); as well as concerns about the common assumption that scattering from soot in the infrared can be neglected when estimating flame radiation properties (Tien and Lee, 1982; Viskanta and Mengüc, 1987). Finally, these results showed that soot the refractive index properties do not approach a resonance condition in the near ultraviolet which is observed for graphite, see Chang and Charalampopoulos (1998); instead, refractive indices declined continuously with decreasing wavelength as the near ultraviolet was approached, similar to the findings of Vaglieco et al. (1990) for amorphous carbon and soot.

The present study sought to extend the measurements of Krishnan et al. (1999) into both the infrared and the near ultraviolet in order to help resolve concerns about soot optical properties in these spectral regions. Other issues that were considered included evaluating scattering predictions in the visible and infrared based on RDG-PFA theory, developing information about depolarization ratios in the visible that is needed to properly close scattering predictions based on RDG-PFA theory, and exploiting RDG-PFA theory to evaluate the potential

importance of scattering from soot on flame radiation properties in the infrared. The present study was limited to soot emitted from buoyant turbulent diffusion flames in the long residence time regime, using fuel types and methods similar to Krishnan et al. (1999).

The paper begins with descriptions of experimental and theoretical methods. Results are then described, considering scattering patterns, depolarization ratios, total scattering/absorption ratios, dimensionless extinction coefficients, refractive index functions and soot scattering predictions, in turn.

Experimental Methods

The experimental arrangement was the same as the earlier light scattering measurements of Krishnan et al. (1999) in the visible. The apparatus consisted of either a water-cooled gas-fueled burner having a diameter of 50 mm, or uncooled liquid-fueled burners having diameters of 51 and 102 mm, all injecting fuel gases vertically upward. The burners were located within an enclosure having a hood with a 152 mm diameter vertical exhaust duct at the top. Measurements were made at the exit of the exhaust duct where flow properties were nearly uniform. All operating conditions involved buoyant turbulent diffusion flames in still air within the long residence time regime where soot in the fuel-lean (overfire) region is Independent of position and characteristic flame residence time (Köylü and Faeth, 1992).

Many of the properties of the present overfire soot were available from earlier measurements by Köylü (1992), Köylü and Faeth (1992,1994a,1996), Köylü et al. (1995), Krishnan et al. (1999) and Wu et al. (1997), as follows: density, composition, volume fractions (gravimetrically), primary particle diameters, aggregate size properties $\left(\overline{N}, N_g, \sigma_g\right)$, aggregate fractal dimensions, scattering and extinction properties in the visible, and refractive index properties in the visible. Present measurements emphasized extinction within the wavelength range of 250-5200 nm. The wavelengths that were considered and the light sources that were used are as follows: 351.2, 457.9, 488.0 and 514.5 nm using an argon-ion laser (4W, Coherent Innova 90-4); 632.8 nm using a He-Ne laser (28 mW, Jodon HN10G1R); 248.0, 303.0, 405.0, 4360, 546.0 and 578.0 nm using a mercury lamp (100W, Oriel 6281); 600.0, 800.0, 1100.0, 1550.0 and 2017.0 nm using a Quartz-Tungsten Halogen (QTH) lamp (100W, Oriel 6333); and 3980.0 and 5205.0 nm using an IR emitter source (Oriel 6363). Two detectors were used, as follows: 351.2-800.0 nm using a silicon detector (Newport 818-UV), and 248.0-303.0 nm and 1100.0-5205.0 nm using a pyrodetector (Oriel 70128). Interference filters having 10 nm bandwidths were used for wavelengths up to 1550.0 nm; interference filters having bandwidths of 90-160 nm were used for wavelengths larger than 1500.0 nm. The optical arrangement was designed following Manickavasagam and Mengüc (1993) to reduce contributions of forward scattering to extinction measurements to less than 1 percent. Calcium fluoride lenses were used

for spatial filtering and collimating the incident light due to the large range of wavelengths considered. The light was modulated by a chopper (SR 540) before passing through the soot-containing exhaust flow. The output of the detector was passed through lock-in amplifiers prior to sampling and storage using a laboratory computer. Sampling was done at 2 kHz for a time period of 60s, averaging results for three sampling periods at each wavelength. Experimental uncertainties (95% confidence) of the extinction measurements are estimated to be less than 5%. Experimental uncertainties of other measurements will be presented when they are discussed.

The test conditions were the same as Krishnan et al. (1999). A brief summary of the fuels considered, and the corresponding structure properties of the overfire soot, is presented in Table 1. This range of fuels provides evaluation of soot optical properties for H/C atomic ratios of 1.00-2.28, which is reasonably broad.

Theoretical Methods

RDG-PFA Theory. Analysis of the extinction and scattering measurements to find soot optical properties was based on RDG-PFA theory. Portions of this theory used during the present investigation are briefly summarized in the following, see Julien and Botet (1987), Dobbins and Megaridis (1991), Köylü and Faeth (1994a) and references cited therein for more details.

The main assumptions of RDG-PFA theory are as follows: individual primary particles are Rayleigh scattering objects, aggregates satisfy the RDG scattering approximations, primary particles are spherical and have constant diameters, primary particles just touch one another, the number of primary particles per aggregate satisfies a log-normal probability distribution function, and aggregates are mass fractal objects that satisfy the following relationship (Julien and Botet, 1987):

$$N = k_f (R_g / d_p)^{D_f} \tag{1}$$

These approximations have proven to be satisfactory during past evaluations of RDG-PFA theory for a variety of conditions, including soot populations similar to the present study, see Köylü and Faeth (1992,1994a,b,1996), Wu et al. (1997) and Krishnan et al. (1999); nevertheless, the theory was still evaluated during the present investigation before applying it to find soot optical and scattering properties.

The following formulation will be in terms of volumetric optical cross sections; these can be converted to optical cross sections, as follows:

$$\overline{C}_j^a = \overline{NQ}_j^a / n_p; \quad j=vv,s,a,e \tag{2}$$

The volumetric extinction cross section is simply the sum of the volumetric absorption and total scattering cross sections,

$$\overline{Q}_e^a = \overline{Q}_a^a + \overline{Q}_s^a = (1+\rho_{sa})\overline{Q}_a^a \tag{3}$$

where the last expression introduces the total scattering/absorption cross section ratio:

$$\rho_{sa} = \overline{Q}_s^a / \overline{Q}_a^a \tag{4}$$

Based on RDG-PFA theory, ρ_{sa} can be computed given the structure and refractive index properties of the soot population, when effects of depolarization are small, as follows:

$$\rho_{sa} = 2x_p^3 F(m)\,\overline{N^2 g}/(3E(m)\overline{N}) \tag{5}$$

The specific expression for the aggregate total scattering factor, $g(kR_g,D_f)$, and the method of computing $\overline{N^2 g}$ from known aggregate structure properties, are described by Köylü and Faeth (1994a).

In order to complete predictions of soot extinction and scattering properties using RDG-PFA theory, measurements of soot volume fractions (gravimetrically) and primary particle diameters (by thermophoretic sampling and transmission electron microscopy, TEM) were used to compute primary particle density, as follows:

$$n_p = 6f_v/(\pi d_p^3) \tag{6}$$

Present extinction and scattering measurements in the visible yield $\overline{Q}_e^a$ and $\overline{Q}_s^a$ directly, so that $\overline{Q}_a^a$ can be found from Eq. (3) and ρ_{sa} from Eq. (4). Then the refractive index functions can be completed from the RDG-PFA formulation, as follows:

$$E(m) = k^2\overline{Q}_a^a/(4\pi x_p^3 n_p) \tag{7}$$

$$F(m) = k^2(qd_p)^{D_f}\,\overline{Q}_{vv}^a(qd_p)/(k_f x_p^6 n_p) \tag{8}$$

where qd_p must be large enough so that scattering is in the large-angle (power-law) regime where Eq. (8) is appropriate. This last requirement was readily satisfied because power-law scattering dominated the scattering properties of the present large soot aggregates, see Wu et al. (1997). The fractal properties needed to apply Eq. (8) also were known for the present soot populations, see Table 1. Finally, combining Eqs. (6) and (7) yields a useful expression for $\overline{Q}_a^a$, as follows:

$$\overline{Q}_a^a = 6\pi E(m) f_v / \lambda \tag{9}$$

Large soot aggregates exhibit effects of depolarization which influence $\overline{Q}_{hh}^a$ and thus estimates of $\overline{Q}_s^a$ and ρ_{sa}. Unfortunately, effects of depolarization cannot be predicted using RDG-PFA theory and must be handled empirically instead. This was done as suggested by Köylü and Faeth (1994a) by defining a depolarization ratio, ρ_v, and using it analogous to Rayleigh scattering theory, see Rudder and Bach (1968). Thus, values of $\overline{Q}_{hh}^a(\theta)$ were found, as follows:

$$\overline{Q}^{a}_{hh}(\theta) = \left[(1-\rho_v)\cos^2\theta + \rho_v\right]\overline{Q}^{a}_{vv}(\theta) \tag{10}$$

It follows immediately from Eq. (10) that

$$\rho_v = \overline{Q}^{a}_{hh}(90°)/\overline{Q}^{a}_{vv}(90°) \tag{11}$$

so that ρ_v could be obtained directly from present measurements in the visible.

The formulation of Eqs. (1)-(11) was used in several ways during the present investigation. First of all, normalized parameters, e.g., $\overline{Q}^{a}_{vv}(\theta)/\overline{Q}^{a}_{vv}$ (90°) and $\overline{Q}^{a}_{hh}(\theta)/\overline{Q}^{a}_{vv}(90°)$, yield scattering patterns that are independent of refractive index properties from Eqs. (7)-(11) which can then be used to evaluate RDG-PFA predictions and find values of ρ_v from the measurements. In addition, all quantities on the right hand sides of Eqs. (7) and (8) were known in the visible so that these equations could be used to find E(m) and F(m) in the visible as discussed by Krishnan et al. (1999). Effects of depolarization on predictions of total scattering cross sections were found to be small so that Eq. (5) could be used to predict ρ_{sa} in the visible, given values of E(m) and F(m), providing a means of testing combined effects of RDG-PFA predictions and refractive index property measurements. Then, Eq. (5) was used to estimate ρ_{sa} in the infrared (after finding a correlation for F(m)/E(m) in the infrared to e discussed later) so that E(m) could be found from present measurements of $\overline{Q}^{a}_{e}$ using Eqs. (3) and (9). Finally, Eq. (5) in

conjunction with values of E(m) and F(m) developed from the measurements, were used to estimate the potential importance of scattering from soot during computations to find the properties of flame radiation.

Dimensionless Extinction Coefficients. For conditions where soot properties are uniform along an optical path, the dimensionless extinction coefficient, k_e, provides a simple relationship between extinction and soot volume fractions, as follows (Dobbins et al., 1994):

$$K_e = \lambda \ln(I/I_o)/(Lf_v) \tag{12}$$

Soot properties, including f_v, were nearly constant over the present optical path; nevertheless, an appropriate average values of f_v was used to evaluate K_e from Eq. (12) based on several gravimetric measurements of f_v along the optical path, similar to Krishnan et al. (1999).

In the same manner as Eq. (12), the volumetric extinction cross section for a uniform path of length L is given by (Köylü and Faeth, 1994a):

$$\overline{Q}_e^a = -\ln(I/I_o)/L \tag{13}$$

Then, introducing the volumetric absorption coefficient from Eq. (3) and combining Eqs. (12) and (13) yields the following:

$$K_e = \lambda(1+\rho_{sa})\overline{Q}_a^a / f_v \tag{14}$$

Finally, substituting for $\overline{Q}_a^a$ from Eq. (9) yields

$$K_e = 6\pi E(m)(1+\rho_{sa}) \tag{15}$$

Equation (15) implies that variations of the dimensionless extinction coefficient with wavelength result from variations of E(m) and ρ_{sa} with wavelength.

Results and Discussion

Scattering Patterns. Scattering patterns were used to evaluate RDG-PFA theory for the present overfire soot because they are independent of refractive index properties. Typical examples of these evaluations are illustrated by the measured and predicted scattering patterns of ethylene soot at wavelengths of 351.2-632.8 nm appearing in Fig. 1, see Köylü and Faeth (1994a), Wu et al. (1997) and Krishnan et al. (1999) for other examples involving similar overfire soot populations. Experimental uncertainties (95% confidence) of the normalized scattering properties illustrated in Fig. 1, $\overline{Q}_{vv}^a(\theta)/\overline{Q}_{vv}^a$ (90°) and $\overline{Q}_{hh}^a(\theta)/\overline{Q}_{vv}^a(90°)$, are estimated to be smaller than 10%, except for the latter near 90°where small values of this ratio make uncertainties somewhat larger as discussed later.

The agreement between measurements and predictions in Fig. 1 is excellent with discrepancies smaller than experimental uncertainties. In particular, there is no deterioration of predictions at small wavelengths where relatively large values of x_p create concerns about the

validity of RDG-PFA theory. Similarly, there is no deterioration of performance at large wavelengths where progressively increasing values of the real and imaginary parts of the refractive indices of soot with increased wavelength also cause concerns about the validity of RDG-PFA theory. Similar performance was achieved at other conditions implying acceptable use of RDG-PFA theory for soot at values of x_p as large as 0.46.

Depolarization Ratios. A limitation of RDG-PFA theory, noted earlier, is that it provides no estimates of depolarization ratios that are needed to accurately compute $\overline{Q}^a_{hh}(\theta)$ from Eq. (10). Thus, measurements of ρ_v in the near infrared could be undertaken. This work involved exploiting the available data base of scattering patterns in the literature from Köylü and Faeth (1994a,b), Wu et al. (1997), Krishnan et al. (1999) and the present investigation, using Eq. (11) to find ρ_v. It was found that ρ_v became progressively smaller with increasing wavelength, for example, see the scattering patterns at different wavelengths plotted in Fig. 1. There also was a tendency for ρ_v to become progressively smaller with decreasing primary particle size. Considering both these trends, correlations of ρ_v in terms of the primary particle size parameter, x_p, proved to be the most successful approach and will be discussed in the following.

Available measurements of ρ_v are plotted as a function of x_p in Fig. 2. Measurements illustrated in the plot include results from Köylü and Faeth (1994a,b), Wu et al. (1997), Krishnan

et al. (1999) and the present investigation. Experimental uncertainties (95% confidence) of these determinations are somewhat larger than those of $\overline{Q}^a_{vv}(\theta)/\overline{Q}^a_{vv}(90^\circ)$ due to the small magnitude of ρ_v but are still estimated to be smaller than 20%. Results for soot in the overfire region of buoyant turbulent diffusion flames in the long residence time regimes, due to Köylü and Faeth (1994a), Wu et al. (1997), Krishnan et al. (1999) and the present investigation, are relatively independent of fuel type and are in reasonable agreement with each other, yielding the following correlation for ρ_v:

$$\rho_v = 0.14x_p \tag{16}$$

which also is shown on the plot. The standard error of the power of x_p in Eq. (16) is 0.1, the standard error of the coefficient is 0.03, and the correlation coefficient of the fit is 0.83, which is reasonably good. In contrast, the measurements for underfire soot in laminar diffusion flames due to Köylü and Faeth (1994a) are consistently smaller (by roughly 35%) than results for the overfire soot, although the variation of ρ_v with x_p is similar. This behavior suggests that the coefficient of Eq. (16) may be a function of aggregate size because the underfire soot involved $\overline{N}$ in the range 30-80 whereas the overfire soot involved $\overline{N}$ in the range 260-552 (see Table 1 for the latter). Finally, the values of ρ_v for soot aggregates illustrated in Fig. 3 are roughly an order of magnitude larger than typical values of ρ_v for Rayleigh scattering from gases, see Rudder and

Bach (1968). This behavior is consistent with the much smaller values of x_p for gases than for soot, due to the much smaller size of gas molecules than primary soot particles.

Total Scattering/Absorption Ratios. In addition to scattering patterns, predictions of RDG-PFA theory were further evaluated using present measurements of total scattering/absorption ratios, ρ_{sa}, in the visible. Study of ρ_{sa} is also useful for gaining a better understanding of the scattering properties of soot and their variation with wavelength, and for establishing methods for estimating ρ_{sa} that will be needed to find refractive index properties in the near infrared based on present measurements of extinction properties.

Values of ρ_{sa} were found by integrating measured differential scattering cross sections to find $\overline{Q}_s^a$ and then applying Eq. (3) and the measured value of $\overline{Q}_e^a$ to find $\overline{Q}_a^a$ and Eq. (4) to find ρ_{sa}. Experimental uncertainties of ρ_{sa} (95% confidence) are estimated to be smaller than 20%, with uncertainties tending to be largest at 632.8 nm for n-heptane and at 351.2 nm for the rest of the fuels because ρ_{sa} reaches minimum values at these conditions. Predictions of ρ_{sa} were obtained from measured soot structure properties using Eq. (5). Values of the soot refractive index function ratio, F(m)/E(m), needed to make these determinations in the visible were obtained from the measurements of Krishnan et al. (1999) for the same soot populations. Unfortunately, all the soot structure properties needed to complete RDG-PFA predictions of ρ_{sa}

were not available for butadiene and cyclohexane; therefore, results for these two fuels will not be considered in the following.

Measured and predicted values of ρ_{sa} are illustrated for wavelengths of 351.1-632.8 nm in Fig. 3. These results are for overfire soot in large buoyant turbulent diffusion flames burning n-heptane, benzene, toluene, ethylene, propylene and acetylene in still air. Measures values of ρ_{sa} are relatively large, in he range 0.1-0.9, tending to increase with increasing propensity to soot as indicated by increasing primary particle diameters. These results suggest significant effects of scattering for the conditions of the present measurements, which is expected in view of he relatively large aggregates found in the overfire region of large buoyant diffusion flames. Finally, RDG-PFA theory is in reasonably good agreement with the measurements.

An interesting feature of the results illustrated in Fig. 3 is that ρ_{sa} increases with increasing wavelength for all the fuels except n-heptane. This behavior is related to aggregate size, noting that n-heptane has the smallest aggregates of all the fuels considered in Fig. 3, e.g., the overfire soot produced by this fuel has the smallest value of $\overline{N}$ all the fuels by a wide margin and nearly the smallest value of d_p, see Table 1. These properties imply that the optical properties of n-heptane soot tend to approach Rayleigh scattering to a closer extent than the other fuels, where ρ_{sa} can be formulated, as follows (Köylü and Faeth, 1994a):

$$\rho_{sa} = (2\pi^3/3)(F(m)/E(m))(d_p/\lambda)^3, \quad \text{Rayleigh scattering} \tag{17}$$

The general expression for d_p for RDG-PFA scattering, Eq. (5), is complex, however, it can be simplified considerably at the limit of large aggregates and wavelengths where scattering is dominated by the large angle regime. Such conditions are representative of the large aggregates considered in Fig. 3, as a limit. At the large aggregate limit, ρ_{sa} independent of the specific distribution of N (the scattering properties of the aggregates saturate) and yields the following asymptotic expression (Köylü and Faeth, 1994a):

$$\rho_{sa} = D(F(m)/E(m))(d_p/\lambda)^{3-D_f}, \quad \text{saturated RDG-PFA scattering} \tag{18}$$

where D is a fractal factor that is independent of length, defined as follows:

$$D = \frac{\pi^3 k_f}{3(4\pi)^{D_f}} \left[\frac{6}{(2-D_f)} - \frac{24}{(6-D_f)(4-D_f)} \right] \tag{19}$$

Adopting a fractal dimension typical of soot, $D_f = 1.8$, yields the following expression for large soot aggregates from Eq. (18):

$$\rho_{sa} = D(F(m)/E(m))(d_p/\lambda)^{1.2}, \quad \text{saturated RDG-PFA scattering} \tag{20}$$

Based on Eqs. (17) and (20), it is evident that small soot aggregates, such as n-heptane soot, exhibit a relatively rapid reduction of ρ_{sa} with increasing wavelength compared to large soot aggregates, given similar variations of F(m)/E(m) with wavelength. Thus, it is plausible that increases of F(m)/E(m) with increasing wavelength that are sufficient to cause ρ_{sa} to increase

with increasing wavelength for large aggregates are still not sufficient to cause corresponding increases of ρ_{sa} for small aggregates that approach the Rayleigh scattering limit.

Dimensionless Extinction Coefficients. Similar to Krishnan et al. (1999), effects of fuel type on dimensionless extinction coefficients were comparable to experimental uncertainties. As a result, present measurements were limited to the gas-fueled flames, in order to check this behavior, with the following measurements presented as averages over all the gas-fueled flames, for conciseness. The resulting values of K_e are plotted as a function of wavelength in Fig. 4. Other measurements for overfire soot in the long residence time regime for various fuels, due to Dobbins et al. (1994), Choi et al. (1995), Mulholland and Chen (1998), Zhou et al. (1998) and Krishnan et al. (1999) are plotted on the figure for comparison with the present measurements.

Dimensionless extinction coefficients from the studies illustrated in Fig. 4 all involve soot emitted from large buoyant turbulent diffusion flames burning a variety of fuels and are in excellent agreement. This behavior supports the idea that effects of fuel type on K_e are small for these conditions for the wavelength range 250-5200 nm. This relative independence of K_e on soot type, however, should not be assumed for all flame conditions. For example, Dobbins et al. (1994) and Colceck et al. (1997) review measurements of specific extinction coefficients which

readily yield values of K_e that exhibit significant differences among soot in large diffusion flames, in premixed flames and in smoldering flames.

Values of K_e illustrated in Fig. 4 increase rapidly with increasing wavelength in the near ultraviolet, at wavelengths smaller than 400 nm which agrees with the observations of Vaglieco et al. (1990) for amorphous carbon and soot in the near ultraviolet. In contrast, graphite approaches a resonance condition which causes extinction levels to increase in the near ultraviolet (Tien and Lee, 1982). For wavelengths in the range 400-5200 nm, however, values of K_e are relatively constant, yielding an average value over all fuels and wavelengths for the measurements of Krishnan et al. (1999) and the present investigation of 8.7 with a standard deviation of 1.5 which is plotted in the figure. This mean value is slightly larger than the value of 84 with a similar standard deviation for wavelengths of 400-800 nm. The present slightly larger value of K_e reflects the relatively slow increase of K_e with increasing wavelength over the wavelength range 400-5200 nm seen in Fig. 4.

It is of interest to examine the relative variation of K_e with wavelength for the conditions illustrated in Fig. 4, resulting from the predictions of RDG-PFA theory. These considerations can be based on Eq. (15) with the wavelength variation of ρ_{sa} estimated from Eq. (2) for large soot aggregates because values of K_e were only obtained for the gaseous fuels (and not for n-heptane)

over the full wavelength range illustrated in Fig. 4. Based on these considerations, $K_e/E(m)$ varies proportional to λ^0 to $\lambda^{-1.2}$ as ρ_{sa} varies from small to large values compared to unity. Thus, the behavior of K_e seen in Fig. 4 requires a relatively rapid increase of E(m) with increasing wavelength in the near ultraviolet at wavelengths smaller than 400 nm, followed by a more gradual increase with increasing wavelength for wavelengths in the range 400-5200 nm, with the rate of increase tending to be larger for soot having relatively large values of ρ_{sa} in this wavelength range, such as the overfire soot considered during the present investigation. This observation will be helpful for interpreting values of E(m) and F(m) to be considered next.

Refractive Index Functions. Values of F(m)/E(m) and E(m) are needed to find spectral radiation properties and nonintrusive measurements of soot volume fractions, see Eqs. (5), (7), (8), (9) and (15). Thus, the spectral variations of these properties based on earlier and present measurements are considered in the following.

Values of F(m)/E(m) for wavelengths of 350-9000 nm are illustrated in Fig. 5. Results shown include the *ex situ* reflectometry measurements of Dalzell and Sarofim (1969), Felske et al. (1984) and Stagg and Charalampopoulos (1993), and the *in situ* absorption and scattering measurements in the visible of Wu et al. (1997) and Krishnan et al. (1999). The measurements of Dalzell and Sarofim (1969) are averages of their results for acetylene- and propane-fueled

flames. The measurements of Wu et al. (1997) have been adjusted to correct an error in their gravimetric determinations of soot volume fractions by matching their dimensionless extinction coefficients to the present measurements at 514.5 nm as discussed by Krishnan et al. (1999). Other measurements due to Batten (1985), Lee and Tien (1980), Chang and Charalampopoulos (1990) and Vaglieco et al. (1990) have not been included on the plot due to concerns about either experimental methods or about methods used to interpret measurements as discussed by Krishnan et al. (1999). Finally, two empirical correlations of the measurements are illustrated on the plot: one for the measurements of Krishnan et al. (1999) for wavelengths of 350-650 nm and one for all the measurements for wavelengths 350-6000 nm.

The measurements of F(m)/E(m) illustrated in Fig. 5 involve various fuels, sources and methods and are in remarkably good agreement. Exceptions involve the early *ex situ* reflectometry measurements of Dalzell and Sarofim (1969); they provide low estimates in the visible which may be due to the fact that corrections were not made for effects of surface voids on scattering properties which are important in the visible (Felske et al., 1984); and they provide high estimates in the far infrared at wavelengths larger than 6000 nm where small scattering levels and corresponding poor signal-to-noise ratios may be a factor. The relatively good agreement among the measurements at other conditions is no doubt promoted by the fact that F(m)/E(m) involves ratios of scattering to absorption cross sections which tends to normalize the

measurements and reduce errors compared to absolute measurements of absorption and scattering alone.

The absorption and scattering measurements of Krishnan et al. (1999) and the corrected absorption and scattering measurements of Wu et al. (1997), both in the visible, provide complete information needed to find ρ_{sa} and E(m) in the visible using Eqs. (7) and (8). In addition, ρ_{sa} becomes small at the largest wavelengths considered during the present investigation so that present measured values of $\overline{Q}_e^a \approx \overline{Q}_a^a$ and E(m) can be found directly from Eq. (7). At intermediate wavelengths, however, RDG-PFA theory was used to estimate values of ρ_{sa} so that $\overline{Q}_a^a$ could be found from the extinction measurements and then E(m) from Eq. (7). These estimates of ρ_{sa} were obtained using the correlation of F(m)/E(m) illustrated in Fig. 5, the known structure properties of the present soot and the RDG-PFA results of Eq. (5). Another set of *in situ* measurements of E(m) was obtained from the earlier extinction measurements of Köylü and Faeth (1996): this was done by matching values of E(m) from Krishnan et al. (1999) with these results at 514.5 nm and then using present measurements and estimates of ρ_{sa} in the visible and infrared to find E(m) from Eq. (7). Finally, the *ex situ* reflectometry measurements of Dalzell and Sarofim (1969), Felske et al. (1984) and Stagg and Charalampopoulos (1993) directly provide values of E(m).

The various determinations of E(m) for wavelengths of 350-9000 nm are illustrated in Fig. 6. The various *in situ* measurements of E(m) agree within experimental uncertainties over the entire wavelength range of the measurements which is encouraging. The *in situ* and *ex situ* measurements of E(m) in the visible agree within experimental uncertainties, with the somewhat smaller values of E(m) for the *ex situ* measurements attributed to uncorrected effects of surface voidage, at least for the measurements of Dalzell and Sarofim (1969). More disconcerting, however, are the unusually small values of E(m) found from the *ex situ* reflectometry measurements of Dalzell and Sarofim (1969) and Felske et al. (1984) in the infrared at wavelengths of 2000-9000 nm. In particular, it is difficult to see how trends of constant or progressively decreasing values of E(m) with increasing wavelength could yield the slightly increasing values of K_e with increasing wavelength in the infrared seen in Fig. 4 for RDG scattering objects. In contrast, present values of E(m) expressly yield the trends of K_e illustrated in Fig. 4 due to the method used to find E(m). Nevertheless, resolving the differences between the *in situ* and *ex situ* determinations of E(m) seen in Fig. 6 merits priority because these differences clearly can have a large impact on the radiative properties of soot-containing flames which are dominated by continuum radiation from soot in the infrared.

Soot Scattering Predictions. Given the RDG-PFA scattering and refractive index properties of the present overfire soot aggregates, it is of interest to estimate the potential

importance of scattering from such soot in flame environments. This was done by finding ρ_{sa} for the six fuels where required structure properties were known. Values of ρ_{sa} were computed using Eq. (5) and the correlation of F(m)/E(m) illustrated in Fig. 5 along with the appropriate structure properties. The results of these computations are illustrated in Fig. 7.

Referring to Fig. 5, the general correlation for F(m)/E(m) is not as steep in the visible as specific correlations for the present measurements; therefore, values of ρ_{sa} in Fig. 7 begin to decrease with increasing wavelength somewhat sooner than corresponding results for present test conditions illustrated in Fig. 3. The results shown in Fig. 7 indicate maximum values of ρ_{sa} for wavelengths of 450-600 nm, with n-heptane soot reaching a maximum before the rest as discussed earlier. The progressive increase of F(m)/E(m) with increasing wavelength seen in Fig. 5, however, tends to maintain relatively large values of ρ_{sa} well into the infrared, particularly for the very large soot aggregates resulting from the combustion of benzene, toluene and acetylene, where scattering is still roughly 20% of absorption at wavelengths approaching 2000 nm. This behavior suggests that scattering should be considered for accurate estimates of continuum radiation from soot in flame environments, at least for large soot aggregates similar to those considered during the present investigation and representative of natural fires.

Conclusions

The extinction and scattering properties of soot were studied using *in situ* methods at wavelengths of 250-5200 nm. Test conditions were limited to soot in the fuel-lean (overfire) region of buoyant turbulent diffusion flames in the long residence time regime where soot properties are independent of position and characteristic flame residence time. Flames burning in still air and fueled with eight liquid and gas hydrocarbon fuels were considered to provide atomic H/C ratios in the range 1.00-2.28. The major conclusions of the study are as follows:

1. Measured scattering patterns and ratios of total scattering/absorption cross sections in the visible were in good agreement with the predictions of RDG-PFA theory.
2. Measured depolarization ratios yielded a simple correlation in terms of the primary particle size parameter alone which completes the methodology needed to estimate soot scattering properties using RDG-PFA theory. Effects of aggregate size on this correlation were observed, however, and merit further study in the future.
3. Present dimensionless extinction coefficients were relatively independent of fuel type, increasing rapidly with increasing wavelength in the near ultraviolet but becoming relatively independent of wavelength over the range 400-5200 nm. Present measurements were in good agreement with earlier measurements for similar soot populations due to

Dobbins, et al. (1994), Choi et al. (1995), Mulholland and Choi (1998) and Zhou et al. (1998).

4. Present *in situ* measurements of the ratios of the scattering/absorption refractive index function, F(m)/E(m), were independent of fuel type and were in good agreement with earlier *ex situ* measurements in the literature. Present *in situ* measurements of the refractive index function for absorption, E(m), were also independent of fuel type and were in good agreement with earlier *in situ* measurements but were somewhat larger than earlier *ex situ* reflectometry measurements in the infrared.

5. Ratios of total scattering/absorption cross sections, ρ_{sa}, were relatively large in the visible and near infrared (reaching maximum values as large as 0.9) suggesting potential for greater effects of scattering from soot particles on the properties of flame radiation than previously thought.

Extending these conclusions to other types of soot should be approached with caution. In particular, the present soot has been exposed to oxidation in flame environments and involves relatively large soot aggregates due to large characteristic flame residence times; thus, such soot may not be representative of unoxidized and weakly aggregated soot typical of fuel-rich soot growth regions.

Acknowledgments

This research was supported by the Building and Fire Research Laboratory of the Institute of Standards and Technology, Grant Nos. 60NANB4D-1696 and 60NANB8D0084, with H. R. Baum serving as Scientific Officer and by NASA Grants NAG3-1878 and NAG3-2048 under the technical management of D.L. Urban and Z.-G. Yuan of the NASA Glenn Research Center.

References

Batten, C.E., 1985 "Spectral Optical Constants of Soots from Polarized Angular Reflectance Measurements," *Appl. Optics*, Vol. 24, pp. 1193-1199.

Chang, H.Y., and Charalampopoulos, T. T., 1990 "Determination of the Wavelength Dependence of Refractive Indices of Flame Soot," *Proc. R. Soc. London A*, Vol. 430, pp. 577-591.

Charalampopoulos, T.T., 1992, "Morphology and Dynamics of Agglomerated Particulates in Combustion Systems Using Light Scattering Techniques," *Prog. Energy Combust. Sci.*, Vol. 18, pp. 13-45.

Choi, M.Y., Mulholland, G.W., Hamins, A., and Kashiwagi, T., 1995, "Comparisons of the Soot Volume Fraction Using Gravimetric and Light Extinction Techniques," *Combust. Flame*, Vol. 102, pp. 161-169.

Colbeck, I., Atkinson, B., and Johar, Y., 1997, "The Morphology and Optical Properties of Soot Produced by Different Fuels," *J. Aerosol Sci.*, Vol. 28, pp. 715-723.

Dalzell, W.H., and Sarofim, A.F., 1969, "Optical Constants of Soot and Their Application to Heat Flux Calculations," *J. Heat Trans.*, Vol. 91, pp. 100-104.

Dobbins, R.A., and Megaridis, C.M., 1991, "Absorption and Scattering of Light by Polydisperse Aggregates," *Appl. Optics*, Vol. 30, pp. 4747-4754.

Dobbins, R.A., Mulholland, G.W., and Bryner, N.P., 1994, "Comparison of a Fractal Smoke Optics Model with Light Extinction Measurements," *Atmospheric Environment*, Vol. 28, pp. 889-897.

Dyer, T.M., 1979, "Rayleigh Scattering Measurements of Time-Resolved Concentration in a Turbulent Propane Jet," *AIAA J.*, Vol. 17, pp. 912-914.

Faeth, G. M., and Köylü, Ü.Ö., 1995, "Soot Morphology and Optical Properties in Nonpremixed Turbulent Flame Environments," *Combust. Sci. Tech.*, Vol. 108, pp. 207-229.

Felske, J.D., Charalampopoulos, T.T., and Hura, H., 1984, "Determination of the Refractive Indices of Soot Particles from the Reflectivities of Compressed Soot Pellets," *Combust. Sci. Tech.*, Vol. 37, pp. 263-284.

Jullien, R., and Botet, R., 1987, *Aggregation and Fractal Aggregates*, World Scentific Publishing Co., Singapore, pp. 45-60.

Köylü, Ü.Ö., 1992, "Emission, Structure and Optical Properties of Overfire Soot from Buoyant Turbulent Diffusion Flames," Ph.D. Thesis, The University of Michigan, Ann Arbor, MI.

Köylü, Ü.Ö., and Faeth, G.M., 1992, "Structure of Overfire Soot in Buoyant Turbulent Diffusion Flames at Long Residence Times," *Combust. Flame*, Vol. 89, pp. 140-156.

Köylü, Ü.Ö., and Faeth, G.M., 1993, "Radiative Properties of Flame-Generated Soot," *J. Heat Trans.*, Vol. 111, pp. 409-417.

Köylü, Ü.Ö., and Faeth, G.M., 1994a, "Optical Properties of Overfire Soot in Buoyant Turbulent Diffusion Flames at Long Residence Times," *J. Heat Trans.*, Vol. 116, pp. 152-159.

Köylü, Ü.Ö., and Faeth, G.M., 1994b, "Optical Properties of Soot in Buoyant Laminar Diffusion Flames," *J. Heat Trans.*, Vol. 116, pp. 971-979.

Köylü, Ü.Ö., and Faeth, G.M., 1996, "Spectral Extinction Coefficients of Soot Aggregates from Turbulent Diffusion Flames," *J. Heat Trans.*, Vol. 118, pp. 415-421.

Köylü, Ü.Ö., Faeth, G.M., Farias, T.L., and Carvalho, M.G., 1995, "Fractal and Projected Structure Properties of Soot Aggregates," *Combust. Flame*, Vol. 100, pp. 621-633.

Lee, S.C., and Tien, C.L., 1980, "Optical Constants of Soot in Hydrocarbon Flames," *Eighteenth Symposium (International) on Combustion,* The Combustion Institute, Pittsburgh, pp. 1159-1166.

Manickavasagam, S., and Mengüc, M.P., 1993, "Effective Optical Propeties of Coal/Char Particles Determined from FT-IR Spectroscopy Experiments," *Energy and Fuel*, Vol. 7, pp. 860-869.

Mulholland, G.W., and Choi, M. Y., 1998, "Measuremenent of the Mass Specific Extincion Coefficient for Acetylene and Ethene Smoke Using the Large Agglomerate Optics Facility," *Twenty-Seventh Symposium (International) on Combustion*, The Combustion Institute, Pittsburgh, pp. 1515-1522.

Rosner, D.E., Mackowski, D.W., and Garcia-Ybarra, P., 1991 "Size- and Structure-Insensitivity of the Thermophoretic Transport of Aggregated 'Soot' Particles in Gases," *Combust. Sci. Tech.* Vol. 80, pp. 87-101.

Rudder, R.R., and Bach, D. R., 1968, "Rayleigh Scattering of Ruby-Laser Light by Neutral Gases," *J. Opt. Soc. Amer.*, Vol. 58, pp. 1260-1266.

Sivathanu, Y.R., and Faeth, G.M., 1990, "Soot Volume Fractions in the Overfire Region of Turbulent Diffusion Flames," *Combust. Flame* , Vol. 81, pp. 133-149.

Stagg, B.J., and Charalampoulos, T.T., 1993, "Refractive Indices of Pyrolytic Graphite, Amorphous Carbon, and Flame Soot in the Temperature Range 25° to 600° C.," *Combust. Flame*, Vol. 94, pp. 381-396.

Tien, C. L., and Lee, S. C., 1982, "Flame Radiation," *Prog. Energy Combust. Sci.,* Vol. 8, pp. 41-59.

Vaglieco, B.M., Beretta, F., and D'Alessio, A., 1990, "In Situ Evaluation of the Soot Refractive Index in the UV-Visible from the Measurements of Scattering and Extinction Coefficients in Rich Flames," *Combust. Flame* , Vol. 79, pp. 259-271.

Viskanta, R., and Mengüc, M.P., 1987, "Radiation Heat Transfer in Combustion Systems," *Prog.* Energy Combust. Sci., Vol. 13, pp. 511-524.

Wu, J.-S., Krishnan, S.S., and Faeth, G.M., 1997, "Refractive Indices at Visible Wavelengths of Soot Emitted from Buoyant Turbulent Diffusion Flames," *J. Heat Trans.*, Vol. 119, pp. 230-237.

Zhou, Z.-Q., Ahmed, T.U., and Choi, M.Y., 1998, "Measurements of Dimensionless Soot Extinction Constant Using a Gravimetric Sampling Technique," *Experimental Thermal and Fluid Science*, Vol. 18, pp. 27-32.

Table 1. Summary of Soot Structure Properties[a]

Fuel[b]	d_p (nm)	$\overline{N}$	N_g	σ_g
Toluene (f)	51	526	252	3.2
Benzene (f)	50	552	261	3.5
Acetylene (g)	47	417	214	3.3
Butadiene (g)	42[c]	---	---	---
Propylene (g)	41	460	227	3.0
Cyclohexane (f)	37[c]	---	---	---
n-Heptane (f)	35	260	173	2.4
Ethylene (g)	32	467	290	2.7

[a]Soot in the overfire region of buoyant turbulent diffusion flames burning in still air in the long residence time regime with ambient pressures and temperatures of 99 ± 0.5 kPa and 298 ± 3 K, respectively. Soot density of 1880 kg/m^3 from Wu et al. (1997); k_f = 8.5 with a standard deviation of 0.5 from Köylü et al. (1995); D_f = 1.79 with a standard deviation of 0.05 from Krishnan et al. (1999). Values of d_p, $\overline{N}$, N_g and σ_g from Köylü et al. (1992) and Köylü and Faeth (1994a) except when noted otherwise. Listed in order of decreasing primary particle diameter.
[b]Parameter in parentheses denotes gas (g) or liquid (f) fuel.
[c]From Krishnan et al. (1999).

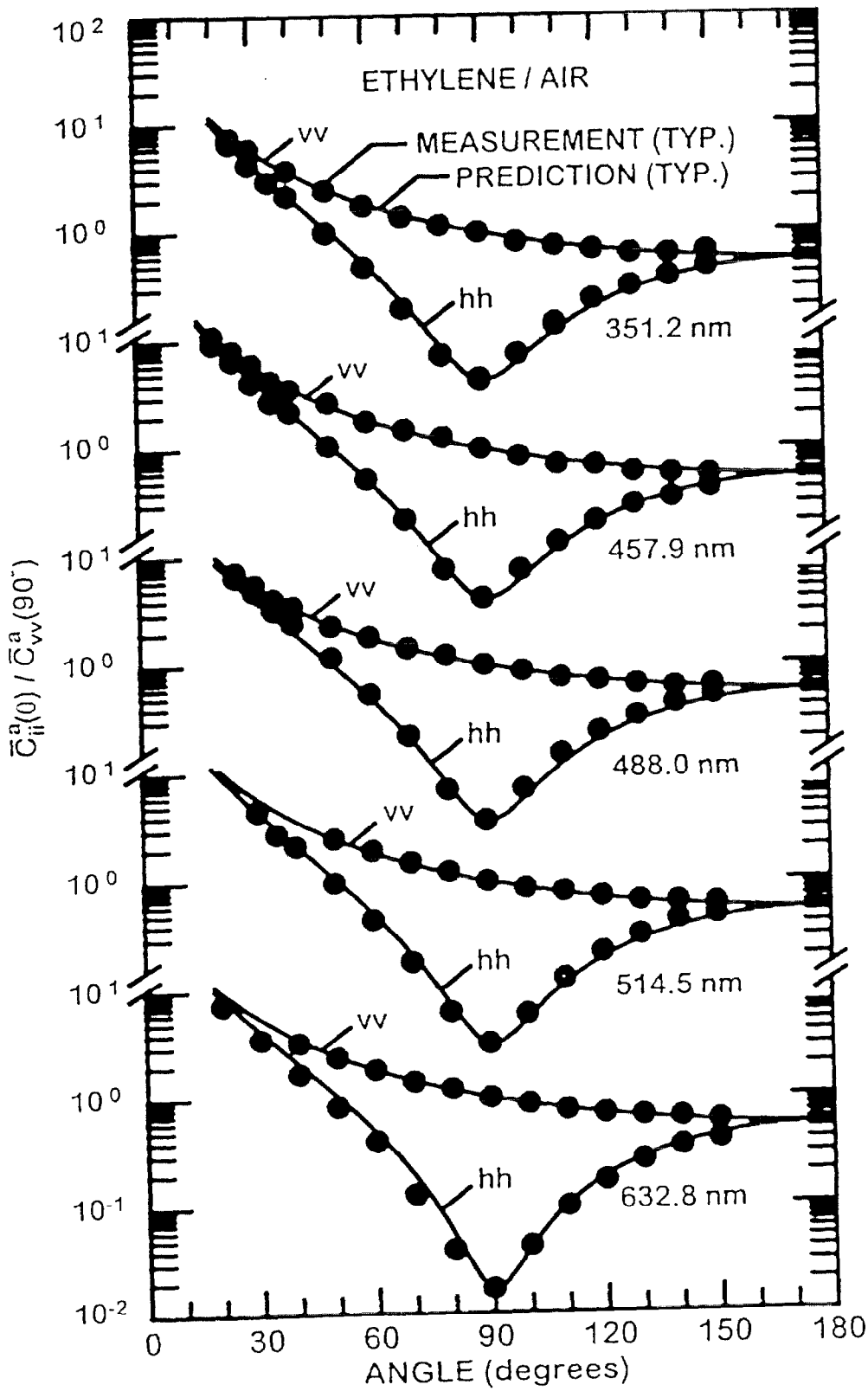

Fig. 1 Measured and predicted scattering patterns for soot in ethylene/air flames at wavelengths in the visible (351.2-632.8 nm).

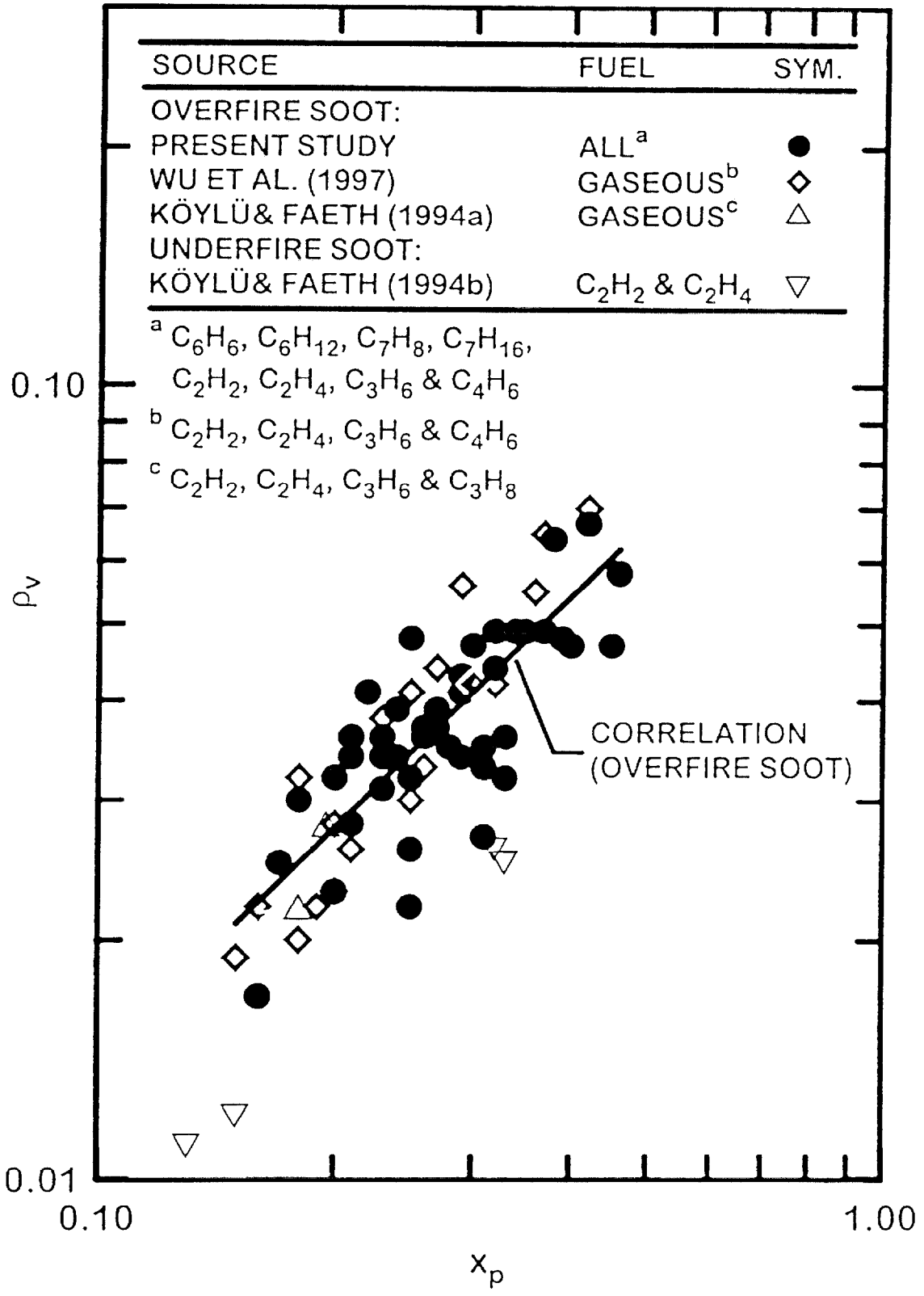

Fig. 2 Measurements of depolarization ratios for various fuels as a function of primary particle size parameter in the visible (351.2-632.8 nm). Measurements of Köylü and Faeth (1994a,b), Wu et al. (1997) and the present investigation.

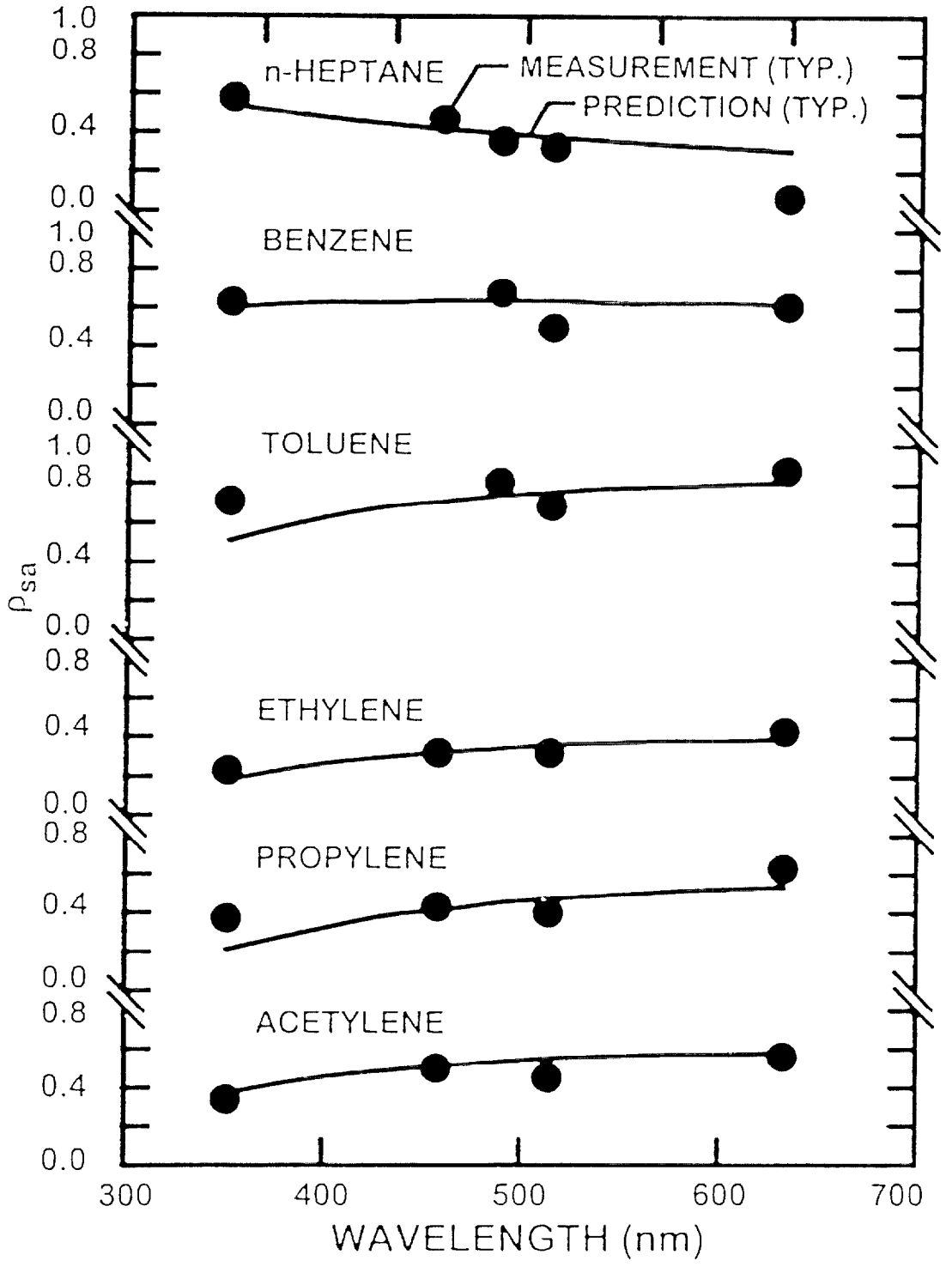

Fig. 3 Measured and predicted total scattering /absorption cross section ratios for various fuels as a function of wavelength in the visible (351.2-632.8 nm).

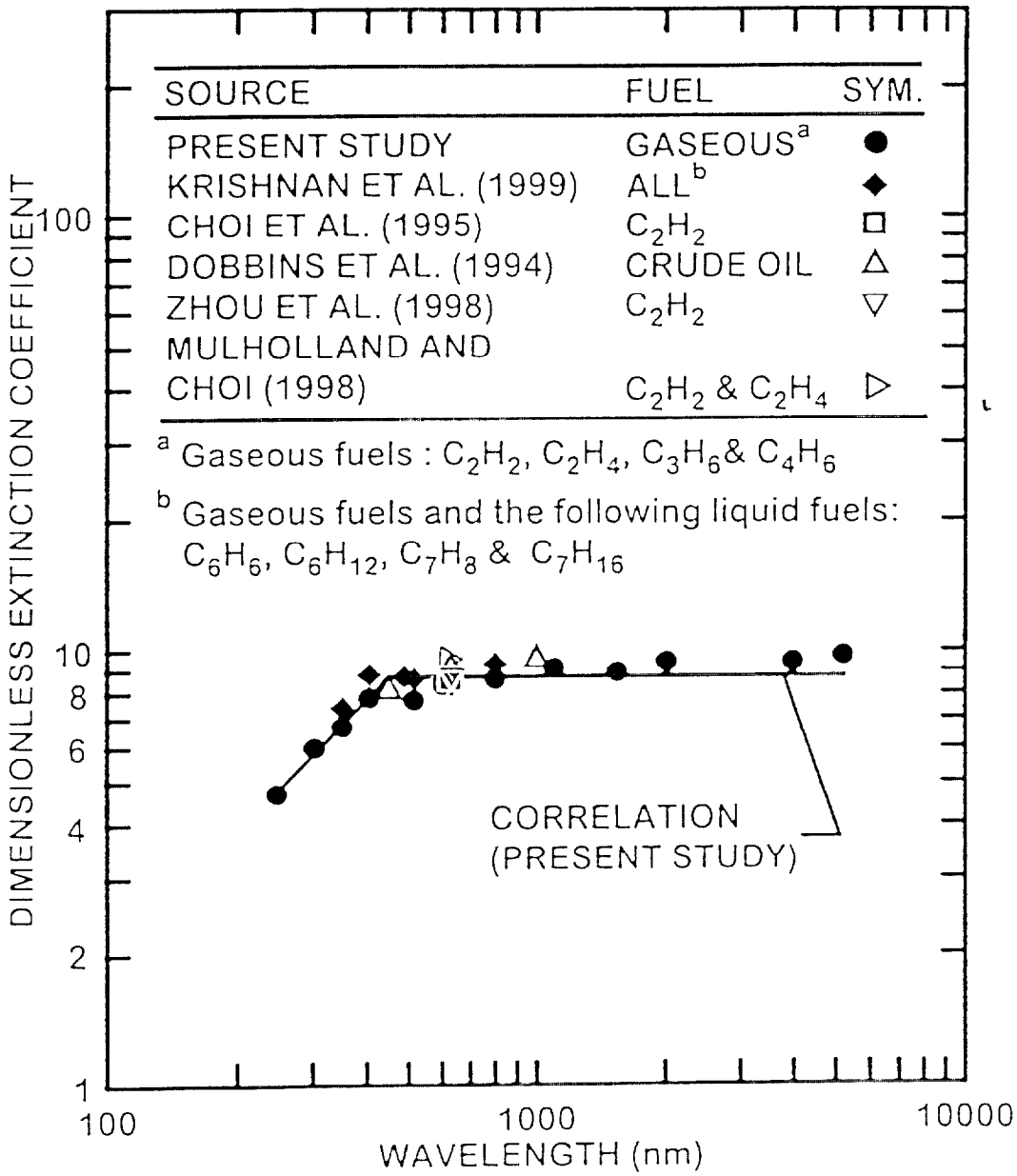

Fig. 4 Measured dimensionless extinction coefficients of soot for various fuels at wavelengths of 250-5200 nm. Measurements of Dobbins et al. (1994), Choi et al. (1995), Mulholland and Choi (1998), Zhou et al. (1998) and the present investigation.

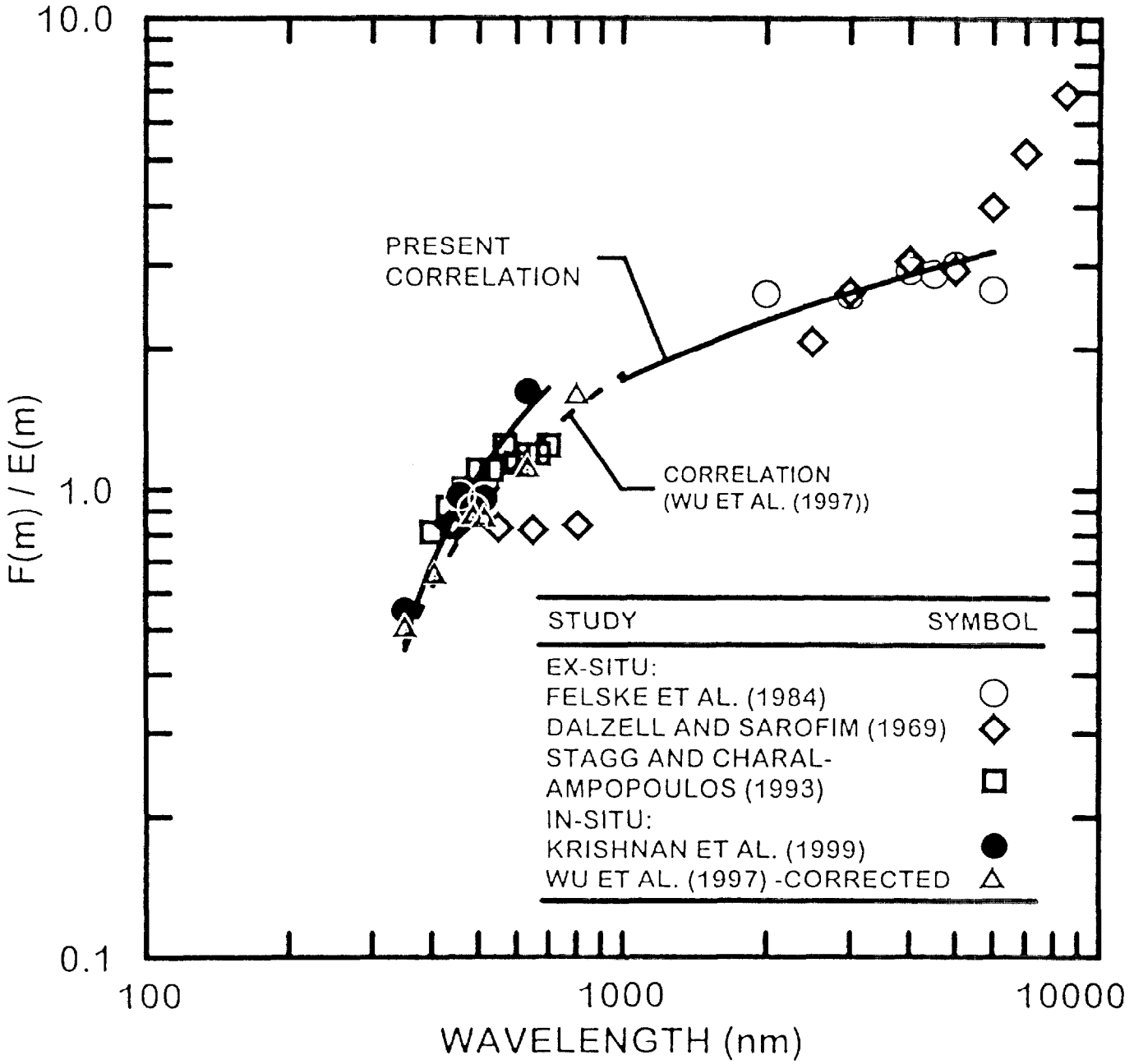

Fig. 5 Measurements of the refractive index function ratios, F(m)/E(m), for various fuels as a function of wavelength for wavelengths of 250-9000 nm. *Ex situ* measurements of Dalzell and Sarofim (1969), Felske et al. (1984), Stagg and Charalampopoulos (1993); *in situ* measurements of Wu et al. (1997) and Krishnan et al. (1999).

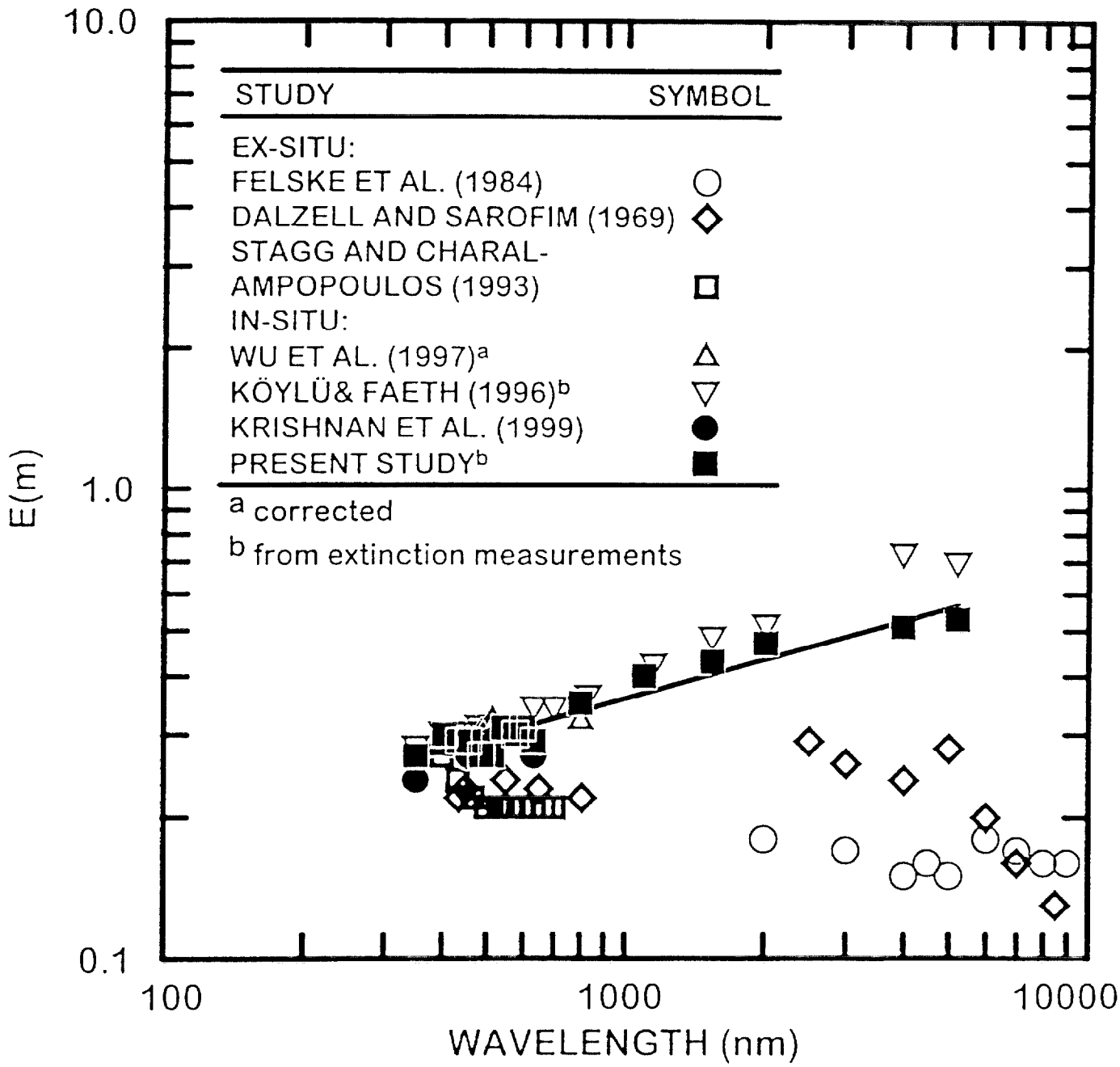

Fig. 6 Measurements of the refractive index function for absorption, E(m), as a function of wavelength for wavelengths of 250-9000 nm. *Ex situ* results of Dalzell and Sarofim (1969), Felske et al. (1984) and Stagg and Charalampopoulos (1993); *in situ* results of Köylü and Faeth (1996), Krishnan et al. (1999) and the present investigation.

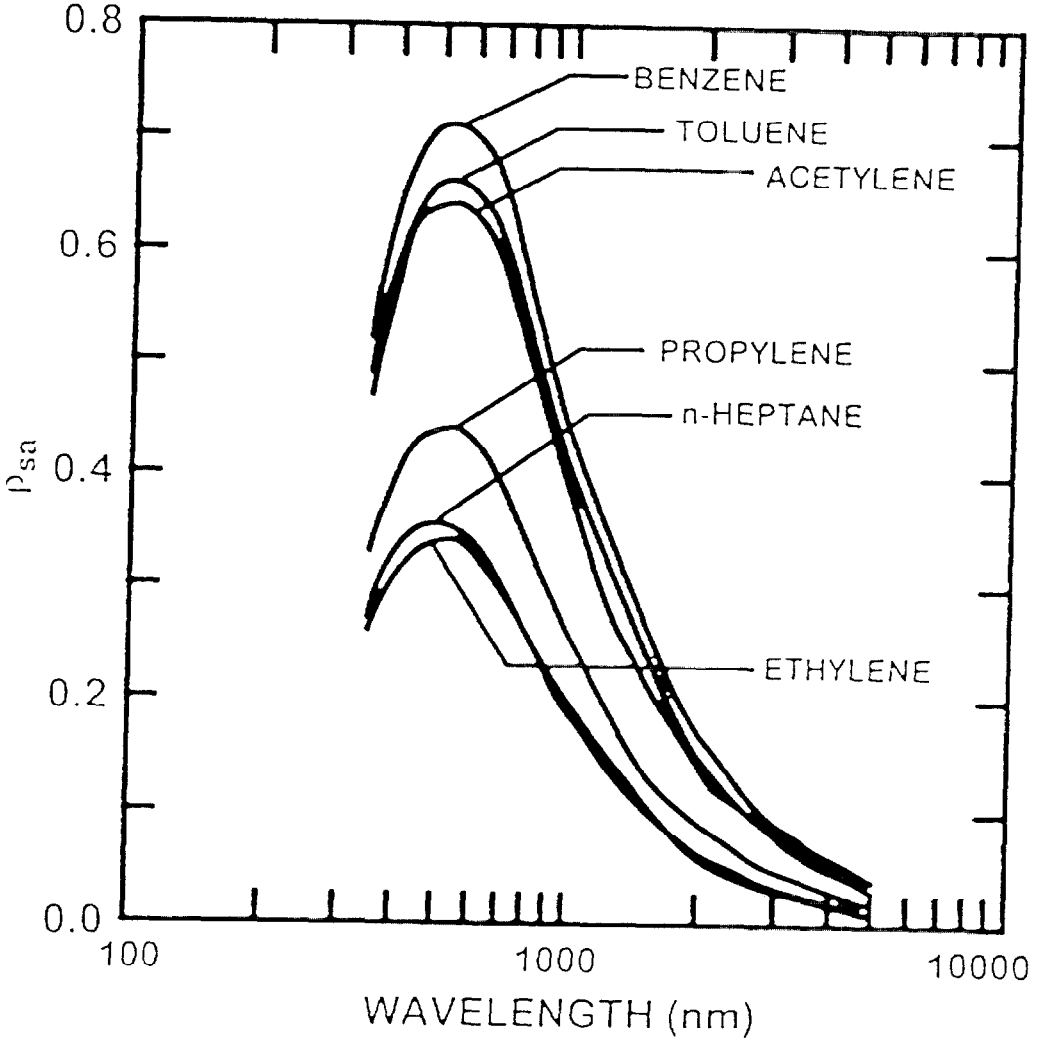

Fig. 7 Estimates of total scattering /absorption cross section ratios for various fuels as a function of wavelength for wavelengths in the visible and infrared (350-5200 nm).